**YANKEE ATOMIC ELECTRIC COMPANY**

Telephone (617) 872-8100
TWX 710-380-7619

1671 Worcester Road, Framingham, Massachusetts 01701

July 1, 1985

2.C.2.1
FYR 85-72

United States Nuclear Regulatory Commission
Washington, D. C. 20555

Attention: Mr. John A. Zwolinski, Chief
Operating Reactors Branch No. 5
Division of Licensing

References:
(a) License No. DPR-3 (Docket No. 50-29)
(b) License No. DPR-28 (Docket No. 50-271)
(c) License No. DPR-36 (Docket No. 50-309)
(d) USNRC Letter to YAEC and MYAPCO, dated May 11, 1984
(e) Topical Report: "RELAP5YA - A Computer Program for Light Water Reactor System Thermal-Hydraulic Analysis," Yankee Atomic Electric Company, YAEC-1300P, October 1982
(f) MYAPCO Letter to USNRC, dated January 31, 1985
(g) YAEC Letter to USNRC, dated February 26, 1985
(h) YAEC Letter to USNRC, dated March 1, 1985
(i) YAEC Letter to USNRC, dated April 30, 1985

Subject: Response to the NRC Questions on RELAP5YA

Dear Sir:

Reference (d) requested answers to 197 questions on YAEC's Topical Report on RELAP5YA [Reference (e)]. Our schedule called for the submittal of responses to 79 RELAP5YA questions by July 1, 1985. Responses to 11 of these questions have already been submitted to you in Reference (i). Responses to the remaining 68 questions are provided as an attachment to this letter. The attachment contains 12 extra responses belonging to the next group of questions scheduled for August 15, 1985. These are provided to you in advance to facilitate the review process.

Question Q.IX.13, instead of Q.IX.8, was erroneously identified as deleted in Reference (h). To correct this mistake, Question Q.IX.8 and its response have been identified as deleted in this submittal. The response to Q.IX.13 will be provided later.

We trust this information is satisfactory. However, if you have any questions please contact us.

Very truly yours,

YANKEE ATOMIC ELECTRIC COMPANY

G. Papanic
Senior Project Engineer - Licensing

GP/mmt

# RESPONSE TO 80 QUESTIONS ON RELAP5YA

July 1, 1985

## I. CONDENSATION HEAT TRANSFER AND NONCONDENSIBLE GASES

Nine potential sources of noncondensible gases are listed on Page VIII-49 of Reference 4 for a PWR: "(1) dissolved hydrogen in the primary coolant, (2) dissolved nitrogen in the accumulator water, (3) dissolved air in the refueling water storage tank, (4) hydrogen released from the zirconium-water reaction, (5) free nitrogen used to pressurize accumulators, (6) hydrogen released from radiolytic decomposition of injected water, (7) fission and fill gas in reactor fuel, (8) hydrogen gas (free and dissolved) in makeup tank, and (9) pressurizer steam space gas."

Q.I.3

Clarify which of these are treated by RELAP5YA and what rates are used to predict the amounts entering the system from each source.

A.I.3

Noncondensible gases are expected to have a negligible effect on the outcome of small break LOCAs. Hence, the treatment of noncondensibles in our calculations is not warranted. Appendix I.3-1 provides the justification for excluding the treatment of noncondensibles in our analyses.

## APPENDIX A.I-3

## BOUNDING ESTIMATES OF NONCONDENSIBLE GAS SOURCES AND THEIR IMPACT ON SBLOCAS

### 1.0 INTRODUCTION

During normal operation, a concentration between 25-50 cc of hydrogen/kg of water is dissolved in the Reactor Coolant System with an associated buildup in the pressurizer vapor space. Some concerns have been raised that this noncondensible gas can be released during a SBLOCA and inhibit adequate core cooling. The major concern is centered around the belief that the noncondensibles generated may migrate to the steam generator U-tubes and inhibit flow or sufficiently degrade heat transfer to inhibit adequate decay heat removal.

The steam generators are the preferred mode of decay heat removal for a significant period of time in only very small breaks. For example, licensing analyses for breaks larger than 0.02 $ft^2$ in the Maine Yankee plant show that most of the decay heat is removed through the break (Reference I.3-1). For breaks smaller than 0.02 $ft^2$, the steam generators are relied upon to remove some decay heat for a significant period of time.

Section 2 describes the method used to estimate the nine potential noncondensible gas sources. Plant-specific calculations for the Maine Yankee plant and Yankee plant at Rowe are provided. Section 3 provides an estimation of the noncondensibles' impact on the heat transfer capability of the two plants.

### 2.0 ESTIMATION OF NONCONDENSIBLE GAS SOURCES

The release of noncondensibles from the nine potential sources are calculated below. These calculations are performed for both the Maine Yankee plant and Yankee plant at Rowe.

## MAINE YANKEE PLANT

1. Dissolved hydrogen in the primary coolant: The calculation assumed the maximum RCS concentration of 50 cc of $H_2$/kg of water (Reference I.3-2) at STP. It is conservatively assumed that all the hydrogen is released and remains in the primary system.

2. Dissolved nitrogen in the accumulator water: The concentration of dissolved nitrogen is determined from Henry's Law (Reference I.3-3) at 104$^{o}$F and 230 psig to be 2.04 x $10^{-4}$ lbm $N_2$/lbm $H_2O$. This concentration is used to calculate the nitrogen introduced during accumulator water injection.

3. Dissolved air in refueling water storage tank: The pumped safety injection water from the RWST was calculated to contain 19.9 cc of air/kg of water at STP based upon Henry's Law (Reference I.3-3). The entire RWST inventory is assumed to be injected.

4. Hydrogen released from zirconium-water reaction: The calculation is based on 1% zirconium reacted and 37840 fuel rods.

5. Free nitrogen used to pressurize accumulators: The nitrogen contained in the accumulator gas space is assumed to be released when the accumulator liquid empties.

6. Hydrogen released from radiolytic decomposition of injected water: The time when the $H_2$ concentration in the primary system falls below 5 cc of $H_2$/kg of water is determined to be the time to start the calculation of radiolytic decomposition of water. For the 0.02 $ft^2$ Maine Yankee SBLOCA, a concentration of 5 cc $H_2$/kg $H_2O$ is reached at approximately 4700 seconds. At this time, the steam generators are not relied on to remove decay heat.

7. Fission and fill gas in reactor fuel: The calculation is performed assuming all fuel rods are at end-of-life conditions.

8. Hydrogen in the make-up tank: For the Maine Yankee plant, the make-up tank does not release water into the primary system during a SBLOCA.

9. Pressurizer vapor space: 630 cubic feet of hydrogen at STP is assumed to be contained in the pressurizer vapor space. This represents 90% of the available gas volume.

For Maine Yankee, Table I.3-1 provides the volume at (STP) and mass of the noncondensibles from all the nine sources identified above.

It is to be recognized that the core would have to undergo transients that are not predicted to occur for applicable small breaks, in order for many of the sources identified above to be important. Present Appendix K small break plant licensing analyses show that clad temperatures remain low and no cladding rupture is predicted. In addition for breaks of 0.02 $ft^2$ (Reference I.3-1) in area and lower, the system pressure does not reduce to the safety injection tank pressure. The only sources that may be introduced are: (a) hydrogen dissolved in the primary coolant, (b) air dissolved in the refueling water and (c) hydrogen contained in the pressurizer vapor space. The noncondensible gas volume from these sources amounts to 2011 $ft^3$ at STP.

For the Maine Yankee plant, the total primary tube volume is 688 $ft^3$ per steam generator. The noncondensible gas volume at the steam generator safety relief valve setpoint (1000 psia) is about 60 $ft^3$. The reactor vessel upper head volume is 1476 $ft^3$. Most of the noncondensibles are expected to migrate to the upper head without causing any impact on decay heat removal capability of the steam generators. However, if all the gas generated in this conservative calculation were to migrate to the steam generator U-tubes and reside there, the gas would occupy about 3% of the U-tube volume at stable conditions.

## YANKEE PLANT AT ROWE

1. Dissolved hydrogen in the primary coolant: The calculation assumed a maximum concentration of 40 cc of $H_2$/kg of water

(Reference I.3-4) at STP. It is conservatively assumed that all the hydrogen is released and remains in the primary system.

2. Dissolved nitrogen in the accumulator water: The dissolved concentration of nitrogen is determined from Henry's Law (Reference I.3-3) at 14.7 and 70°F to be $1.9027 \times 10^{-5}$ lbm $N_2$/lbm $H_2O$. This concentration is used to calculate the introduction of nitrogen during accumulator water injection.

3. Dissolved air in refueling water storage tank: The concentration of dissolved air is determined from Henry's Law (Reference I.3-3) to be $1.6364 \times 10^{-5}$ lbm air/lbm $H_2O$ at 14.7 psia and 130°F. The entire RWST inventory is assumed to be injected.

4. Hydrogen released from zirconium water-reaction: The calculation is based on 1% zirconium reacted and 17336 fuel rods.

5. Free nitrogen used to pressurize accumulators: The accumulator at the Yankee plant is isolated just before the liquid is completely depleted. This is done to avoid accumulator nitrogen injection into the reactor vessel.

6. Hydrogen released from radiolytic decomposition of injected water: The radiolytic decomposition of water is initiated when the $H_2$ concentration in the primary system falls below 5 cc of $H_2$/kg of water. For a 1" break in Yankee Rowe, this concentration is reached at about 3000 seconds. At this time, the steam generators are not needed to remove decay heat.

7. Fission and fill gas in reactor fuel: The calculation is performed assuming all fuel rods are at end-of-life conditions.

8. Hydrogen in the make-up tank: For the Yankee plant, the make-up tank does not release water into the primary system during a SBLOCA.

9. Pressurizer vapor space: 185 cubic feet of hydrogen at STP are assumed to be contained in the pressurizer vapor space. This represents 90% of the available gas space.

For the Yankee plant at Rowe, Table I.3-2 provides the volume (at STP) and mass of the noncondensibles from all the nine sources identified above.

For breaks of 1" diameter and lower (for which the steam generator is desired to remove decay heat), the system pressure does not reduce to the accumulator actuation pressure (Reference I.3-5). Also, the clad temperatures remain low and no cladding rupture is predicted. The only sources that may be introduced are: (a) hydrogen dissolved in the primary coolant, (b) air dissolved in the refueling water and (c) hydrogen contained in the pressurizer vapor space.

The conservative calculations performed indicate that for the Yankee plant 440 $ft^3$ at STP of noncondensible are available during the period the steam generators are desired for some decay heat removal.

For the Yankee plant, the total primary tube volume (4 steam generators) is 538 $ft^3$. The noncondensible gas volume at the steam generator safety relief valve setpoint (900 psia) is about 13 $ft^3$. The reactor vessel upper head volume is about 378 $ft^3$. Most of the noncondensibles are expected to migrate to the upper head region without causing any impact on the decay heat removal capability of the steam generators. However, if all the gas generated in this conservative calculation were to migrate to the steam generator U-tubes and stay there, the gas would occupy less than 3% of the U-tube volume at stable conditions.

## 4.0 EFFECT OF NONCONDENSIBLES ON CONDENSATION HEAT TRANSFER

The impact of the noncondensibles on heat transfer and thermal hydraulics of the two plants is assessed in this section. It is concluded that the noncondensible gases released at the Maine Yankee and the Yankee plants during small break LOCAs will have a negligible effect on the hydraulic and thermal aspects of the two plants.

The two effects of noncondensible gases are:

1. Reduction in the available temperature difference for given primary and secondary system pressures.

2. Reduction in condensation heat transfer due to the resistance of the noncondensible gas boundary layer.

The reduction in the available temperature difference is negligible as illustrated in Tables I.3-3 and I.3-4 for the Maine Yankee plant, and Tables I.3-5 and I.3-6 for the Yankee plant at Rowe. These tables assume that 2011 $ft^3$ (STP) at Maine Yankee and 440 $ft^3$ (STP) at Yankee Plant of noncondensibles are evenly distributed in either the primary system or the steam generators. The presence of noncondensibles affects the saturation temperature due to the partial pressure of the noncondensible gas. These temperature differences of less than $3^{o}F$ will not significantly affect the small break calculations.

The presence of noncondensible gas in a condensing vapor influences the resistance to heat transfer in the region of the vapor liquid interface. This increased resistance results in reduced heat transfer. The increased resistance is due to the formation of a noncondensible boundary layer. The noncondensible gas is carried with the vapor towards the liquid vapor interface where it accumulates. Therefore, the partial pressure of gas at the liquid vapor interface increases above that in the bulk of the mixture. This situation is shown in Figure I.3-1. The effect of noncondensibles on the condensation heat transfer is calculated using the method outlined in Reference I.3-6.

The overall heat conduction through the liquid film when equated to the sensible heat transfer in the diffusion layer plus the latent heat liberated at the film interface results in the equation:

$$h_c(T_{GI} - T_W) = h_s(T_{GO} - T_{GI}) + K_g \rho_g h_{fg}(P_{GO} - P_{GI})/P_{am} \qquad (1)$$

where:

$h_c$ = heat transfer coefficient in liquid film, Btu/hr $ft^{2o}F$

$h_s$ = sensible heat transfer coefficient, Btu/hr $ft^{2o}F$

$K_g$ = mass transfer coefficient, ft/hr

$h_{fg}$ = latent heat of vaporization, Btu/lb

$P_{am}$ = log mean partial pressure of noncondensible.

$$P_{am} = \left[\frac{P_{AI} - P_{AO}}{\ln P_{AI}/P_{AO}}\right].$$

Other terms are defined in Figure I.3-1.

For the case where the gas mixture is stagnant, the sensible heat transferred through the diffusion layer need not be considered. Kg, the mass transfer coefficient, is defined in Reference I.3-6 as:

$$K_g = \frac{1.02D}{H}\left[\frac{gH^3\,\bar{\rho}\,(\frac{\rho_o}{\rho_i} - 1)}{\mu D}\right]^{0.373} \qquad (2)$$

where:

D = volumetric diffusivity, $ft^2/hr$

H = tube height, ft

g = acceleration of gravity, $ft/hr^2$

$\bar{\rho}$ = mixture density, $lb/ft^3$

$\rho_o$ = vapor density in bulk mixture, $lb/ft^3$

$\rho_i$ = vapor density at interface, $lb/ft^3$

$\mu$ = mixture viscosity, lb/ft-hr

The film heat transfer coefficient, $h_c$, was evaluated using the Nusselt film condensation model.

$$h_c = 0.943\left[\frac{\rho_l(\rho_l - \rho_v)\, g\, h_{fg}\, k_l^3}{\mu_l\, H(T_{GI} - T_w)}\right]^{0.25} \qquad (3)$$

where:

$\rho_l$ = liquid density, $lb/ft^3$

$\rho_v$ = vapor density, $lb/ft^3$

$k_l$ = liquid thermal conductivity, Btu/hr ft$^{0}$F

$\mu_l$ = liquid viscosity, lb/ft-hr

All liquid properties are evaluated at:

$$T_{ref} = T_w + 0.31\ (T_{GI} - T_w)$$

The solution can be arrived at by iterating on $T_{GI}$, until Equation (1) is satisfied.

Two sets of calculations have been performed to illustrate the effect of noncondensibles on heat transfer from the primary side to the secondary side of the steam generators. These calculations assumed:

For Maine Yankee:

a) A secondary side pressure of 1000 psia.

b) 2011 ft$^3$ (at STP) of noncondensible (hydrogen) are released.

c) The noncondensible was evenly dispersed throughout either the entire primary system or in the four steam generators.

For the Yankee plant at Rowe:

a) A secondary side pressure of 900 psia.

b) 440 ft$^3$ (at STP) of noncondensible (hydrogen) are released.

c) The noncondensible was evenly dispersed throughout either the entire primary system or in the four steam generators.

Figure I.3-2 and I.3-3 give the results of these calculations as a function of primary side pressure for the Maine Yankee and Yankee plants, respectively. The top curve corresponds to the case where the noncondensible was evenly mixed throughout the entire primary system. The bottom curve in each graph corresponds to the case where the noncondensible was uniformly

distributed in the steam generators only. The graph's ordinate represents the heat flux with noncondensibles divided by the heat flux without noncondensibles for the same primary side pressure. As the curves show, for a primary side pressure which is approximately 200 psia greater than the secondary side pressure, the reduction in heat transfer is less than 10% for Maine Yankee and about 13% for the Yankee plant. Due to the large heat transfer area (151403 $ft^2$ for Maine Yankee and 42575 $ft^2$ for Yankee) available for condensation, this type of reduction presents no problem.

If the primary side begins to approach the secondary side pressure and the effect of noncondensible becomes more pronounced, the net effect will only be to stabilize at a slightly higher primary pressure (about 25 psia) than that for the case without noncondensible. The significant margin in overall heat transfer is illustrated in Figures I.3-4 and I.3-5, which gives the heat removal rate from the secondary side for various primary side pressures. For reference, the core decay heat at 500 seconds has been noted on the ordinate. The top curve in Figures I.3-4 and I.3-5 corresponds to the case without any noncondensible present. The middle curve represents the situation where the noncondensibles are mixed evenly throughout the primary system. The bottom curve corresponds to a case where the noncondensible gas is only present in the steam generators. Comparison between the steam generator heat removal rates and the core decay heat rate at 500 seconds illustrates the significant available margin in steam generator heat removal capability even when the maximum amount of noncondensible is assumed to be present at the most detrimental location.

In summary, the following conclusions can be drawn.

Noncondensible Gases in Steam Generators - Stagnant Conditions

1. The effect of the presence of noncondensible gas source on steam generator heat transfer rate is small (10% for MY and 13% for YR), for primary pressures that are 200 psia or higher than the steam generator secondary side pressure. This small heat transfer degradation has no significant impact on the primary side pressure.

2. For primary pressures that approach the secondary side pressure, the steam generator heat transfer degradation due to the presence of noncondensible gas is higher. However, this will only lead to increasing the primary system pressure by about 25 psia for the same decay heat rate.

3. The core heat transfer is not affected for these cases since all the noncondensible gas is assumed to reside in the steam generators.

Noncondensible Gases Evenly Distributed - Stagnant Conditions

1. For these cases, the heat transfer rates in the steam generators and the core are not significantly affected.

References

(I.3-1) Liliane Schor, et al., "Justification of Reactor Coolant Pump Operation During Small Break LOCA Transients for Maine Yankee," YAEC-1423, April 1984.

(I.3-2) Maine Yankee Plant, Reactor Coolant System, System Description No. 4467-010, Revision 0, Combustion Engineering, Inc.

(I.3-3) Perry, Robert H and Chilton, Cecil H., "Chemical Engineers' Handbook," Fifth Edition, McGraw Hill Book Company.

(I.3-4) Yankee Plant at Rowe Technical Specifications.

(I.3-5) J. N. Loomis, et al., "Reactor Coolant Pump Operation During Small Break LOCA Transients at the Yankee Nuclear Power Station," YAEC-1437, July 1984.

(I.3-6) Collier, John G., "Convective Boiling and Condensation," Second Edition, McGraw Hill Book Company.

TABLE I.3-1

Sources of Noncondensibles for the Maine Yankee Plant

| | Source | Volume (STP) | Mass |
|---|---|---|---|
| 1. | Dissolved hydrogen in the primary coolant | 515.0 $ft^3$ | 2.69 lb |
| 2. | Dissolved nitrogen in the accumulator water | 768.0 $ft^3$ | 56.0 lb |
| 3. | Dissolved air in RWST | 866.0 $ft^3$ | 65.09 lb |
| 4. | Hydrogen released from zirconium water reaction | 4127.0 $ft^3$ | 21.57 lb |
| 5. | Free nitrogen used to pressure accumulators | 96780.0 $ft^3$ | 7057.0 lb |
| 6. | Hydrogen released from radiolytic decomposition and injected water | N/A | N/A |
| 7. | Fission and fill gas in reactor fuel | 1236.9 $ft^3$ | He 10.08 lbm<br>Ar 0.30 lbm<br>N 0.31 lbm<br>Kr 5.52 lbm<br>Xe 61.42 lbm |
| 8. | $H_2$ gas in makeup tank | N/A | N/A |
| 9. | Pressurizer steam space gas | 630.0 $ft^3$ | 3.292 lb |

Note:

a) For breaks requiring the return to natural circulation no fuel rod rupture or oxidation is predicted.

b) For breaks requiring the return to natural circulation, the SIT's do not inject water.

TABLE I.3-2

Sources of Noncondensibles for the Yankee Plant at Rowe

| | Source | Volume (STP) | Mass |
|---|---|---|---|
| 1. | Dissolved hydrogen in the primary coolant | 117.3 $ft^3$ | 0.613 lb |
| 2. | Dissolved nitrogen in the accumulator water | 11.38 $ft^3$ | 0.8298 lb |
| 3. | Dissolved air in RWST | 137.89 $ft^3$ | 10.365 lb |
| 4. | Hydrogen released from zirconium water reaction | 813.74 $ft^3$ | 4.2526 lb |
| 5. | Free nitrogen used to pressure accumulators | N/A | N/A |
| 6. | Hydrogen released from radiolytic decomposition and injected water | N/A | N/A |
| 7. | Fission and fill gas in reactor fuel | 103.37 $ft^3$ | He 1.05 lb<br>Ar 0.05 lb<br>N $5.85 \times 10^{-4}$ lb<br>Kr 0.044 lb<br>Xe 0.49 lb<br>H $9.0 \times 10^{-5}$ lb |
| 8. | $H_2$ gas in makeup tank | N/A | N/A |
| 9. | Pressurizer steam space gas | 184.5 $ft^3$ | 0.9642 lb |

Note:

a) For breaks requiring the return to natural circulation no fuel rod rupture or oxidation is predicted.

b) For breaks requiring the return to natural circulation, the SIT's do not inject water.

TABLE I.3-3

Maine Yankee
Primary Temperatures With and Without Noncondensibles
Assumes Noncondensibles Evenly Distributed in Primary System

| Primary Pressure (psia) | T($^{o}$F) w/o Noncondensibles | T($^{o}$F) w/ Noncondensibles | $\Delta$ T($^{o}$F) |
|---|---|---|---|
| 1050.0 | 550.53 | 549.89 | 0.64 |
| 1200.0 | 567.19 | 566.59 | 0.60 |
| 1400.0 | 587.07 | 586.53 | 0.54 |
| 1600.0 | 604.87 | 604.38 | 0.49 |
| 1800.0 | 621.02 | 620.57 | 0.45 |
| 2000.0 | 635.80 | 635.39 | 0.4 |

TABLE I.3-4

Maine Yankee
Primary Temperatures With and Without Noncondensibles
Assumes Noncondensibles Only in Steam Generators

| Primary Pressure (psia) | T(°F) w/o Noncondensibles | T(°F) w/ Noncondensibles | Δ T(°F) |
|---|---|---|---|
| 1050.0 | 550.53 | 547.26 | 3.27 |
| 1200.0 | 567.19 | 564.19 | 3.00 |
| 1400.0 | 587.07 | 584.36 | 2.71 |
| 1600.0 | 604.87 | 602.38 | 2.49 |
| 1800.0 | 621.02 | 618.72 | 2.30 |
| 2000.0 | 635.80 | 633.66 | 2.14 |

TABLE I.3-5

Yankee Rowe
Primary Temperatures With and Without Noncondensibles
Assumes Noncondensibles Evenly Distributed in Primary System

| Primary Pressure (psia) | T(°F) w/o Noncondensibles | T(°F) w/ Noncondensibles | Δ T(°F) |
|---|---|---|---|
| 1000.0 | 544.58 | 544.05 | 0.53 |
| 1050.0 | 550.53 | 550.01 | 0.52 |
| 1200.0 | 567.19 | 566.72 | 0.47 |
| 1400.0 | 587.07 | 586.65 | 0.42 |
| 1600.0 | 604.87 | 604.49 | 0.38 |
| 1800.0 | 621.02 | 620.67 | 0.35 |
| 2000.0 | 635.80 | 635.48 | 0.32 |

TABLE I.3-6

Yankee Rowe
Primary Temperatures With and Without Noncondensibles
Assumes Noncondensibles Only in Steam Generators

| Primary Pressure (psia) | T(°F) w/o Noncondensibles | T(°F) w/ Noncondensibles | $\Delta$ T(°F) |
|---|---|---|---|
| 1000.0 | 544.58 | 541.74 | 2.84 |
| 1050.0 | 550.53 | 547.78 | 2.75 |
| 1200.0 | 567.19 | 564.66 | 2.53 |
| 1400.0 | 587.07 | 584.79 | 2.28 |
| 1600.0 | 604.87 | 602.78 | 2.09 |
| 1800.0 | 621.02 | 619.09 | 1.93 |
| 2000.0 | 635.80 | 634.01 | 1.79 |

THE INFLUENCE OF NONCONDENSIBLES ON
INTERFACIAL RESISTANCE

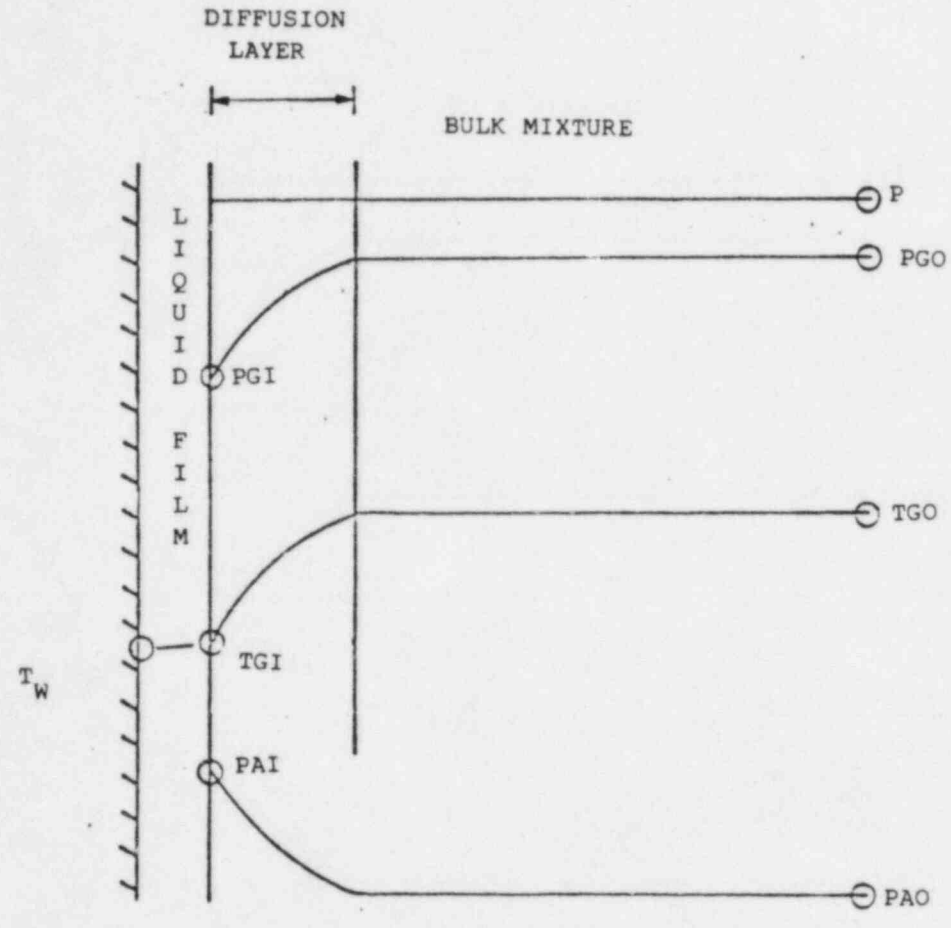


P = TOTAL SYSTEM PRESSURE
PGO = STEAM PARTIAL PRESSURE IN BULK MIXTURE
PGI = STEAM PARTIAL PRESSURE AT INTERFACE
PAO = NONCONDENSIBLES PARTIAL PRESSURE IN BULK MIXTURE
PAI = NONCONDENSIBLES PARTIAL PRESSURE AT INTERFACE
TW = WALL TEMPERATURE
TGO = BULK MIXTURE TEMPERATURE
TGI = INTERFACE TEMPERATURE

Figure I.3-1 The Influence of Noncondensibles on Interfacial Resistance

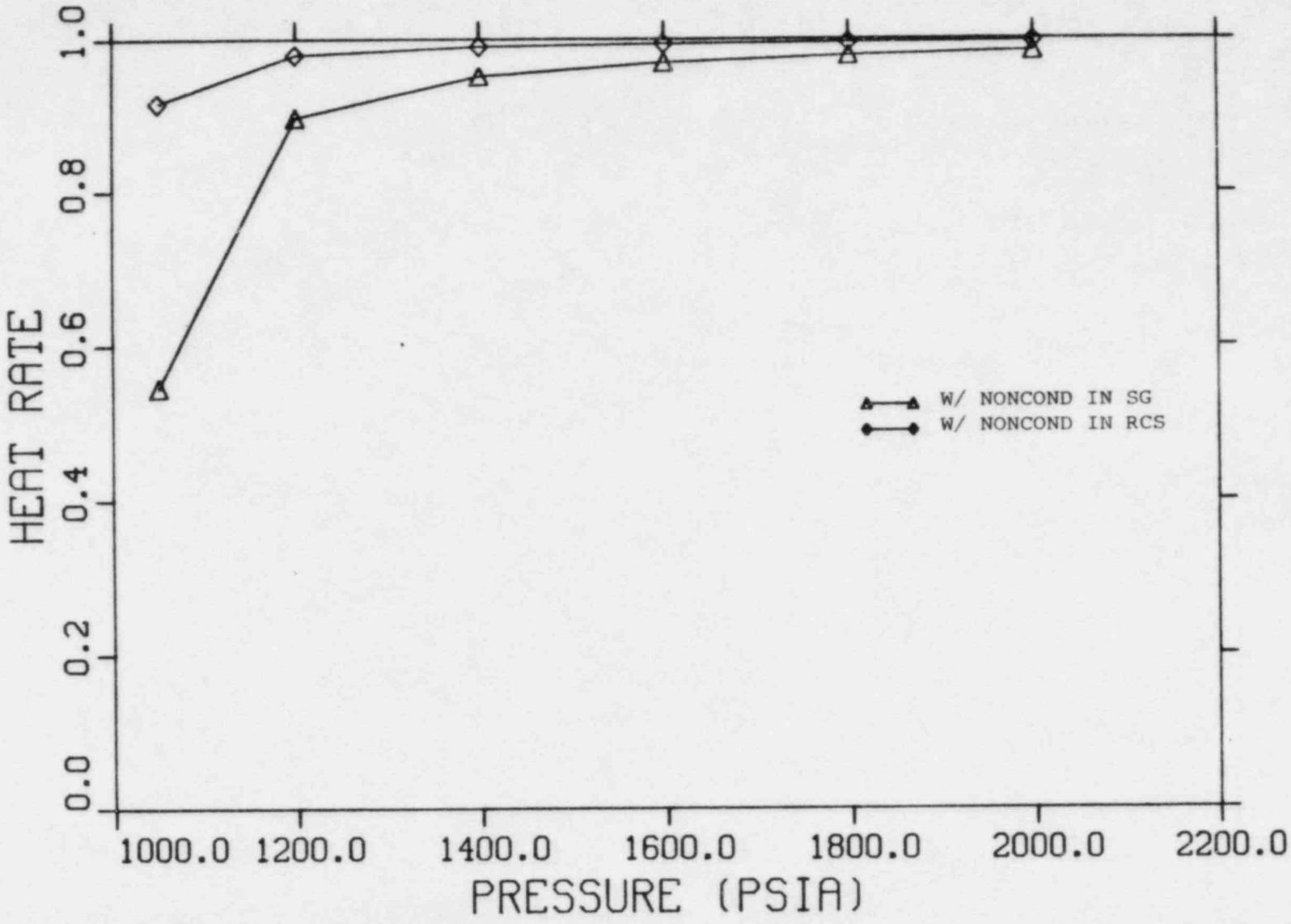


Figure I.3-2 Effect of Noncondensibles on Heat Rate - Maine Yankee

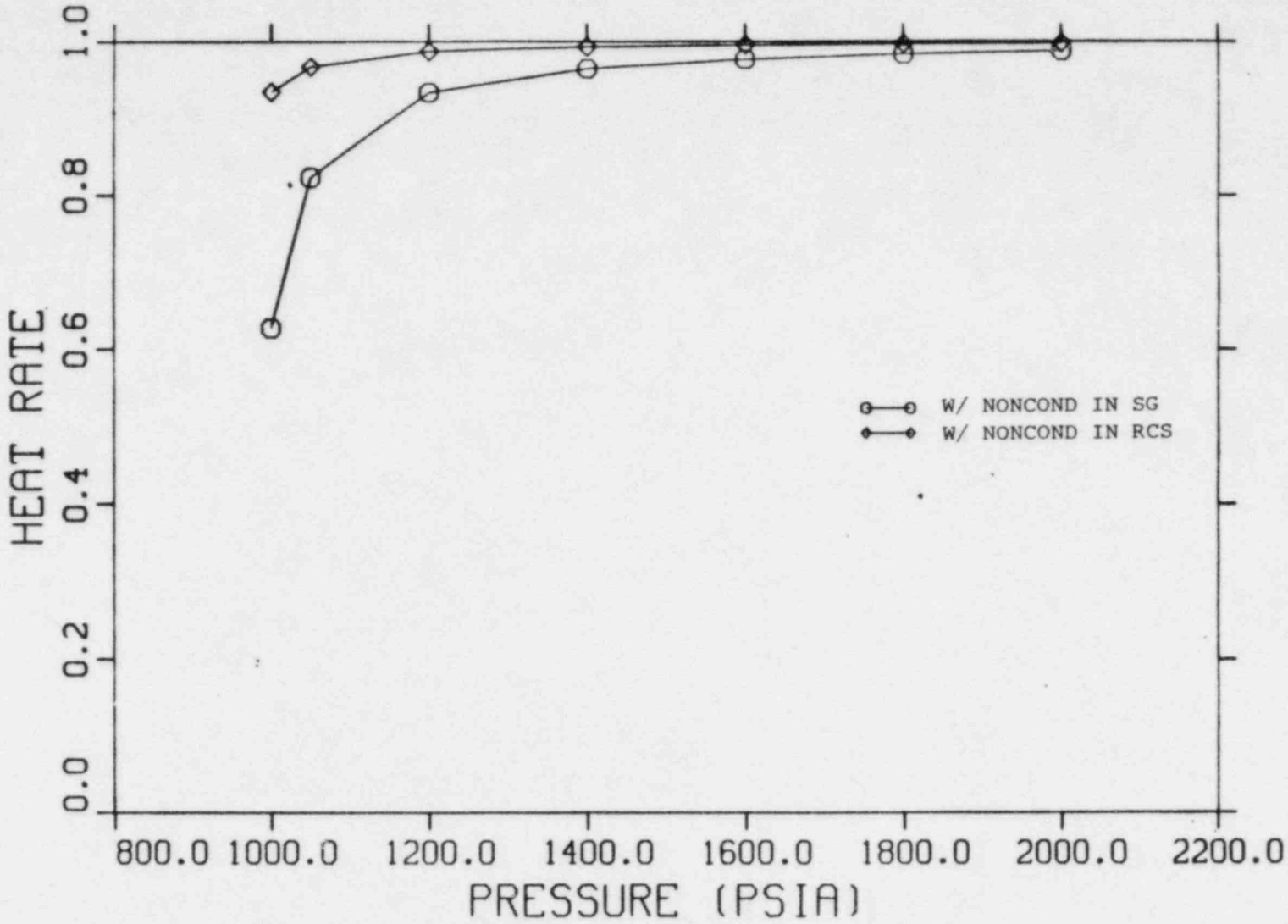


Figure I.3-3 Effect of Noncondensibles On Heat Rate
Yankee Plant at Rowe

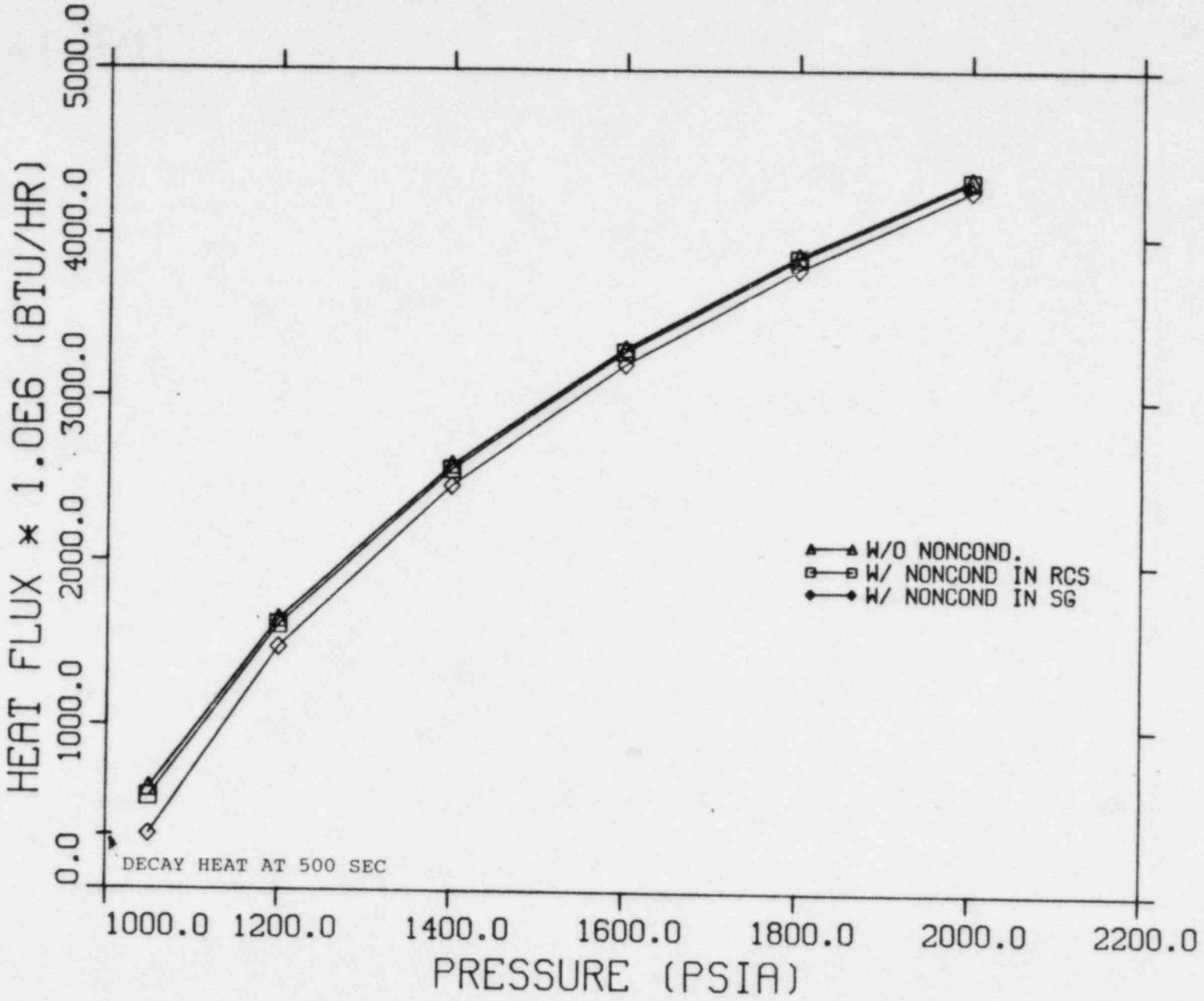


Figure I.3-4 Heat Flux With and Without Noncondensibles - Maine Yankee

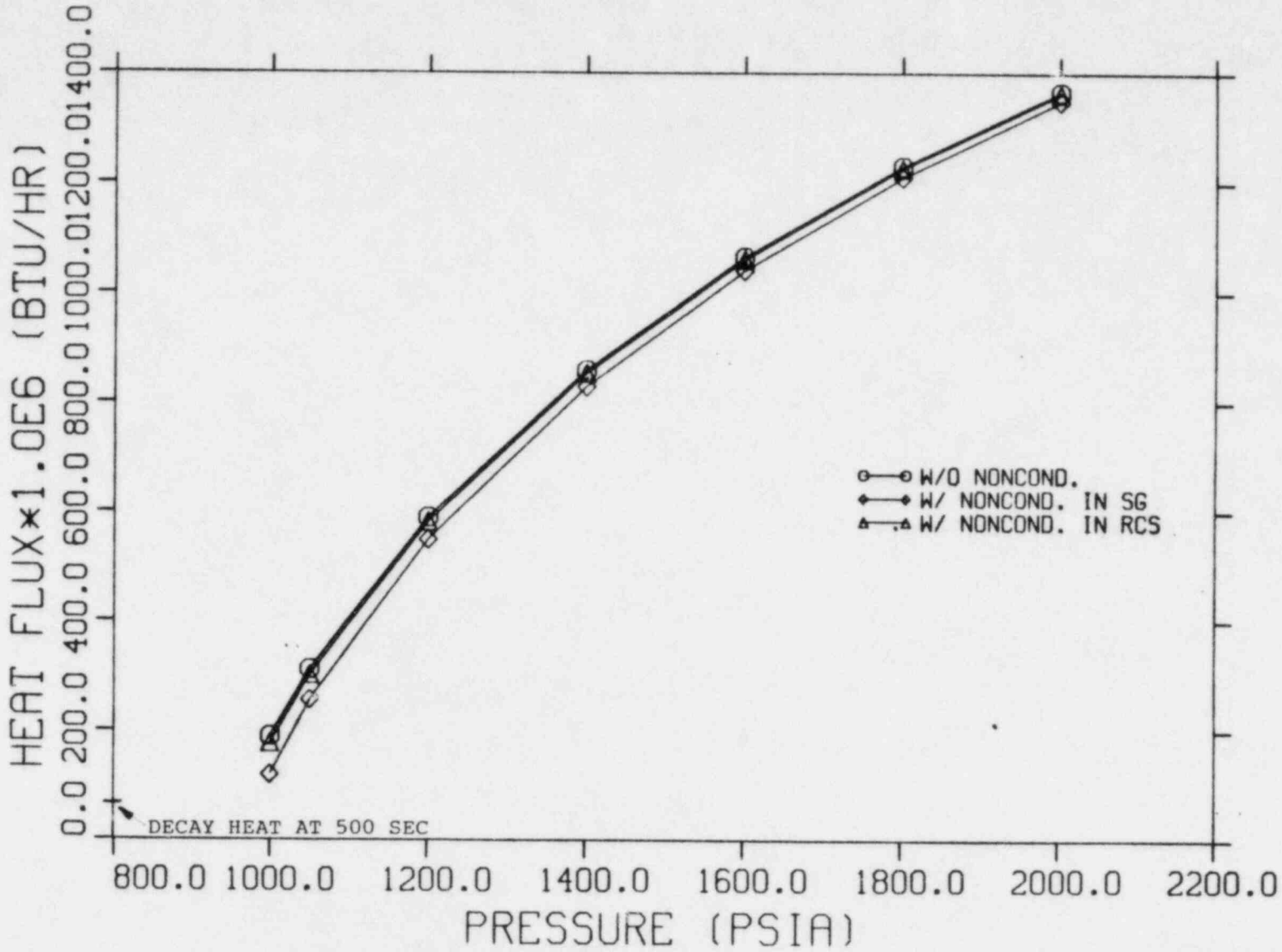


Figure I.3-5 Heat Flux With and Without Noncondensibles
Yankee Plant at Rowe

Q.I.4

Justify why any sources are omitted.

A.I.4

Please see Response A.I.3.

Q.I.5

Clarify how mixtures of more than one noncondensible gas such as nitrogen and hydrogen are modeled, especially if fractions of each are changing in space and time.

A.I.5

Please see Response A.I.3.

Q.I.6

Clarify under what conditions natural circulation flow can be interrupted by the accumulation of noncondensible gas plus steam in the U-bends, and what conditions are necessary to re-establish natural circulation flow.

A.I.6

Please see Response A.III.1.

Q.I.7

Clarify how the pump curves are changed if noncondensibles are present.

A.I.7

Input data that represent the pump homologous curves are not changed for cases where some noncondensible gas might be present for the following reasons:

a. The most prevalent constituents in pump components will generally be water and/or steam. Large concentrations of noncondensible gases are not expected in pump components for LOCA cases that comply with the ECCS criteria in 10CFR50.46. For example, see the answer to Question Q.I.3.

b. Since large concentrations of noncondensible gases are not expected, they are excluded from our LOCA analyses. For example, see the answer to Question Q.I.3.

c. Perhaps the most systematic comparison of steam water versus air-water mixtures on pump two-phase performance is presented in Reference I.7-1. This study indicates that both two-phase mixtures show similar trends of head and torque degradation as a function of void fraction. There is some indication that the air-water data may involve somewhat more head and torque degradation than the steam water data (see Figures 6-2, 6-4, 6-5 and 6-7 from Reference I.7-1 attached). However, the data scatter (particularly in the air-water data) preclude drawing quantitative conclusions with a high degree of confidence.

Therefore, we use pump homologous data derived from steam water tests for all LOCA analyses.

Reference

(I.7-1) Kamath, P. S., Swift, W. L., "Two-Phase Performance of Scale Models of a Primary Coolant Pump," EPRI NP-2578, Electric Power Research Institute, Palo Alto, CA, September 1982.

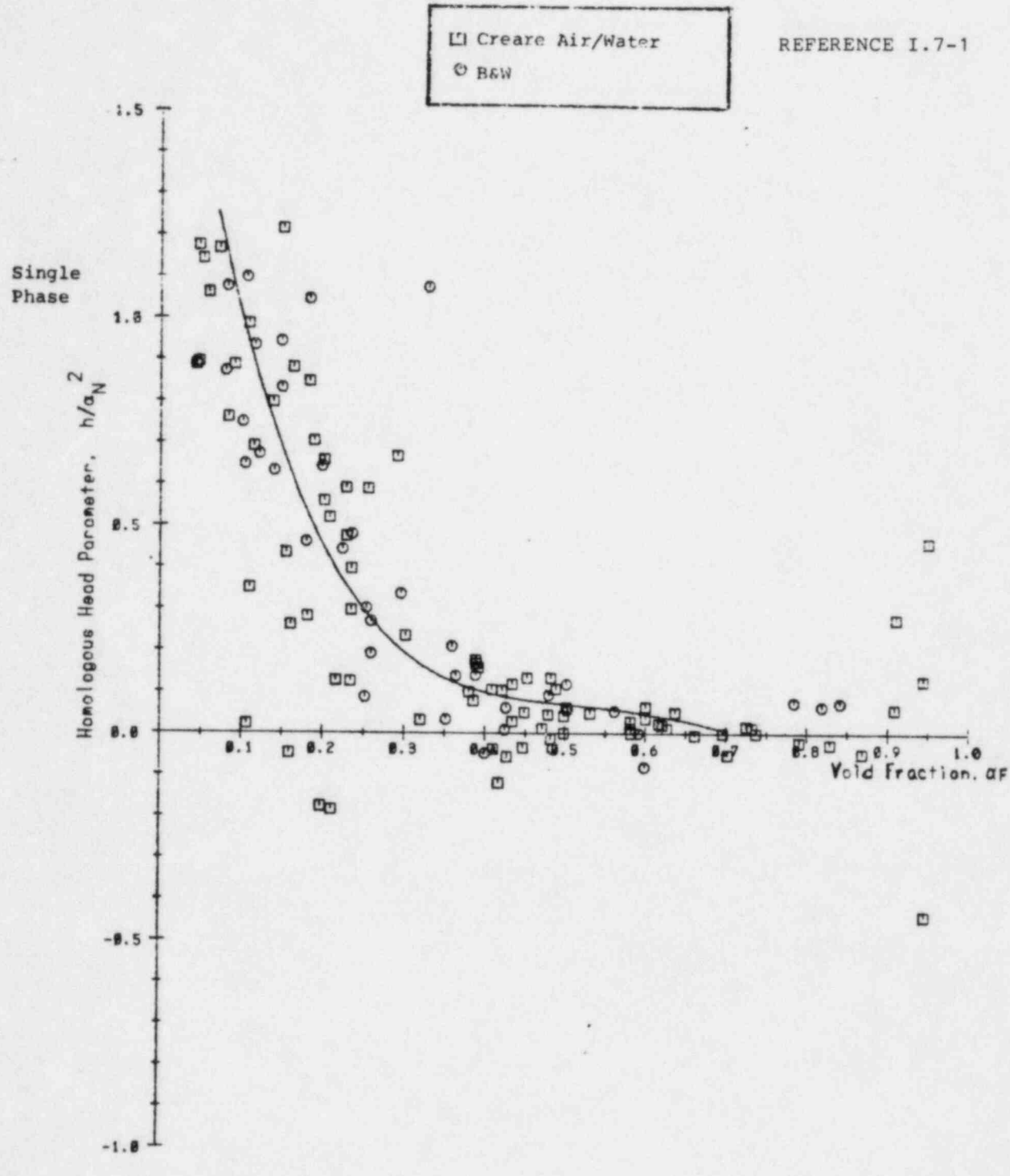


Figure 6-2. Comparison of Creare Air/Water Head Correlation with Creare and B&W Data For $\nu/\alpha_N$ Between 0.80 and 1.20

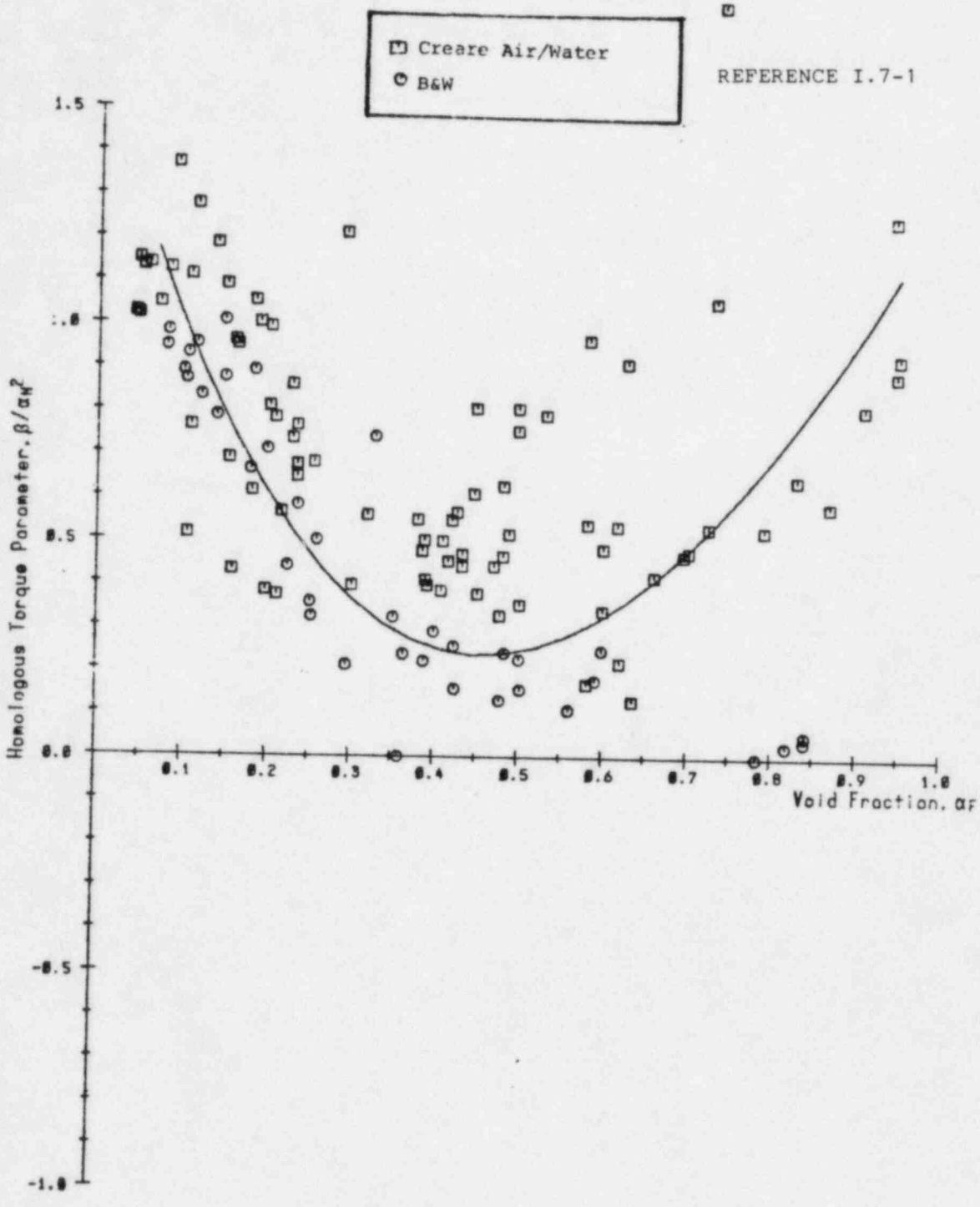


Figure 6-4. Comparison of Creare Air/Water Torque Correlation with Creare Air/Water vs B&W Data For $\nu/\alpha_N$ Between 0.80 and 1.20

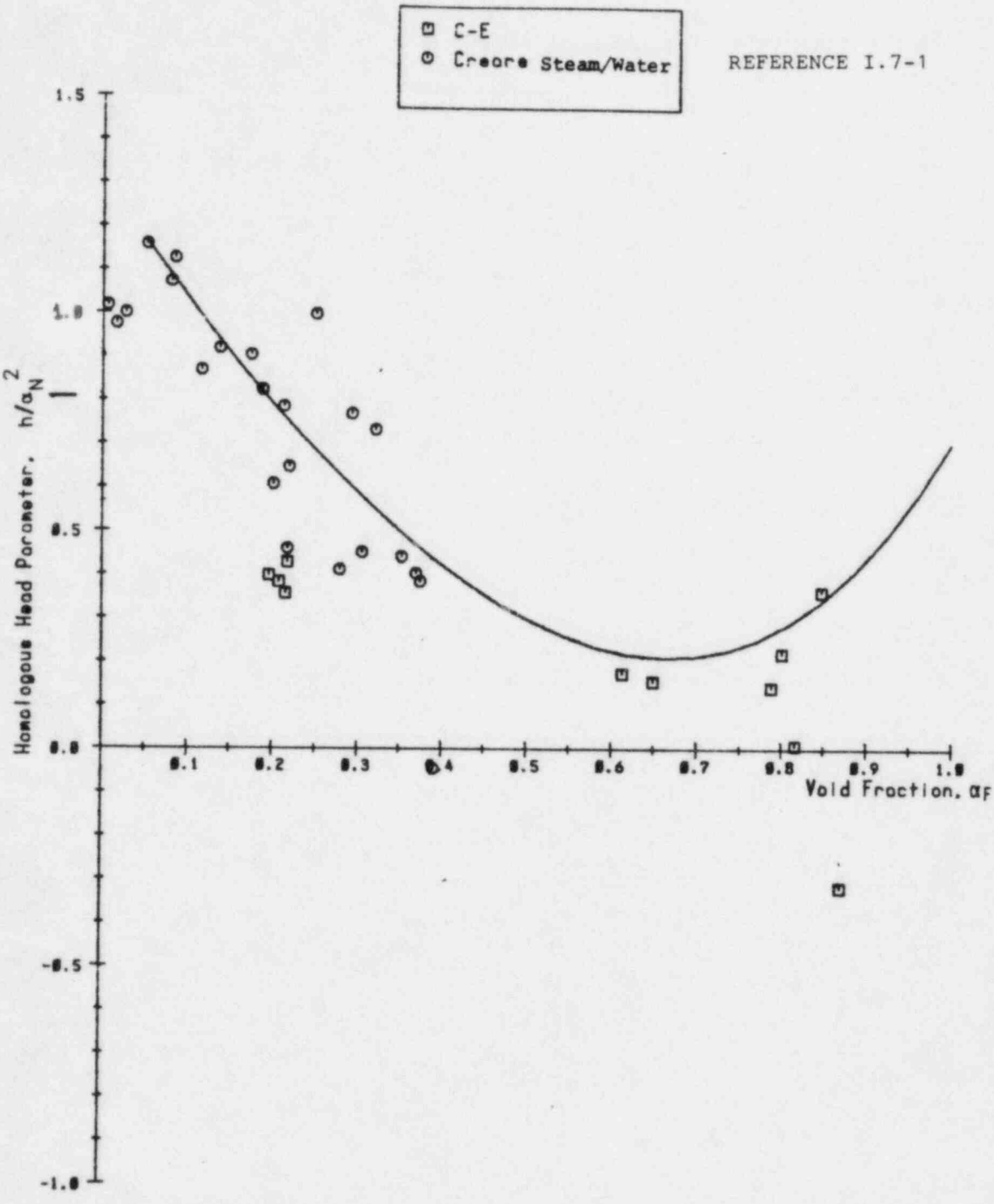


Figure 6-5. Comparison of Creare Steam/Water Head Correlation with Creare and C-E Data For $p_{ups} \leq 500$ psia For $v/\alpha_N$ Between 0.90 and 1.10

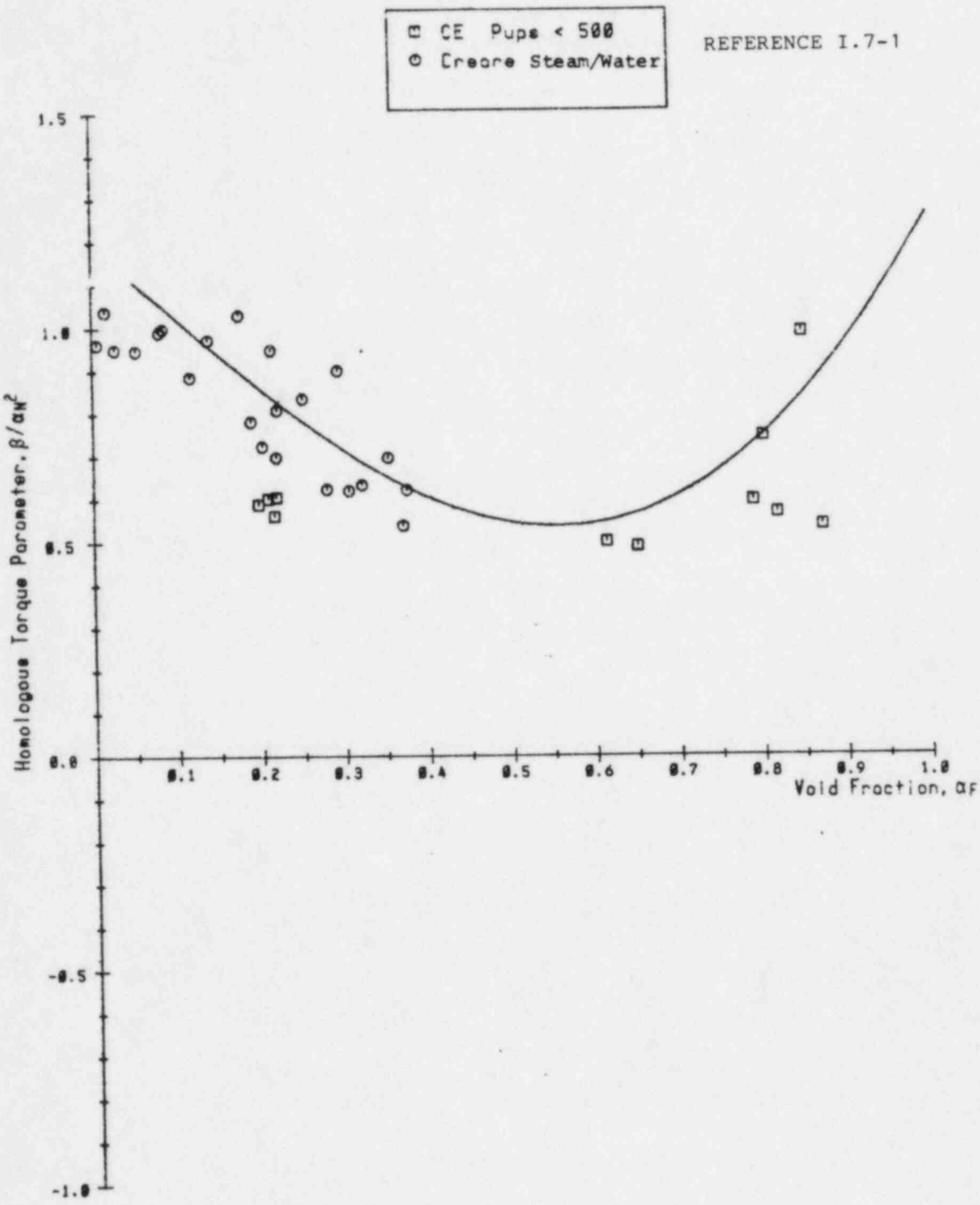


Figure 6-7. Comparison of Creare Steam/Water Torque Correlation with Creare Steam/Water and C-E Data For $\nu/\alpha_N$ Between 0.90 and 1.10 and p < 500 psia

Q.I.8

The condensation model is described as follows on p. 35 of Ref. 10:

"$\Gamma_g = K\ (1-X+X_c)\ (X_e-X)$, where:

$K = 1.0 \times 10^{5}$ ($Kg/m^3$-sec), empirical constant

$X_c = 1.0 \times 10^{-5}$, empirical constant."

"From the code assessment, we have inferred that this model tends to overpredict the condensation rate when subcooled ECC is injected into a steam environment. This causes the system pressure to be low and results in degraded heat transfer in the fuel bundle region as seen in the TLTA and LOFT code assessment cases discussed in Section 5.0 of Volume III. An improved model in this area is desirable for best-estimate analyses. For licensing analyses, the degraded heat transfer effect and the conservative assumptions imposed by Appendix K yield conservative results."

"The presence of a noncondensible gas is taken into account in the vaporization and condensation models described above." Clarify how the presence of a noncondensible gas is taken into account in this equation.

A.I.8

Significant quantities of noncondensible gas are not expected within the primary or secondary coolant systems as discussed in the answers to questions I.3 and I.21. However, the current RELAP5YA condensation model described above does account for the presence of noncondensible gas. For the same total pressure and gas mixture quality, increasing amounts of noncondensible gas will decrease the static quality difference, $X_e-X$, and therefore decrease the condensation rate. This is further explained below.

The static quality of a gas mixture is defined by equation (77) on page 21 of Appendix A in Reference I.8-1 as follows:

$$X = X_n + X_v \tag{1}$$

where:

$X$ = static quality of the gas mixture
$X_n$ = static quality of the noncondensible gas
$X_v$ = static quality of the vapor

Note that for a fixed value of the mixture quality, X, the vapor quality will decrease as the noncondensible quality increases toward X. This causes a corresponding decrease in the vapor partial pressure for a fixed total pressure.

The two-phase, multicomponent mixture specific internal energy is defined by equation (80) in Reference I.8-1 as follows:

$$U = (1-X)U_f + X_n U_n + X_v U_v \tag{2}$$

where:

$U$ = mixture specific internal energy
$U_f$ = liquid specific internal energy
$U_n$ = noncondensible specific internal energy
$U_v$ = vapor specific internal energy

Equation (1) can be used to eliminate $X_v$ in equation (2) to obtain:

$$U = (1-X)U_f + X_n U_n + (X-X_n)U_v \tag{3}$$

The equilibrium quality for the gas mixture, $X_e$, is obtained from equation (3) by setting

$$X = X_e, \qquad U_f = U_{fs}, \qquad U_v = U_{vs}$$

where $U_{fs}$ and $U_{vs}$ are the liquid and vapor specific internal energies at the saturation state corresponding to the vapor partial pressure, $P_v\ (T_e)$. We then obtain:

$$X_e = [U-U_{fs} + (U_{vs}-U_n)X_n]/(U_{vs}-U_{fs}) \tag{4}$$

The static quality difference, $(X_e-X)$, is obtained by subtracting X from equation (4) and then substituting equation (3) in to eliminate U. This yields:

$$(X_e-X) = [(1-X)(U_f-U_{fs}) + (X-X_n)\ (U_v-U_{vs})]/(U_{vs}-U_{fs}) \tag{5}$$

We now examine the limiting condition where the noncondensible quality, $X_n$, approaches the fixed gas mixture quality, X. When $X \geq 0.5$, the least massive phase is the liquid. Therefore the 5 equation model sets the liquid phase to saturation conditions, $U_f = U_{fs}\ (P_v)$. Then equation (5) reduces to:

$$(X_e-X) = (X-X_n)(U_v-U_{vs})/(U_{vs}-U_{fs}) \tag{6}$$

which tends towards zero as $X_n$ tends toward X. When $X < 0.5$, the least massive phase is the gas. Therefore the 5 equation model sets the vapor phase to saturation conditions, $U_v = U_{vs}\ (P_v)$. Then equation (5) reduces to:

$$(X_e-X) = (1-X)(U_f-U_{fs})/(U_{vs}-U_{fs}) \tag{7}$$

From pages 21 and 22 of Appendix A, Reference I.8-1:

$$U_f = U_f\ (P,\ T_f)$$

$$U_{fs} = U_{fs}\ [P_v(T_e)]$$

As the noncondensible quality increases toward X, the vapor pressure decreases and the equilibrium temperature approaches the liquid temperature. In the limit,

$$U_{fs} \simeq U_f$$

and the static quality difference tends to zero. Therefore, the condensation rate approaches zero as the noncondensible quality approaches the gas quality.

References

(I.8-1) R. T. Fernandez, R. K. Sundaram, J. Ghaus, A. Husain, J. N. Loomis, L. Schor, R. C. Harvey and R. Habert, "RELAP5YA - A Computer Program for Light-Water Reactor System Thermal-Hydraulic Analysis, Volume I: Code Description," Yankee Atomic Electric Company Report YAEC-1300P, Volume I (October 1982). (Proprietary)

Q.I.22

Clarify how the effect of any buildup of noncondensible gas in the volume attached to the HPI or accumulator is included in the condensation rate during injection.

A.I.22

See the answer to Question Q.I.8.

Q.I.23

Pages 166-168 of Reference 10 describe the energy transfer to the accumulator nitrogen as the sum of three terms: (1) the heat convected from the wall to the nitrogen, (2) the heat convected from the liquid surface to the nitrogen, and (3) the additional energy transfer caused by condensation in the gaseous phase of the liquid that is vaporized at the interface. In the presence of mass transfer, the driving potential for heat transfer (Lewis number assumed equal to 1) is the enthalpy difference rather than the temperature difference (Reference 14). Clarify why the heat convected from the liquid water is in terms of temperature rather than enthalpy.

A.I.23

The accumulator model presently incorporated into RELAP5YA corresponds to the RELAP5/MOD1 Cycle 18 version described in Appendix A of Reference I.23-1. The present model supersedes the model described in Chapter 3 of Reference I.23-1.

The heat convected from the liquid water is given in terms of an enthalpy difference as indicated in Equation (208) of Appendix A to Reference I.23-1; shown below:

$$Q_{cond} = \dot{M}_{vap} \left[h_g^s(T_w) - h_f^s(T_D)\right]$$

The temperature difference which appears in Equation (206) is one of the terms used to assess the water vapor concentration gradient at the liquid-gas interface. The concentration gradient is used in the context of Fick's law with the objective of assessing the evaporation rate $\dot{M}_{vap}$, as described in Appendix I.23-1.

## APPENDIX I.23-1

## Assessment of the Evaporation Rate at the Liquid-Gas Interface

Equation (206) of Appendix A to Reference I.23-1 can be derived by assuming that the vaporization at the liquid-gas interface in the accumulator can be approximated by a quasi-steady diffusion formulation. Then, applying Fick's law, which is given by Equation (3-12) of Reference I.23-2 in the form:

$$\dot{M}_{vap} = -A_w \cdot \rho \cdot d \cdot \vec{\nabla} m_{vap} \qquad (1)$$

where:

$\dot{M}_{vap}$ = vaporization mass transfer rate, (Kg/s)

$A_w$ = liquid-gas interfacial area, ($m^2$)

$d$ = diffusivity of water vapor in air, ($m^2/s$), equal to that in nitrogen

These quantities are defined consistently with the nomenclature of Appendix A to Reference I.23-1. Furthermore, $\rho$ is the mixture (Nitrogen and vapor) density at the interface (which is assumed to be equal to the saturated water vapor density, $\rho_g$, at the liquid surface). Finally, $m_{vap}$ is the concentration of vapor at the liquid-gas interface (kg of vapor per kg of mixture), i.e.:

$$m_{vap} = \frac{\rho_{vap} \cdot V_{vap}}{V \cdot \rho} \qquad (2)$$

Assuming that the mixture density is approximately equal to the vapor density, applying the perfect gas assumption to the volume ratio in Equation (2) and substituting the result into Equation (1) gives:

$$\dot{M}_{vap} = -A_w \cdot \rho_g \cdot d \cdot \left[\frac{d}{dx}(P_{vap}/P_D)\right] \qquad (3)$$

where $P_{vap}$ is the vapor partial pressure at the interface and $P_D$ is the mixture or dome pressure, which is not dependent on x.

The perfect gas law can be once again used to estimate:

$$\frac{d}{dx} P_{vap} \approx \frac{P_D}{T_D} \frac{d}{dx} T \qquad (4)$$

Substituting Equation (4) into Equation (3) and integrating over a diffusion length, $L_D$, leads to Equation (203) of Appendix A to Reference I.23-1 in the form:

$$\dot{M}_{vap} = -\rho_g \bullet A_w \bullet h_3 \bullet \beta_e \bullet (T_w - T_D) \qquad (5)$$

where $\beta_e = T_D^{-1}$ represents the equilibrium compressibility for a perfect gas and $h_3 = d/L_D$ in (m/s) is a mass transfer coefficient.

The mass transfer coefficient can be written in terms of the heat transfer coefficient by applying Reynolds' analogy as in (Equation 11-31) of Reference I.23-3, which is easily rewritten in the form of Equation (204) of Appendix A to Reference I.23-1 after minor algebraic transformations.

References


(I.23-1) R. T. Fernandez, R. K. Sundaram, J. Ghaus, A. Husain, J. N. Loomis, L. Schor, R. C. Harvey and R. Habert, "RELAP5YA - A Computer Program for Light-Water Reactor System Thermal-Hydraulic Analysis, Volume I: Code Description," Yankee Atomic Electric Company Report YAEC-1300P, Volume I (October 1982). (Proprietary)

(I.23-2) W. M. Kays, "Convective Heat and Mass Transfer," McGraw-Hill, 1966.

(I.23-3) J. P. Holman, "Heat Transfer," McGraw-Hill, Fourth Edition, 1976, Chapter 11.

Q.I.24

Clarify how the energy transfer from evaporation of water at the liquid surface is included. Assuming the heat- and mass-transfer analogy, the mass flow of vapor leaving the liquid surface is equal to $g_m(w_v - w_{v_i})/(w_{v_i} - 1)$ (Reference 14), where $g_m$ is the mass transfer coefficient and $w_v$ is the mass fraction of water at i the interface or at $\infty$ in the main nitrogen volume.

A.I.24

The primary objective of the accumulator component model is to calculate the injection rates into the cold leg. An important parameter in the calculation of these flow rates is the accumulator gas dome pressure history. The gas dome pressure is somewhat sensitive to the condensation rate of steam in the gas space. Therefore, the energy transfer to the gas space from the evaporation of water at the liquid surface is estimated by assuming that all the evaporated water (Equation (203) of Appendix A to Reference I.23-1 which is derived in Appendix I.23-1) recondenses (Equation (207)) and that the heat of condensation (Equation (208)) is added to the gas space. The impact on the injection rates due to variations of the energy (temperature) of the liquid slug (caused by heat removal from the liquid slug due to evaporation) is negligible. Therefore, the evaporation energy, which is supplied by the liquid slug is neglected and the liquid is assumed to remain at constant temperature.

In summary, the condensation energy is accounted for in the gas space. In the liquid slug, the evaporation energy is neglected because it has no effect on the injection rates.

Q.I.25

Justify Equation (3.4-32) of Reference 10. Please supply a copy of Reference 3.4-1 of Reference 10.

A.I.25

This equation corresponds to Equation (206) of Appendix A to Reference I.23-1 in the current accumulator model. The equation is justified in Appendix I.23-1. Requested reference is supplied as Appendix I.25-1.

# APPENDIX I.25-1

## A MECHANISTIC ACCUMULATOR MODEL FOR LIGHT WATER REACTOR TRANSIENT ANALYSIS*

K. E. Carlson, D. L. Siegel, V. H. Ransom and J. A. Trapp
EG&G Idaho, Inc.
Idaho National Engineering Laboratory
Idaho Falls, Idaho

ABSTRACT

A lumped parameter accumulator model has been developed and installed into the computer program RELAP5. The model includes heat transfer from the wall of the tank, from the water surface to the dome, vaporization from the water surface to the dome, and condensation of vapor in the dome. The last feature also includes heat addition to the nitrogen dome due to the condensing process. Results from data comparisons are presented

NOMENCLATURE

| | |
|---|---|
| | Cross-sectional flow area |
| C | Multiplier for heat transfer correlation |
| $C_v$ | Specific heat at constant volume |
| D | Diameter |
| d | Diffusivity |
| f | Coefficient of friction |
| g | Gravitational constant |
| Gr | Grashof number |
| h | Enthalpy |
| $h_1$, $h_2$ | Heat transfer coefficients |
| $h_3$ | Mass transfer coefficient |
| k | Thermal conductivity |
| L | Length |
| M | Mass |
| $\dot{m}$ | Mass transfer rate |
| P | Pressure |
| Pr | Prandit number |
| Q | Total heat transfer |
| R | Nitrogen gas constant |
| T | Temperature |
| t | Time |
| U | Internal energy |
| V | Volume |
| v | Velocity |
| z | Elevation |

Greek

| | |
|---|---|
| $\alpha$ | Thermal diffusivity |
| $\beta$ | Coefficient of isobaric thermal expansion |
| $\Delta$ | Change of |
| $\rho$ | Density |
| $\nu$ | Kinematic viscosity |

Subscripts

| | |
|---|---|
| c | Condense |
| f | Liquid |
| g | Vapor |
| K | Upstream volume index (Accumulator) |
| L | Downstream volume index (System) |
| l | Surge line |
| n | Nitrogen |
| S | Saturated |
| t | Tank |
| v | Vaporization |

INTRODUCTION

This paper describes an accumulator model that has been developed for installation into a systems analysis computer code (RELAP5[a]), for analysis of light water reactor (LWR) behavior. This model features mechanistic relationships for heat transfer from the tank wall and water surface, condensation in the vapor dome, and vaporization from the water

a. The RELAP5 computer code and its documentation, RELAP5/MOD1, Code Description Vol. I and II by V. H. Ransom et al., are available from the National Energy Software Center, Bldg. 208-Room C-230, 9700 South Cass Avenue, Argonne, Illinois.

*Work supported by the U. S. Nuclear Regulatory Commission, Office of Nuclear Regulatory Research under DOE Contract No. DE-AC07-76IDO1570.

surface to the dome. The accumulator model consists of a hydrodynamic model and a heat transfer model. The latter includes the vaporization and condensation effects.

The hydrodynamic model is described along with the heat transfer models for the accumulator. Performance of the model is verified by data comparisons between the model results and the LOFT L3-1 test and also a Westinghouse Electric Corporation Upper Head Injection (UHI) accumulator performance test.

## HYDRODYNAMIC MODEL

The accumulator is modeled as a lumped-parameter component. This model was chosen over a distributed model because the spatial gradients in the accumulator are expected to be small.

The accumulator model and associated notations are shown in Figure 1. The basic modeling assumptions are:

1. Heat transfer from the accumulator walls. Heat and mass transfer from the liquid are modeled using natural convection correlations assuming similarity between heat and mass transfer from the liquid surface.

2. The nitrogen is modeled as an ideal gas with constant specific heat. The steam in the dome exists at a very low partial pressure and is not modeled directly. The energy released as a result of vapor condensation is transferred to the nitrogen.

3. Because of the high heat capacity and large mass of water below the interface, the water is assumed to remain at its initial temperature.

4. The model for liquid flow includes inertia, wall friction, form loss, and gravity effects.

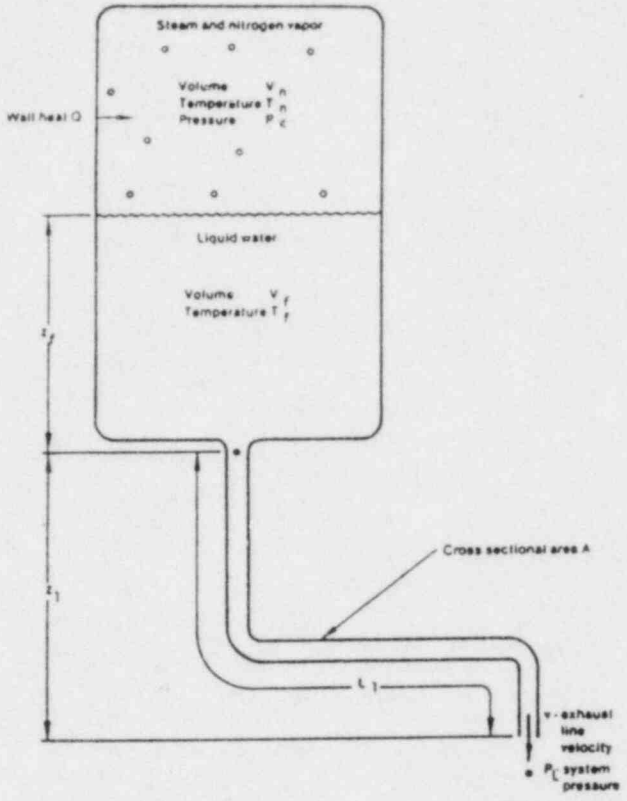


Figure 1. Typical accumulator.

Using these assumptions, the basic equations governing thermal-hydraulics of the tank and discharge line can be written as

1. Conservation of mass (nitrogen)

$$M_n = \text{constant} = \rho_n V_n \tag{1}$$

2. Conservation of energy

Nitrogen

$$M_n \frac{dU_n}{dt} = - P_K \frac{dV_n}{dt} + Q \tag{2}$$

Wall

$$M_t C_{v_t} \frac{dT_t}{dt} = - Q_t \tag{3}$$

3. Momentum equation

$$\rho_f A_1 \left(L_1 \frac{\partial v_f}{\partial t} + \frac{1}{2} v_f^2\right) + \frac{1}{2} \rho_f \frac{f L_f}{D_1} A_1 v_f^2$$

$$= -(P_L - P_K)A_l + \rho_f g (z_f + z_l)A_l \qquad (4)$$

where f is the coefficient of friction.

4. State Relationships

$$P_K V_n = M_n R_n T_n \qquad (5)$$

$$U_n = C_{v_n} T_n. \qquad (6)$$

Using Equations (1) and (6), the nitrogen energy equation (Equation (2)), can be rewritten as

$$M_n C_{v_n} \frac{dT_n}{dt} = -P_K v_f A_l + Q. \qquad (7)$$

Differentiating Equation (5), and solving for the pressure derivative yields

$$\frac{dP_K}{dt} = \frac{P_K}{T_n}\frac{dT_n}{dt} - \frac{P_K}{V_n}\frac{dV_n}{dt} \qquad (8)$$

Equations (4), (7), and (8) comprise the system of three differential equations used in the accumulator model. They are used numerically to advance $T_n$, $V_n$, and $P_K$ in time.

HEAT TRANSFER

The heat transfer to the nitrogen in the dome has been modeled as being due to two distant processes. The first mode is convective heat transfer due to the temperature difference between the nitrogen and the accumulator walls and liquid. The second mode of heat transfer is postulated to be due to condensing water vapor in the accumulator dome. The steam in the dome is assumed to be saturated at the gas temperature. Steam is assumed to be convected from the liquid surface due to the motion of the nitrogen. A mass and energy balance for the steam is then used to calculate the heat transfer to the nitrogen due to convection of vapor from the liquid surface and subsequent condensation in the accumulator dome.

The heat transfer from the tank wall has been modeled with a lumped-parameter model

$$Q_t = A_K n_1 (T_t - T_n). \qquad (9)$$

The wall convective film coefficient has been defined using a correlation for turbulent natural convection[1] for vertical plates as

$$h_1 = 0.1 \left(\frac{k_n}{L}\right) (GrPr)^{1/3} \qquad (10)$$

where L is the sum of the lengths of the tank wall above the liquid surface and the radius of the tank top. The Grashof number is given by

$$Gr = g\beta (T_w - T_n) \frac{L^3}{\nu^2} \qquad (11)$$

where L is as above plus the radius of the liquid surface.

In addition to wall heat transfer, convective heat transfer[1] from the accumulator liquid is assumed to be

$$Q_f = A_K h_2 (T_f - T_n) \qquad (12)$$

where

$$h_2 = 1.11 \left(\frac{k_n}{D}\right) (GrPr)^{1/3}.$$

The variable D is the diameter of the water surface and the Grashof number is the same as above.

Liquid is also assumed to evaporate from the water surface due to the density difference between the vapor at the water surface and in the nitrogen above. The evaporation rate is assumed to be

$$\dot{m}_v = h_3 A_K (\rho_{g_l} - \rho_g)$$

$$= h_3 A_K \rho_{g_l} \beta_g (T_f - T_n) \qquad (13)$$

where

$\rho_{g_l}$ = a function of the liquid temperature.

The mass transfer film coefficient, $h_3$, is

determined assuming similarity between heat and mass transfer from the water surface (both are conserved properties modeled by similar equations), and is given by

$$h_3 = h_2 \left(\frac{d}{k_n}\right)\left(\frac{\alpha}{d}\right)^{1/3} \tag{14}$$

where d is the diffusivity of water vapor in air[2] defined as

$$d = 0.239 \frac{P_o}{P_K} \left(\frac{T}{281}\right)^{2.3} \tag{15}$$

where $P_o$ is atmospheric pressure and 0.239 is a dimensional constant that gives "d" the units of $\{m^2/s\}$.

The mass transfer rate is then

$$\dot{m}_v = h_2 \left(\frac{d}{k_n}\right)\left(\frac{\alpha}{d}\right)^{1/3} A_k \rho_g \beta_g (T_f - T_n). \tag{16}$$

The steam in the accumulator dome will condense as the temperature decreases and the additional heat of vaporization will be transferred to the nitrogen in the dome. The condensation rate is calculated assuming that steam is saturated at the temperature of the dome

$$\dot{m}_c = \dot{m}_v + \frac{d}{dt}(V_n \rho_g). \tag{17}$$

The heat transfer due to this condensation is

$$Q_c = \left[h_{g_s}(T_n) - h_{f_s}(T_n)\right] \frac{d}{dt}(V_g \rho_g)$$

$$+ \dot{m}_v \left[h_{g_s}(T_f) - h_{f_s}(T_n)\right]. \tag{18}$$

The total heat transfer to the nitrogen is then calculated as

$$Q = Q_t + Q_f + Q_c + \dot{m}_v \frac{d U_{g_s}}{dt}. \tag{19}$$

## CALCULATED RESULTS

The accumulator model described previously has been tested in RELAP5 and gives good agreement with experimental data from LOFT Test L3-1, and a Westinghouse UHI accumulator performance test (WCAP-8479[3]). The comparison to the experimental data in both tests is of the form of pressure versus nitrogen volume. This type of comparison makes the effects of heat transfer in the accumulator more apparent than either pressure or temperature versus time comparisons, and also obscures most of the effects of uncertainties of the boundary conditions. The LOFT data used for comparison are liquid level and pressure history; the Westinghouse data used for comparison are integrated mass flow and pressure history.

The LOFT accumulator was simulated using the following measured data.[4] Nitrogen volume is 1.39 $m^3$, water volume was 1.97 $m^3$ (0.45 $m^3$ was surge line and 1.52 $m^3$, in tank), system pressure was 4.37 MPa, and the water and nitrogen temperature was 304.7 K. A form loss of 24.8[5] was included at the surge line exit to model wall form loss as well as wall friction and form loss in the surge line. Time step size was 1 second.

The pressure drop between the accumulator and the system was approximately 0.15 MPa, providing a slow transient for the accumulator model checkout.

Figure 2 shows a pressure versus vapor volume comparison plot between the LOFT measured data and calculated results. Note that the plot includes a calculated isothermal curve (uppermost curve) and a calculated isentropic curve (lowermost curve). In the early part of the blowdown (high pressure and low vapor volume) the expansion of the nitrogen gas is essentially adiabatic. As the gas expands into the accumulator dome, its temperature decreases, causing a temperature difference between the gas and its surroundings. The surroundings then loose heat to the gas, causing the gas pressure to decrease less rapidly. The calculated and experimental pressure versus nitrogen volume curves are seen to be in good agreement, indicating that the heat transfer was accurately predicted. Approximately sixty percent of the heat transfer was calculated to be due to condensation.

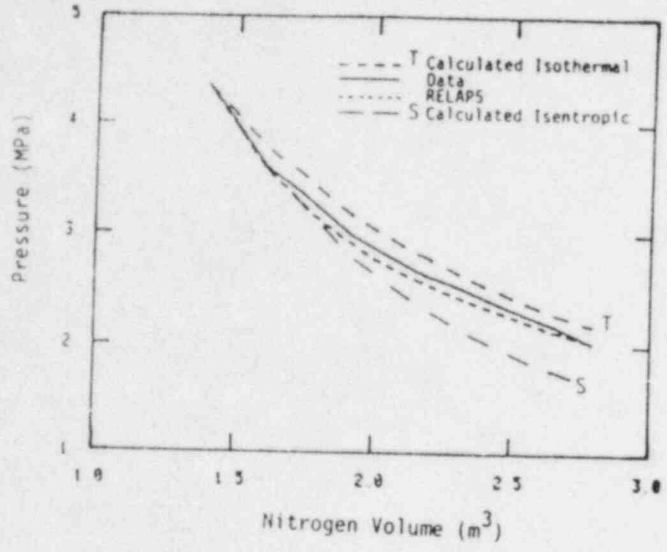


Figure 2. LOFT L3-1 Accumulat

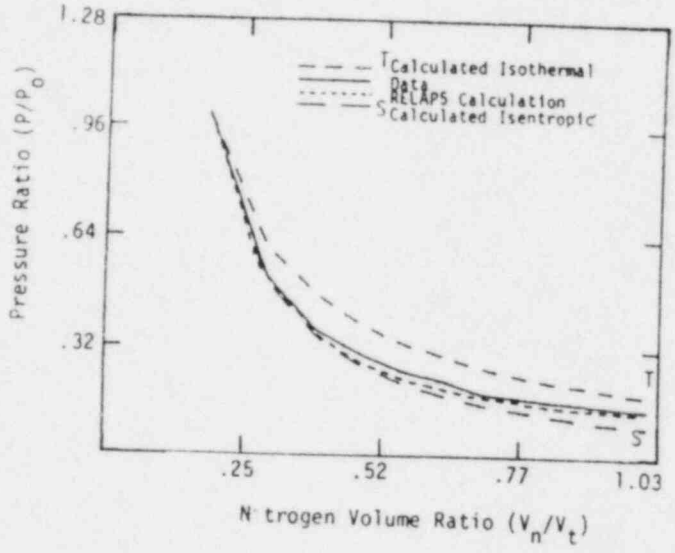


Figure 3. Westinghouse UHI Accumulator.

The Westinghouse UHI accumulator was the secon experiment simulated. This accumulator was tested (in place) by allowing it to discharge into the atmosphere (pressure vessel with cover off). Due to the large pressure drop this performance test resembles a large break type of experiment providing a fast accumulator transient for verifying the accumulator model. This accumulator was simulated by using the measured data and performance information contained in WCAP-8479[3] as input. The uncertainties for the data were not given in this propriatary report

The form of the comparisons between the experimental data and calculated results are of the form of pressure ratios versus volume ratios in order to preserve the integrity of the proprietary data. Figure 3 shows the results of the comparisons between the calculated results and the experimental data. The calculated isothermal (uppermost curve) and isentropic (lowermost curve) curves are included for reference. The experimental data shows a similar behavior seen in the LOFT test, that is, the gas expansion is initially an isentropic process. Then as the temperature difference between the nitrogen and its surroundings increases, the gas pressure decreases less rapidly. The calculated results are again in good agreement with the experimental results.

## SUMMARY

The results of these comparisons to data indicate that heat transfer, especially from the condensing vapor in the dome, is important for accurate representation of accumulator simulations. The RELAP5 accumulator model gives good results for both slow and fast transients, isentropic or polytropic. This technique gives the user a mechanistic accumulator model to use in the nulation of light water reactors.

## REFERENCES

1. J. P. Holman, Heat Transfer, 4th edition, New York: McGraw-Hill Book Company, Inc., 1976, pp. 280, 244-245.

2. R. J. Hanks, 1958 Water Vapor Transfer in Dry Soil, Soil Science Society Procedings, 1958, 22:372-374.

3. WCAP-8479, Westinghouse Electric Corporation Nuclear Energy Systems, P. O. Box 355, Pittsburgh, PA 15230.

4. P. D. Bayless, J. B. Marlow, R. H. Averill, Experimental Data Report for LOFT Nuclear Small Break Experiment, NUREG/CR-1145, EG&G-2007, January 1980, pp. 28, 127, 140.

5. H. J. Welland, LOFT Experiment Operating Specification Small Break Test Series L3, November 1979, ME L3 Series EOS, Rev A, pp. 15.

Q.I.26

Clarify how the analogy between heat and mass transfer was used.

A.I.26

The analogy between heat and mass transfer was used as described in Appendix I.23-1. The expression for the relation between the mass transfer coefficient and the heat transfer coefficient (Equation (204) of Appendix A to Reference I.23-1) is simply an algebraic manipulation of Equation (11-31) of Reference I.23-2.

Q.I.27

Clarify how much effect the evaporation and condensation in the accumulator will have on the calculated pressures and injection rates for SBLOCAs.

A.I.27

The effect of evaporation and condensation in the accumulator on the calculated pressures and injection rates are expected to be negligible. For example, the Maine Yankee test described in Section 2.4.1 of Reference I.23-1 was calculated twice: once with $Q_{cond}$ given by Equation (208) of Appendix A to Reference I.1 and again with $Q_{cond} = 0$. The calculated accumulator pressures and flow rates are essentially identical as indicated in Table I.27-1 and Figures I.27-1 and I.27-2.

| | WITH EVAP/COND. | | WITHOUT EVAP/COND. | |
|---|---|---|---|---|
| TIME (SEC) | FLOW RATE (KG/SEC) | PRESSURE (PA) | FLOW RATE (KG/SEC) | PRESSURE (PA) |
| 0. | 0. | 1.28200E+06 | 0. | 1.28200E+06 |
| 2.5000 | 0. | 1.28200E+06 | 0. | 1.28200E+06 |
| 5.0000 | 0. | 1.28200E+06 | 0. | 1.28200E+06 |
| 7.5000 | 106.41 | 1.27538E+06 | 106.40 | 1.27536E+06 |
| 10.000 | 101.51 | 1.26796E+06 | 101.50 | 1.26783E+06 |
| 12.500 | 333.27 | 1.25255E+06 | 333.21 | 1.25217E+06 |
| 15.000 | 547.24 | 1.22264E+06 | 546.97 | 1.22157E+06 |
| 17.500 | 744.43 | 1.18154E+06 | 743.55 | 1.17898E+06 |
| 20.000 | 920.94 | 1.13295E+06 | 918.63 | 1.12778E+06 |
| 22.500 | 1075.5 | 1.08047E+06 | 1070.5 | 1.07135E+06 |
| 25.000 | 1206.3 | 1.02711E+06 | 1196.9 | 1.01272E+06 |
| 27.500 | 1310.1 | 9.75263E+05 | 1294.2 | 9.56385E+05 |
| 30.000 | 1384.6 | 9.26660E+05 | 1360.4 | 9.08324E+05 |
| 32.500 | 1422.6 | 8.82360E+05 | 1388.5 | 8.45898E+05 |
| 35.000 | 1383.4 | 8.44043E+05 | 1340.0 | 7.99057E+05 |
| 37.500 | 1347.3 | 8.11502E+05 | 1293.9 | 7.57976E+05 |
| 40.000 | 1315.0 | 7.83389E+05 | 1251.4 | 7.21653E+05 |
| 42.500 | 1285.7 | 7.58693E+05 | 1212.2 | 6.89303E+05 |
| 45.000 | 1258.7 | 7.36662E+05 | 1175.6 | 6.60306E+05 |

Table I.27-1 Comparison of Calculated Maine Yankee Accumulator Pressures and Flow Rates With and Without EVAP/COND. Heat Transfer Terms

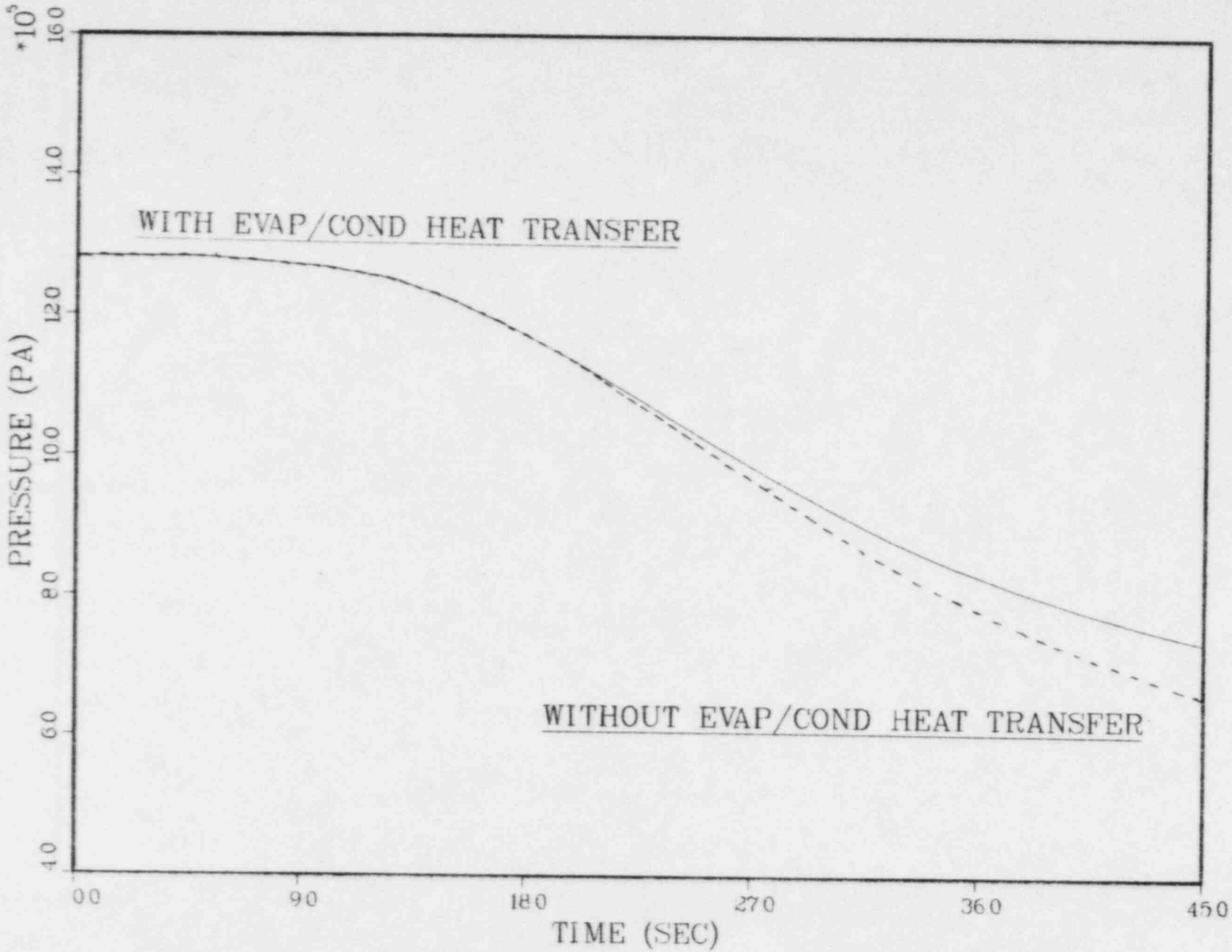


Figure I.27-1 Comparison of Calculated Accumulator Pressures With and Without Evap/Cond. for Maine Yankee Test

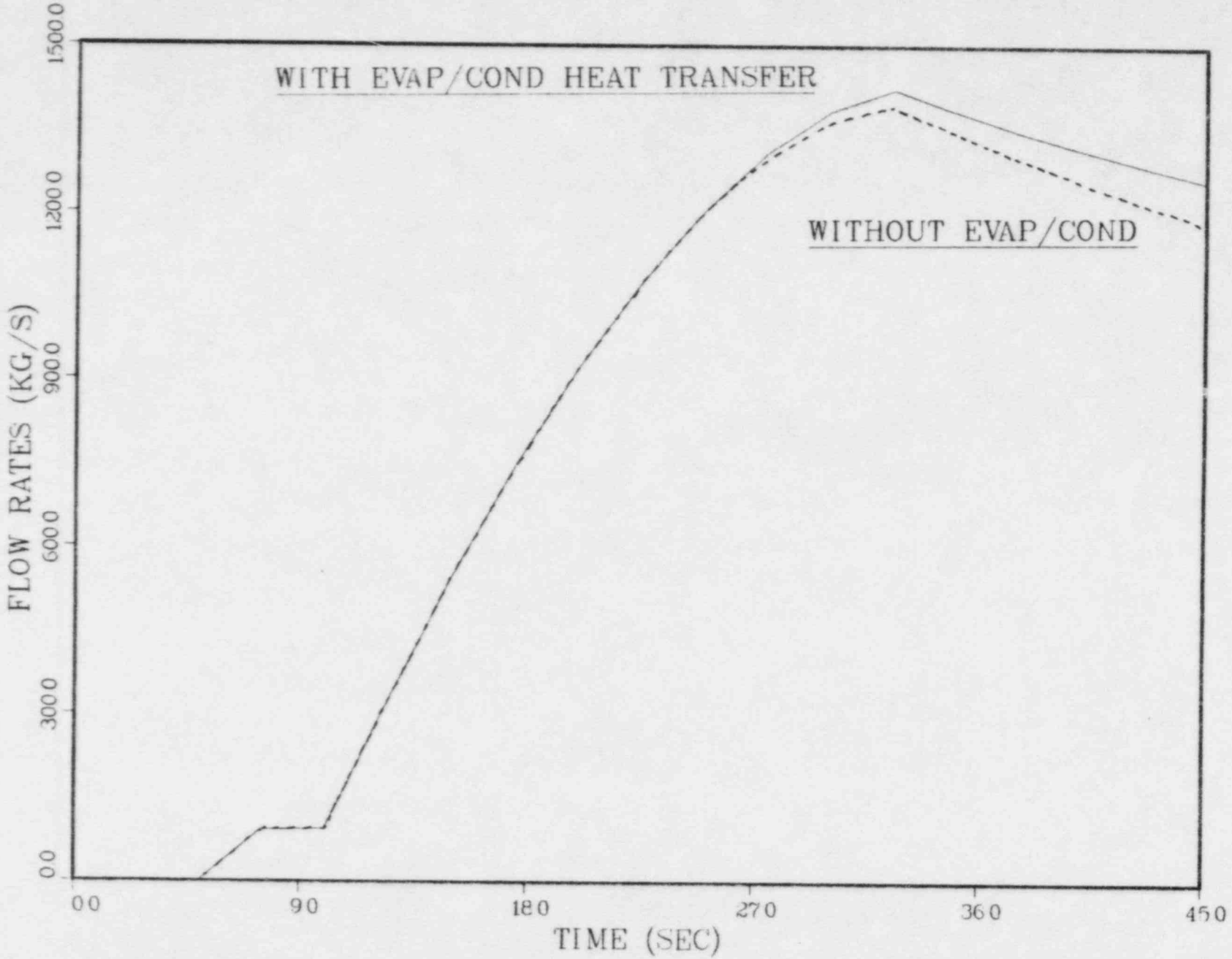


Figure I.27-2 Comparison of Calculated Accumulator Flow Rates With and Without Evap/Cond. for Maine Yankee Test

Q.I.28

The following questions are concerned with the calculation of the Maine Yankee accumulator test presented in Section 2.4.1 of Reference 12. page 87 of Reference 12 says that the "valve took approximately 23 seconds to reach the fully open position." Table 2.4-1 of Reference 12 shows a fixed friction factor and form loss coefficient. Clarify how the valve opening process was modeled, especially because almost half of the 48s transient involved the valve opening time. Figures 2.4-1 and 2.4-2 of Reference 12 do not indicate which curve is the data and which is the RELAP5YA result.

A.I.28

The friction factor and form loss factor given in Table 2.4-1 apply to the surge line and its connection to the accumulator tank. The valve opening process is modeled utilizing the motor valve (MTRVLV) component as described in Section 7.10 of Reference I.23-1. A trip logic is combined with an appropriate valve opening speed resulting in valve throat ratios as shown in Figure I.28-1. This valve area history is believed to simulate the actual valve opening process. The variable form loss coefficient for the valve opening is calculated by the abrupt area change model associated with this component.

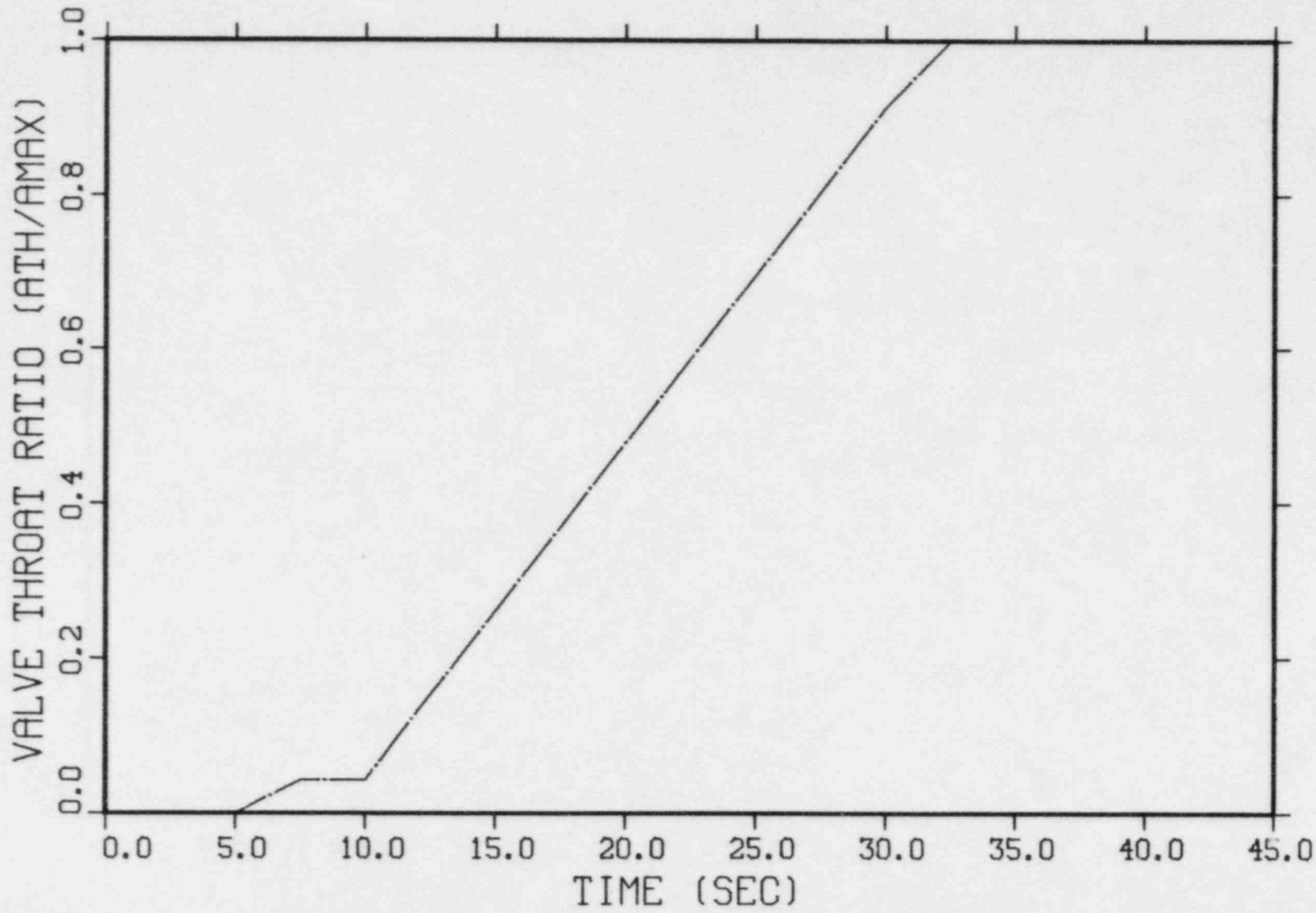


Figure I.28-1 Valve Area History During The Maine Yankee Test

Q.I.29

Clarify which curve is which and why the difference in pressures is increasing after 32 s even though the liquid levels are virtually identical.

A.I.29

As described in A.I.23, the accumulator model described in Chapter 3 of Reference I.23-1 has been replaced by the RELAP5/MOD1 Cycle 18 model. The Maine Yankee accumulator test has been recalculated with the revised model. Figures I.29-1 and I.29-2 compare calculated and measured accumulator pressure and liquid level, respectively. The accumulator pressure and liquid level are well predicted.

Q.I.30

Clarify if any temperature measurements were made in the liquid and nitrogen regions that would indicate the temperature difference that existed during the transient.

A.I.30

No records of temperature measurements in either region have been found.

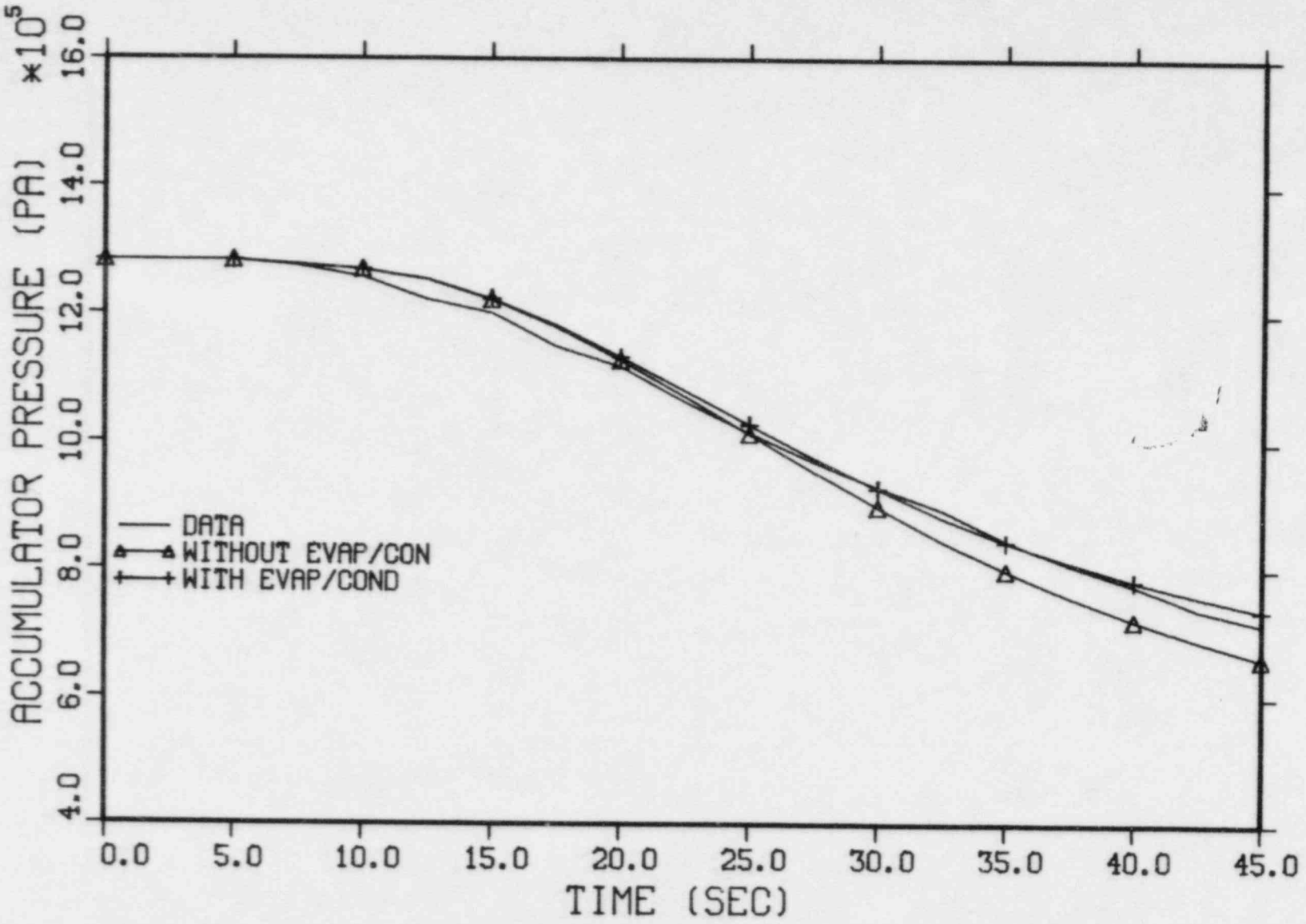


Figure I.29-1 Comparison of Calculated (with and without Evap/Cond.) and Measured Accumulator Pressures for Maine Yankee Test

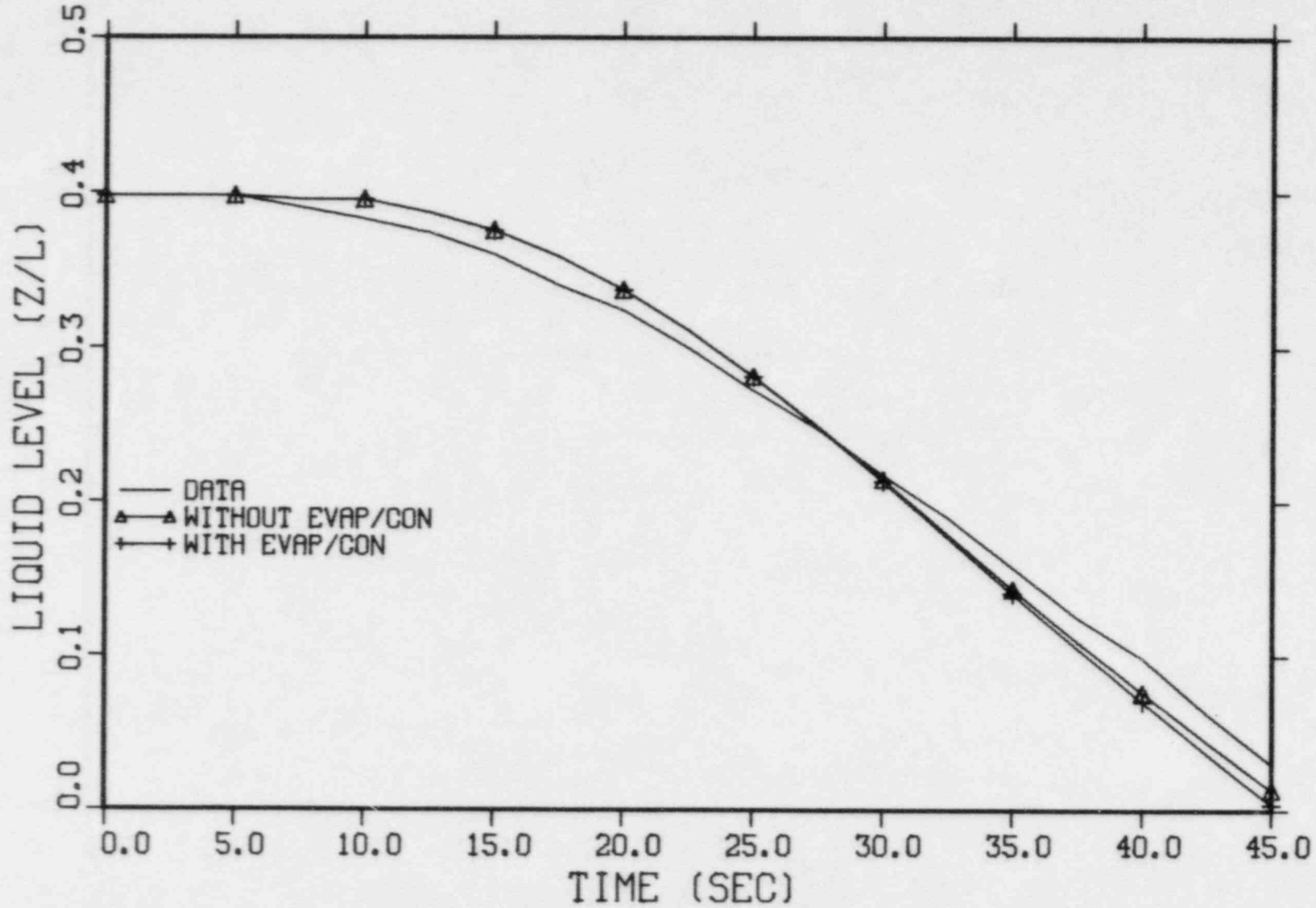


Figure I.29-2 Comparison of Calculated (with and without Evap/Cond.) and Measured Accumulator Liquid Levels for Maine Yankee Test

## III. HOT-LEG OR U-BEND PHASE SEPARATION

### Q.III.1, Q.III.2, Q.III.3 and Q.III.4

The procedures used to interrupt and re-establish natural circulation are not clear. (Q.III.1) Clarify how natural circulation will stop and be restarted as vapor and/or noncondensible gas builds up in the top of the steam generator U-bends. (Q.III.2) Clarify what noding detail is needed to model this process accurately. (Q.III.3) Clarify how the models have been assessed against data. (Q.III.4) Justify that the models for the interruption and re-establishment of natural circulation are mechanistically realistic.

### A.III.1, A.III.2, A.III.3 and A.III.4

Natural circulation is the preferred heat rejection mode for small breaks in which the break flow does not remove the decay heat. From References III.1-1 and III.1-2, the maximum break size for which natural circulation is important is a 3" break for Maine Yankee and a 1" break for the Yankee plant. Break sizes larger than these would not be affected by the loss of natural circulation since sufficient energy would be removed through the break.

From Reference III.1-3, there are two mechanisms which could result in an interruption of natural circulation. One is the collection of noncondensible gas in the top of the steam generator U-bend. The other is an imbalance in the secondary steam generator inventories or heat removal capabilities.

The imbalanced secondary condition does not preclude adequate heat removal since the unaffected steam generators adequately remove decay heat and provide natural circulation flow paths.

The collection of noncondensible gas in the U-bends does not appear to be applicable since the Semiscale tests (Reference III.1-3) showed adequate heat removal and no flow stalling with up to 13% of the primary volume filled with noncondensible gas. This is due to the fact

that the noncondensible gas disperses and does not collect in the U-bends to stall the flow. Only when the noncondensible gas was injected into the steam generator at a rapid rate did the flow stalling occur.

For Maine Yankee and the Yankee plant, small break LOCA conditions for which natural circulation is desired, the amount of noncondensible gas calculated to exist is about 0.5% of the primary system volume. Therefore, interruption of natural circulation is not expected for small break LOCAs for which natural circulation is required for decay heat removal.

Since the interruption and re-establishment of natural circulation is not expected for small break LOCAs, Questions III.2 to III.4 are not applicable.

References

(III.1-1) L. Schor, et al., "Justification of Reactor Coolant Pump Operation During Small Break LOCA Transients Maine Yankee," YAEC-1423, April 1984.

(III.1-2) J. N. Loomis, et al., "Reactor Coolant Pump Operation During Small Break LOCA Transients at the Yankee Nuclear Power Station," YAEC-1437, July 1984.

(III.1-3) D. J. Shimeck and G. W. Johnsen, "Natural Circulation Cooling in a Pressurized Water Reactor Geometry Under Accident-Induced Conditions," Nuclear Science and Engineering 88, 311-320 (1984).

Q.III.5

Clarify how the heat transfer at low flows in the top of the U-bends is modeled for two-phase flow and also if noncondensible gases are present.

A.III.5

No special treatment is given to the heat transfer in the top of the U-bends. The standard RELAP5YA heat transfer models described in Sections 2.1.3.6 and Section 2.1.3.4, Appendix A of Reference III.5-1 are used. The effect of noncondensible gases is not considered and has no significant impact on the heat transfer coefficient.

References

(III.5-1) R. T. Fernandez, et al., "RELAP5YA - A Computer Program for Light-Water Reactor System Thermal-Hydraulic Analysis, Volume I: Code Description," YAEC-1300P, October 1982. (Proprietary)

## IV. STEAM GENERATOR HEAT TRANSFER

Q.IV.1

Page iii of Reference 15 (which modeled FLECHT SEASET Test 23402 where the secondary was hotter than the primary) states that: implementation of the code's time step control algorithm occasionally allowed the primary side temperature to become hotter than the secondary fluid temperature, leading to unphysical oscillations which could be eliminated by the user reducing the time step used." Clarify how this oscillation problem will be avoided in SBLOCA calculations.

A.IV.1

In the analysis performed so far with RELAP5YA, i.e., Pump Trip Study for the Maine Yankee plant (Reference IV.1-1) and the Yankee plant at Rowe (Reference IV.1-2), and the simulation of the LOFT L3-6 experiment (Reference IV.1-3), no such oscillations were encountered. However, if such oscillations are encountered, the time step will be reduced.

References

(IV.1-1) L. Schor, et al., "Justification of Reactor Coolant Pump Operation During Small Break LOCA Transients, Maine Yankee," YAEC-1423, April 1984.

(IV.1-2) J. N. Loomis, et al., "Reactor Coolant Pump Operation During Small Break LOCA Transients at the Yankee Nuclear Power Station," YAEC-1437, July 1984.

(IV.1-3) Fernandez, R. T., R. K. Sundaram, J. Ghaus, A. Husain, J. N. Loomis, L. Schor, R. C. Harvey and R. Habert, "RELAP5YA - A Computer Program for Light-Water Reactor System Thermal-Hydraulic Analysis, Volume III: Code Assessment," Yankee Atomic Electric Company Report YAEC-1300P, Volume III (October 1982). (Proprietary)

Q.IV.2

Clarify what steam generator noding will be used for SBLOCA calculations.

A.IV.2

Figures IV.2-1 and IV.2-2 represent the nodalization used in the Pump Trip Studies for the Maine Yankee plant and Yankee plant at Rowe, respectively. Similar noding schemes will be employed for the small break calculations.

As described below, a detailed nodalization of the steam generator secondary was used for both the plants to ensure realistic heat transfer behavior across the steam generator tubes.

MAINE YANKEE

All the U-tubes in the steam generators are lumped into a single flow path. The primary side of the steam generator is modeled with 10 volumes and the secondary side consists of 14 volumes.

All area changes, baffle plates and dome structures (i.e., separators, dryers) are accounted for in the nodalization through the loss coefficients and geometries that are entered as input. Besides the U-tubes, heat slabs representing the external walls are included in the model.

YANKEE PLANT AT ROWE

For the Yankee plant, a similar nodalization is used for the steam generator as for the Maine Yankee plant. The primary side is modeled with 8 volumes (6 in the tubes) and the secondary side consists of 11 volumes.

All the flow path changes are accounted for in the calculations of the geometry and loss coefficients which are entered as input.

The walls of the steam generator U-tubes and vessel are modeled as heat structures.

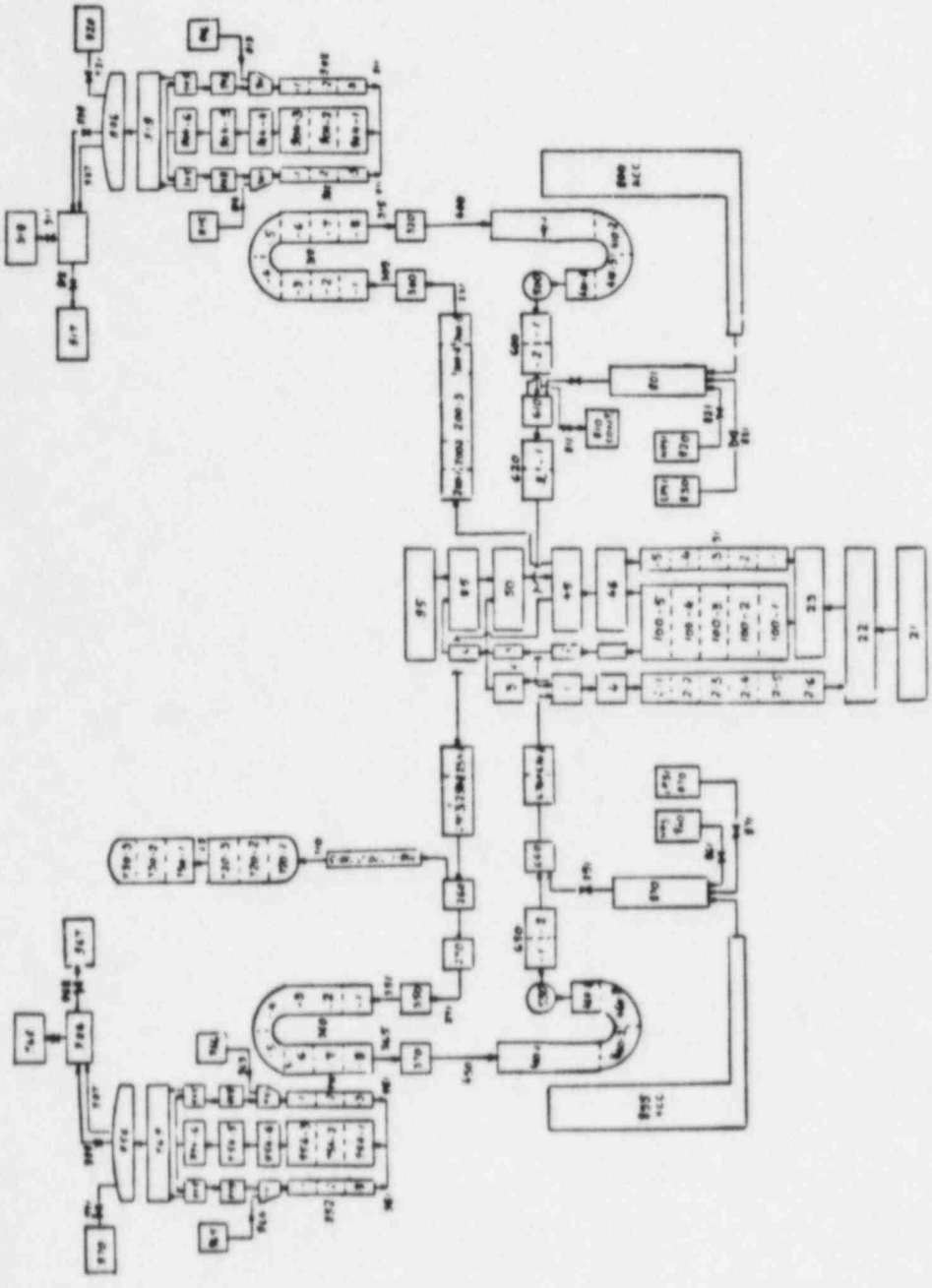

Figure IV.2-1 Proposed Maine Yankee Nodalization
SBLOCA EM Calculations

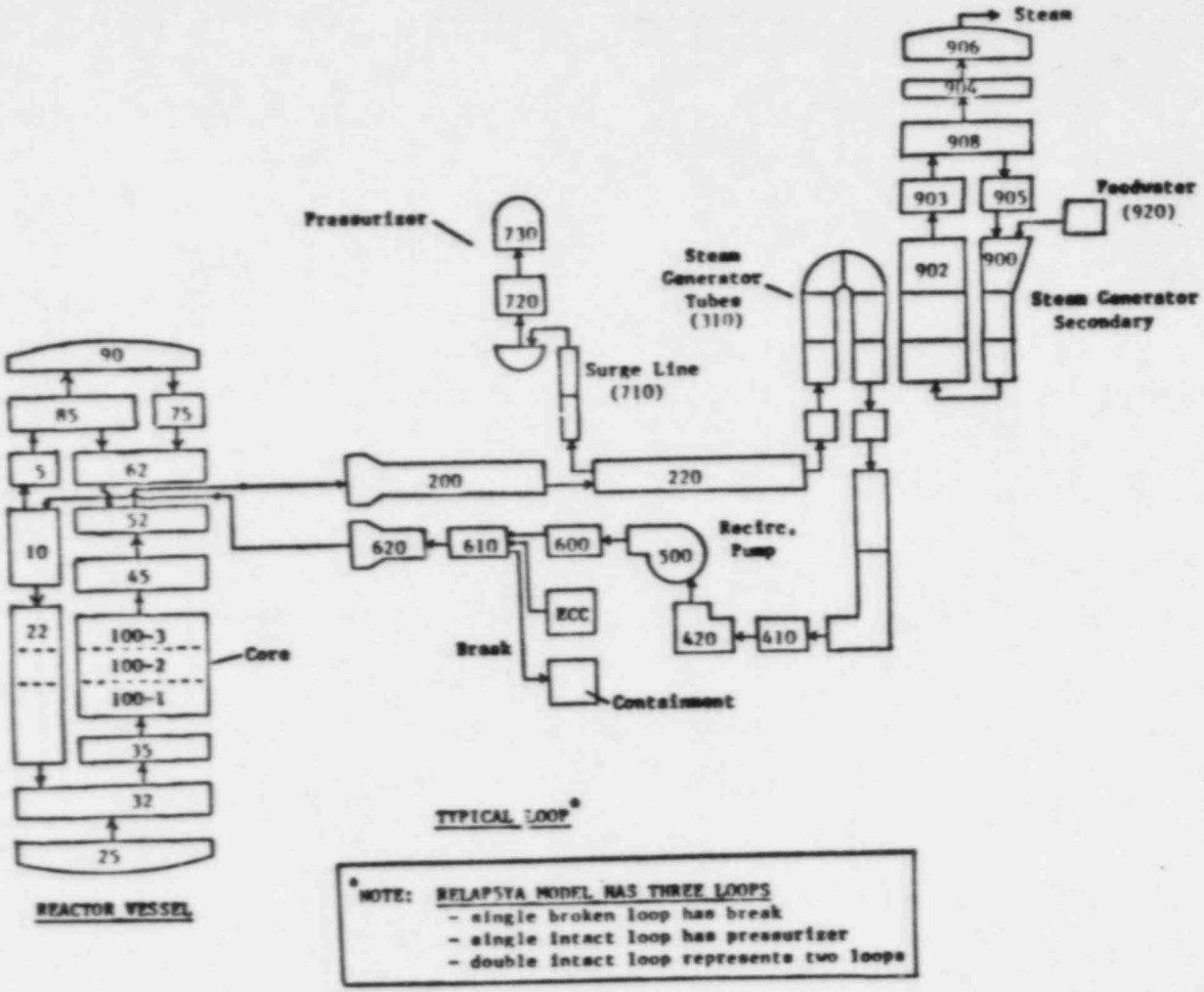


Figure IV.2-2 Proposed Yankee Plant Nodalization
SBLOCA EM Calculations

Q.IV.3

Clarify what noding is needed to model steam generators for low flow and reflux cooling conditions in SBLOCA.

A.IV.3

Figures IV.2-1 and IV.2-2 provide representative noding schemes which will be used for all the phases of a SBLOCA accident, including low flow and reflux cooling conditions.

## V. SYSTEMS VERIFICATION AND OTHER EXPERIMENTAL VERIFICATION

### Q.V.12

Clarify how single-phase and two-phase reverse flow through the pumps is modeled for locked or unlocked rotors.

### A.V.12

Single-phase and two-phase reverse flow through pumps with locked or unlocked rotors would generally be modeled using the Centrifugal Pump Model. This model is described in detail in Section 2.2.6 of Volume I, Section 2.3.1 of Appendix A, Section 3.2.9 of Appendix B and Section 7.11 of Volume II contained in Reference V.12-1. Appropriate input data would be used as discussed in the answers to Questions V.13 and V.15. For the unlocked rotor case with loss of electrical power, the pump angular momentum equation would be solved to determine the time-dependent pump speed. For the locked rotor case, either the pump speed can be entered as zero in a Pump Velocity Table or the Pump Stop Data Card can be used. Note that the Yankee plant has check valves in each cold leg that prevents significant reverse flow from occurring.

### Reference

(V.12) R. T. Fernandez, R. K. Sundaram, J. Ghaus, A. Husain, J. N. Loomis, L. Schor, R. C. Harvey and R. Habert, "RELAP5YA - A Computer Program for Light-Water Reactor System Thermal-Hydraulic Analysis," Yankee Atomic Electric Company Report YAEC-1300P (October 1982). (Proprietary)

Q.V.13

Clarify how prototypical the data used is for full-scale pumps.

A.V.13

Table V.13 summarizes the single- and two-phase steady-state data sources used to assemble the pump performance curves for the Maine Yankee, Yankee and Vermont Yankee reactor coolant pumps.

Single-phase homologous data have been selected to model full scale pump behavior in the following order of availability and preference:

1. Plant-specific full scale pump data.

2. CE-EPRI 1/5 scale pump data (Reference V.13-1).

3. Maine Yankee full scale pump data.

The first preference is to use full scale prototypical data when it is available from the pump manufacturer. The second preference is to use CE-EPRI 1/5 scale pump data for three reasons:

a. The geometry of the CE-EPRI 1/5 scale pump is more similar to that of the Yankee and Vermont Yankee pumps than the Semiscale pump.

b. The specific speed (an important similitude parameter) of the CE-EPRI pump is closer to that of the Yankee and Vermont Yankee pumps than either the Maine Yankee or Semiscale pumps.

| Pump | Specific Speed |
|---|---|
| Vermont Yankee | 3802 |
| Yankee | 4687 |
| Maine Yankee | 5556 |
| CE-EPRI | 4209 |
| Semiscale | 926 |

c. This choice is consistent with the two-phase homologous data base in the principal regions of interest (Curve Types 1-6) discussed below.

The third preference is to use the Maine Yankee pump data since the geometry, scale and specific speed are closer to those for the Yankee and Vermont Yankee pumps than the Semiscale pump parameters and design. These data are only used for Curve Types 7 and 8 in the Yankee and Vermont Yankee pump models.

At the current time, no full scale two-phase homologous pump data are available. Therefore, the choices are limited to the CE-EPRI 1/5 scale steam water data, the Semiscale steam water data and the B&W 1/3 scale air-water data. The CE-EPRI data are used for Curve Types 1 through 6 for the following reasons:

a. Steam water is the two-phase fluid medium of principal interest.

b. The geometry and specific speed for this pump are closer to the full scale pump parameters than those of the Semiscale pump.

c. These data are more consistent with the single-phase homologous data selected for the full scale pumps.

The Semiscale steam water data base is used for Curve Types 7 and 8 (positive flow negative speed) in the two-phase region. Data are entered for these two curve types for completeness. However, these regions are not important since it is unlikely that these conditions will be encountered in LWR LOCAs. In fact, this consideration is the principal reason why these regions were generally excluded from the CE-EPRI 1/5 Scale Test Matrix (Reference V.13-1).

Reference

(V.13-1) W. G. Kennedy et al., "Pump Two-Phase Performance Program," Volume 1 through 8, EPRI NP-1556, Electric Power Research Institute, September 1980.

TABLE V.13

Data Sources For Reactor Coolant Pump Models

| Curve Number | 1 | 2 | 3 | 4 | 5 | 6 | 7[a] | 8[a] |
|---|---|---|---|---|---|---|---|---|
| Head Curves | HAN | HVN | HAD | HVD | HAT | HVT | HAR | HVR |
| Torque Curves | BAN | BVN | BAD | BVD | BAT | BVT | BAR | BVR |
| Maine Yankee | | | | | | | | |
| Single-Phase | MY | MY | MY | MY | MY[b] | MY[b] | MY | MY |
| Two-Phase | EP | EP | EP | EP | EP[b] | EP[b] | SS | SS |
| Yankee Rowe | | | | | | | | |
| Single-Phase | YR | YR | YR[c] | YR[c] | EP[c] | EP[c] | MY | MY |
| Two-Phase | EP | EP | EP[c] | EP[c] | EP[c] | EP[c] | SS | SS |
| Vermont Yankee | | | | | | | | |
| Single-Phase | VY | VY | EP | EP | EP | EP | MY | MY |
| Two-Phase | EP | EP | EP | EP | EP | EP | SS | SS |

Key: MY = Maine Yankee Pump Data
EP = CE-EPRI Pump Data
YR = Yankee Rowe Pump Data
VY = Vermont Yankee Pump Data
SS = Semiscale

Notes:

(a) These regions are very unlikely to occur in LWR LOCAs.

(b) Maine Yankee has anti-reverse rotation devices; therefore, reverse speed (this region) will not occur.

(c) Yankee has nonreturn valves in each cold leg; therefore, reverse flow (this region) will not occur.

Q.V.14

Clarify what range of conditions have been used to test the pump model.

A.V.14

RELAP5YA calculations with pump models have been compared to data from three tests that cover a wide range of conditions. These comparisons are described below:

a. Yankee Pump Coastdown - Single-Phase Conditions

The initial startup test program at the Yankee plant included a test where two pumps were tripped and the remaining two were left running (Reference V.14-1). This caused a normal reactor scram on low pump current, and a rapid flow coastdown in Loop 1 and Loop 4 that contained the canned rotor pumps that were tripped. The primary system pressure was relatively constant at about 2100 psia and maintained a large liquid subcooling of about 120°F in the pumps during this transient. Since each loop contains nonreturn valves, there was no significant backflow in these two loops from continued operation of the remaining two pumps. Plant test records contain the square root of the pressure difference between the inlet and outlet plena, normalized by the initial steady-state value. This was taken as an indication of the "normalized flow" in each tripped loop. These two curves are shown on Figure V.14-1 which is attached.

The Yankee SBLOCA model (Reference V.14-2) was modified to simulate this plant transient. The square root of the pressure difference across the steam generator plena, normalized by the initial value, was monitored by control variables. These parameters yielded similar results for both tripped loops, and are also shown on Figure V.14-1. The comparison shows that the code calculated the coastdown characteristics well. The short coastdown time results from the relatively small inertia of the canned rotor pumps in the Yankee plant. This comparison

provides confidence in the homologous method for predicting single-phase, transient pump performance.

b. TLTA Pump Coastdown - Single-Phase Conditions

TLTA Test 6425/R2 was a large break blowdown test with ECC injection performed in the Two-Loop Test Apparatus by General Electric. This was one of several TLTA tests selected for RELAP5YA code assessment (see Section 5.2 of Reference V.14-3). A review of reported test data indicates that the centrifugal pump in the broken loop was tripped and isolated by two quick closing valves very rapidly to prevent potential damage to that pump. However, the coastdown flow rate for the intact loop centrifugal pump, tripped at time zero, was measured and reported in Figure J-74 of Reference V.14-4. This test data is reproduced in Figure V.14-2 and compared to the transient mass flow rate predicted by the RELAP5YA model of TLTA. This comparison shows that the RELAP5YA model of the TLTA centrifugal pump simulated the coastdown flow rate reasonably well. The corresponding decrease in pump head is shown in Figure V.14-3. No test data were reported for comparing this parameter to, but the calculation shows a well behaved coastdown characteristic. During this 18-second coastdown, the calculated results indicate the pump outlet pressure decreased from 1234 to 1060 psia, the liquid subcooling in the pump decreased from 26$^{o}$F to 17$^{o}$F, and the fluid remained as single-phase liquid.

c. LOFT Pump Operation and Coastdown - Single- and Two-Phase Conditions

LOFT Test L3-6/L8-1 was a PWR small break test that combined a long period of pump operation under single- and two-phase conditions, a subsequent trip of both pumps at 2371 seconds, and continued testing until 7469 seconds. This test has been simulated by the RELAP5YA model of the LOFT facility from 0 to 2460 seconds for code assessment purposes. The pump models used LOFT test data and a fixed inertia rather than the variable

inertia that exists in these components. Many calculated parameters are compared to test data in Section 5.3 of Reference V.14-3. Figures V.14-4 through V.14-6, attached, show additional comparisons of predicted pump performance parameters to available test data.

Figure V.14-4 compares the calculated pump head to the differential pressure across the two pumps (measurement PdE-PC-001). Both curves show essentially the same head degradation as the fluid changes from initially subcooled liquid to predominantly steam at about 1000 seconds and beyond. This comparison provides confidence in the homologous method for modeling pump two-phase performance.

Figure V.14-5 compares the calculated and measured pump speeds. Both curves show essentially a constant speed during the period when electrical power was supplied to the pumps. This was followed by a rapid coastdown when the pumps were tripped at about 2370 seconds. The spikes in the test data from 0 to 300 seconds are attributed to "unexplained noise" by the EG&G test analysts. A slightly lower initial speed (3082 rpm versus the test value of 3200 rpm) was used to match the flow rates and pressure drops around the primary system.

Figure V.14-6 compares the calculated and measured pump speeds during the coastdown period from 2370 seconds to 2450 seconds. The two curves show similar coastdown trends, but with two notable differences. First, the two curves are offset by about 4.4 seconds due to the lower initial speed and the plotting edit frequency for the calculation versus the measured speed history. Second, the slope of the calculated speed history is more negative than the test data for speeds above 1000 rpm, about the same for speeds between 700 and 1000 rpm, and less negative for speeds below 700 rpm. These differences are primarily due to the fixed value for the pump moment of inertia used in the calculation versus the variable moment of inertia in the LOFT pumps. Table V.14-1 compares the approximate LOFT

inertia values to the value of 274 $lb_f$-$ft^2$ used for our simulation. The slope of the pump speed equals the shaft torque divided by the moment of inertia for a free-wheeling pump:

$$dw/dt = -\tau_{SHAFT}/I$$

For speeds above 1000 rpm, our inertia is too small leading to a more rapid coastdown than measured. For speeds below 700 rpm, our inertia is to large leading to a slower coastdown than measured. However, the variable inertia of the LOFT pumps is atypical. Reactor coolant pumps at power plants have fixed inertias.

TABLE V.14-1

| W (rpm) | $I_{LOFT}$ ($lb_f$ - $ft^2$) | $I_{RELAP5YA}$ ($lb_f$ - $ft^2$) |
|---|---|---|
| 3200 | 273 | 274 |
| 3000 | 289 | 274 |
| 2500 | 318 | 274 |
| 2000 | 325 | 274 |
| 1500 | 311 | 274 |
| 1000 | 274 | 274 |
| 500 | 216 or 34* | 274 |
| 100 | 154 or 34 | 274 |
| 0 | 136 or 34 | 274 |

*The test report does not make clear whether the variable inertia flywheel was engaged or disengaged below 750 rpm. If disengaged, then the lower inertia value applies.

References

(V.14-1) _____, "The Startup Experiment Program for the Yankee Reactor," YAEC-184, Yankee Atomic Electric Company, June 1961.

(V.14-2) J. N. Loomis, J. H. Phillips, A. Husain, "Reactor Coolant Pump Operation During Small Break LOCA Transients at the Yankee Nuclear Power Station," YAEC-1437, Yankee Atomic Electric Company, July 1984.

(V.14-3) Fernandez, R. T., R. K. Sundaram, J. Ghaus, A. Husain, J. N. Loomis, Lo Schor, R. C. Harvey and R. Habert, "RELAP5YA - A Computer Program for Light-Water Reactor System Thermal-Hydraulic Analysis, Volume III: Code Assessment," Yankee Atomic Electric Company Report YAEC-1300P, Volume III, October 1982. (Proprietary)

(V.14-4) L. S. Lee, G. L. Sozzi, S. A. Allison, "BWR Large Break Simulation Tests - BWR Blowdown/Emergency Core Cooling Program," Volume 2, NUREG/CR-2229, EPRI NP-1783, GEAP-24962-2, General Electric Company, July 1982.

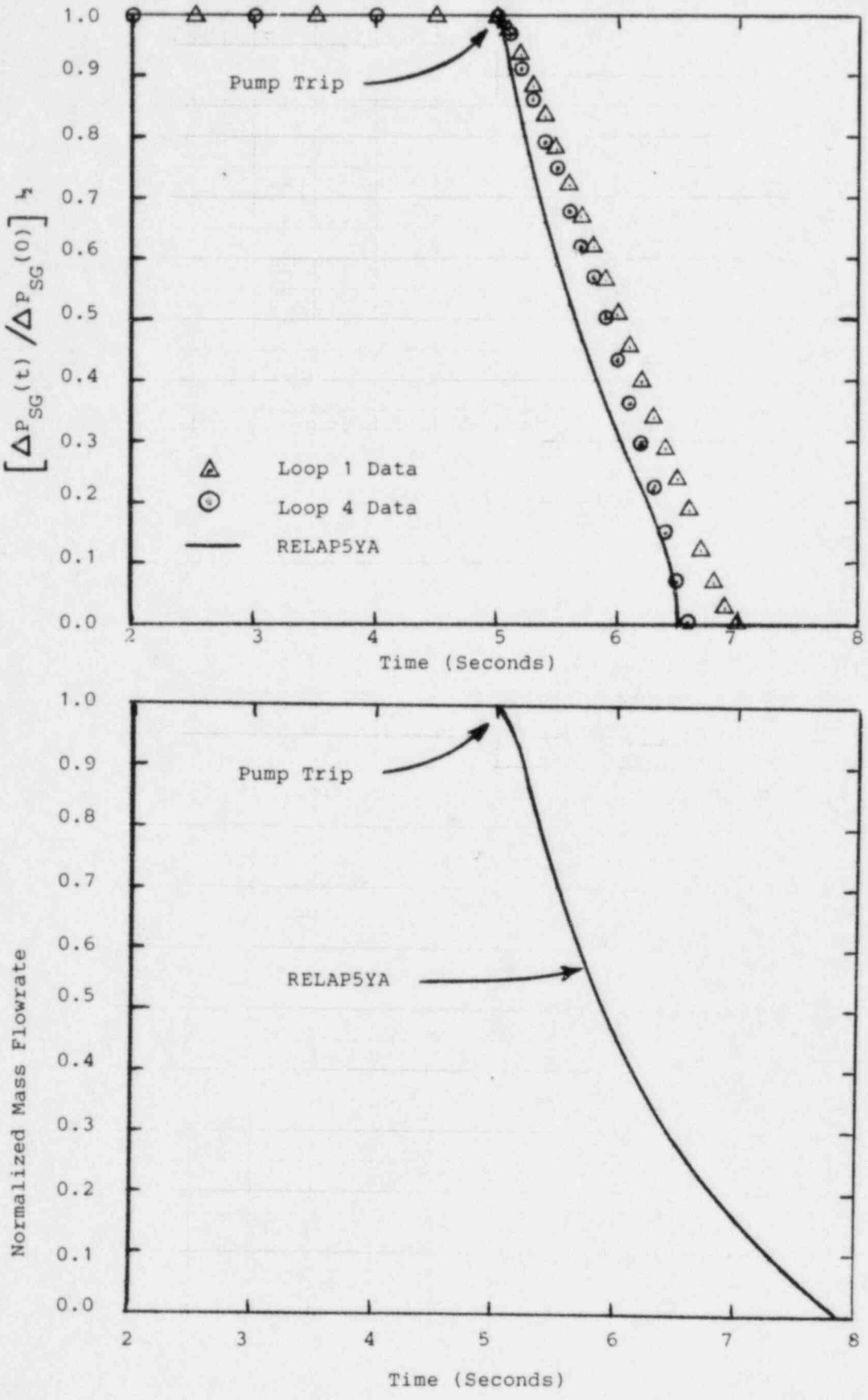


Figure V.14-1: RELAP5YA Comparison to Yankee Rowe Pump Trip Test Data

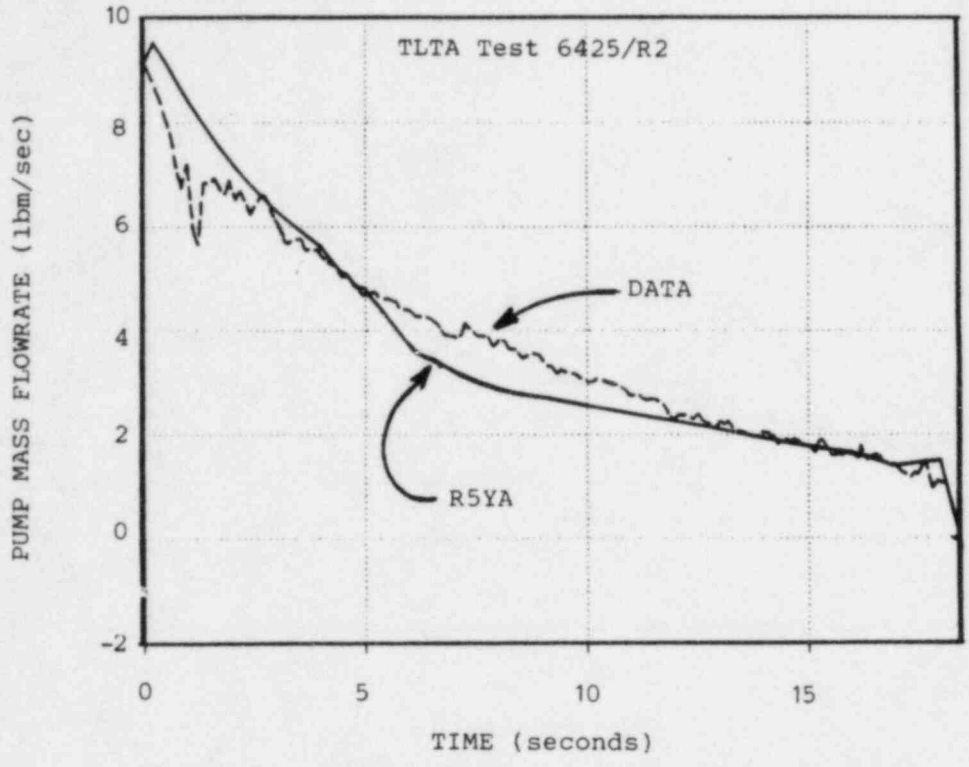


FIGURE V.14-2: INTACT LOOP RECIRCULATION PUMP MASS FLOWRATE

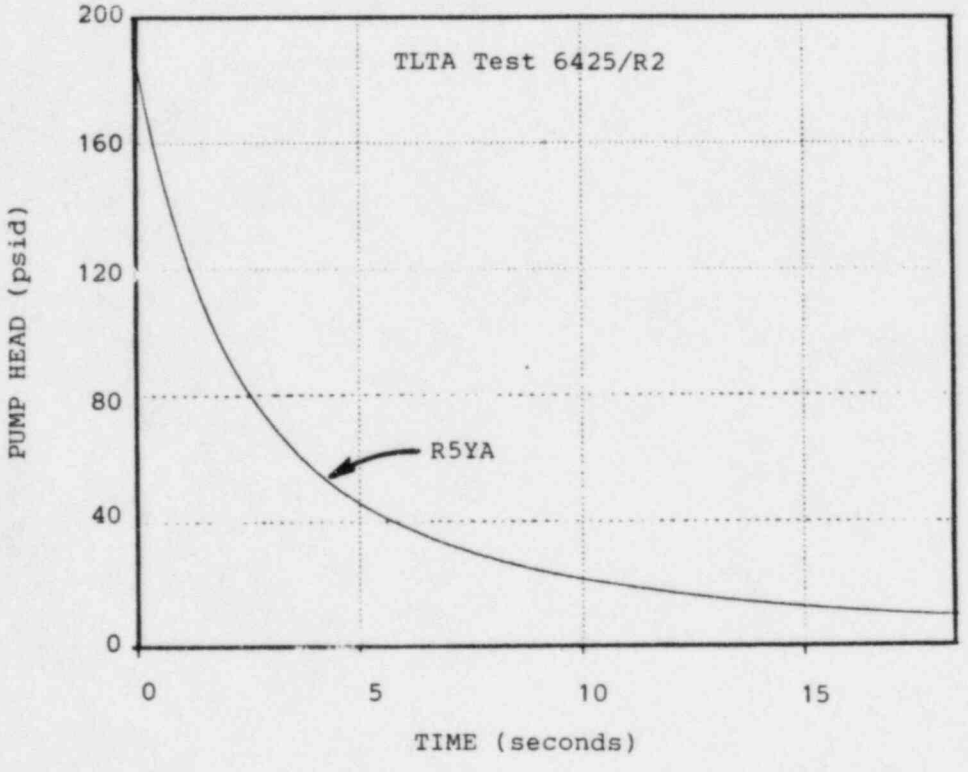


FIGURE V.14-3: INTACT LOOP RECIRCULATION PUMP HEAD

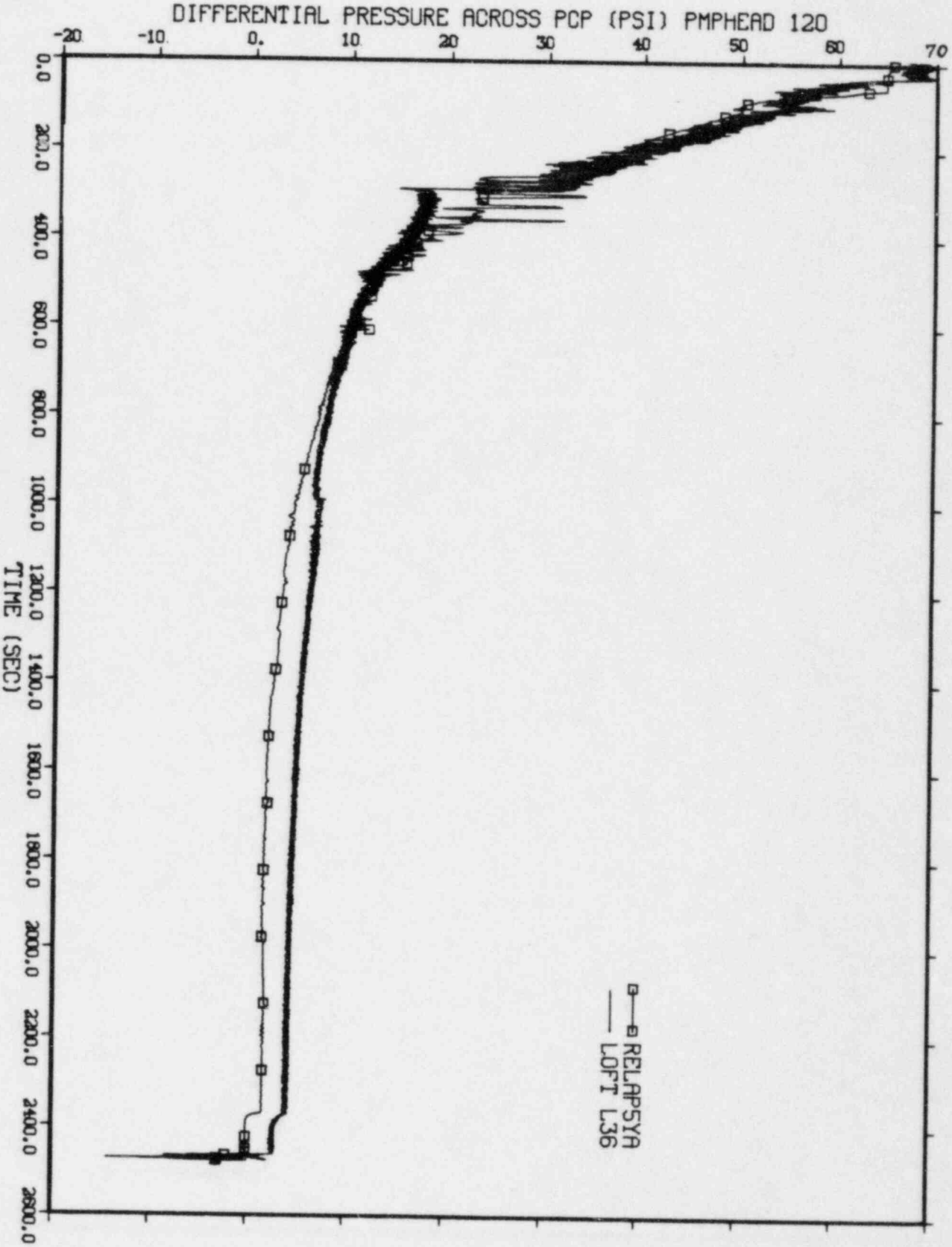


Figure V.14-4 RELAP5YA Comparison to LOFT L3-6 Data
Pump Differential Pressure

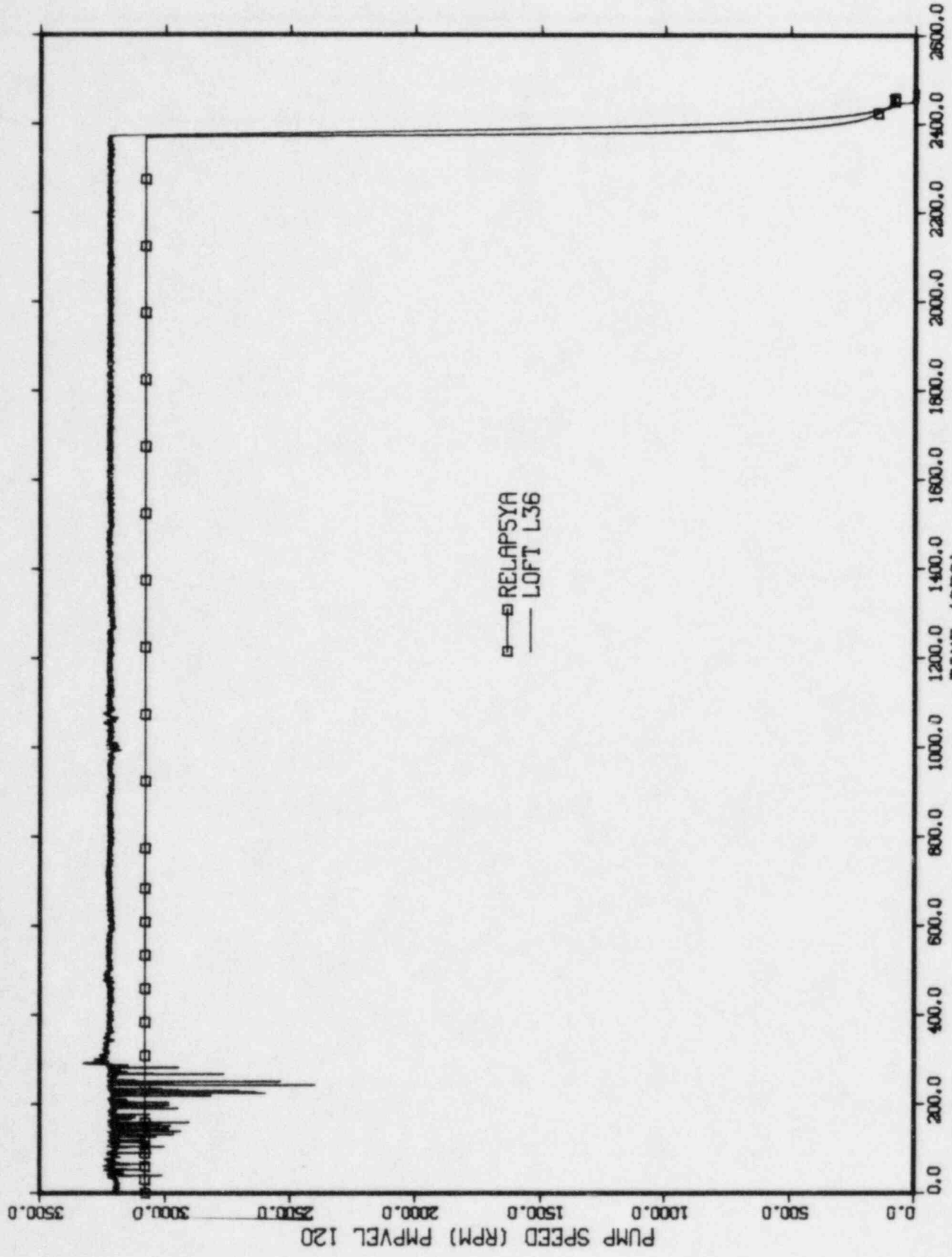


Figure V.14-5 RELAP5YA Comparison to LOFT L3-6 Data
Long Term Pump Speed

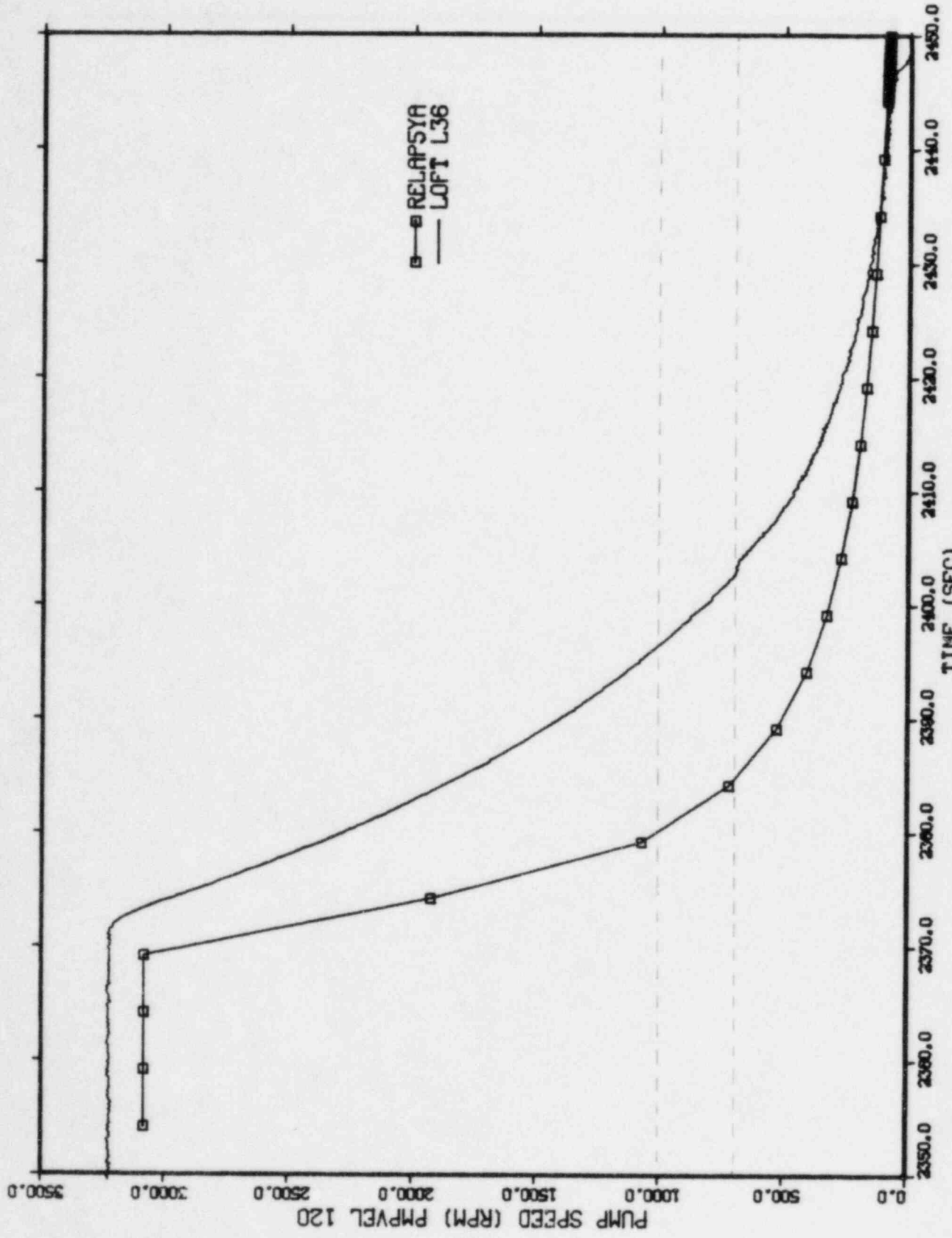


Figure V.14-6 RELAP5YA Comparison to LOFT L3-6 Data
Pump Coastdown Speed History

Q.V.15

Justify which set of pump curves will be used for SBLOCA applications: Bingham, Westinghouse, LOFT, Semiscale or other.

A.V.15

The data bases that were used to develop performance curves for the Maine Yankee, Yankee and Vermont Yankee reactor coolant pumps are described and justified in Answer A.V.13. Additional pump modeling information is provided in answers A.I.7, A.V.12 and A.V.14.

The most preferred source of information is full-scale pump manufacturer's data where available. The second source is the CE-EPRI pump data base due to its completeness (nearly 1000 steady-state tests) and similitude parameters. The Semiscale pump data base is only used to define the two-phase difference tables for Curve Types 7 and 8; however, operation in these regions is very unlikely. None of the Bingham, Westinghouse nor LOFT data bases are used.

## VI. FLOW REGIMES

Page 8 of Reference 9 states that "the horizontal flow regime map is used rather than the vertical flow regime map when the angle ... is less than 15 degrees."

Q.VI.4

Clarify the basis for the 15-degree switching criteria.

A.VI.4

The criterion for switching from the vertical to the horizontal flow map in RELAP5YA is when the absolute value of the angle from the horizontal is less than $15^{\circ}$. The main impact of switching maps is to allow for the occurrence of stratified flow. Recent work by Bornea et al. (Reference VI.4-1) has shown that stratified flow will not occur for angles greater than about $20^{\circ}$ from the horizontal. Hence, the choice of $15^{\circ}$ in RELAP5YA appears reasonable.

Reference

(VI.4-1) Bornea, D., et al., "Gas-Liquid Flow in Inclined Tubes: Flow Pattern Transition for Upward Flow," Chemical Engineering Sciences, Volume 40, (1983).

Q.VI.5

Clarify if the stratified flow model is also used up to angles of 15 degrees.

A.VI.5

The stratified flow model is used up to angles of $15^{\circ}$ from the horizontal if stratified flow is calculated to exist.

Q.VI.6

Clarify if there are any SBLOCA analyses that will use the stratified flow model for situations where the pipe area is changing and, if so, how the model would have to be changed to handle the nonuniform area.

A.VI.6

All the active hydrodynamic volume components in RELAP5YA (SNGLVOL, BRANCH, PIPE, etc.) are assigned a constant flow area over the length of the volume. In normal plant applications, horizontal piping runs with constant flow area are usually long enough that they are treated as separate volumes. If it becomes necessary to combine pipes of different flow areas into one volume, the usual practice is to preserve the combined volume and the combined length and calculate an equivalent flow area. Horizontal pipes with nonuniform flow area are not expected, but if they exist, they will also be modeled with a constant equivalent flow area. The stratified flow model utilizes this constant flow area.

Q.VI.7

Clarify how the slip is treated for the two-phase critical flow when the upstream volume switches from nonstratified to stratified flow and what effect this has on the break flow.

A.VI.7

In RELAP5YA, the determination of the slip between phases is primarily influenced by the interphase drag term, $F_I$ defined in Section 3.1 of Volume I of the RELAP5YA Code Manual. This is a junction-related parameter and its calculation depends on the junction void fraction. In horizontal cocurrent flow, when the flow is not stratified, the junction void fraction is donored from the upstream volume. This applies whether the flow at the junction is choked or not choked. When the flow in the upstream volume is stratified, the junction void fraction is not donored directly from the upstream volume, but is modified to account for the stratified liquid level in the upstream

volume being above or below the junction location and for the mechanism of vapor pull-through or liquid entrainment. The method for estimating this junction void fraction is described in Section 2.2.1.3 of Appendix A of Volume I of the RELAP5YA Code Manual. The junction void fraction, along with the phasic velocities, is also used to compute the junction flow.

Q.VI.10

Clarify how the stopping of natural circulation and reestablishment of natural circulation has been verified analytically and experimentally.

A.VI.10

Please see the response to questions Q.III.1 through Q.III.4.

Q.VI.11

Clarify how the effect of noncondensable gases on natural circulation has been verified.

A.VI.11

Please see the response to questions Q.III.1 through Q.III.4.

Q.VI.13

Submittals need to consider the degree of mixing in the vessel when the loops each have different conditions such as break in one loop, a pressurizer voided in one loop, steam generator heat removal in only one loop, and flow stopped or much less in one loop than the other(s). If complete vessel mixing is assumed, it needs to be justified if different conditions exist in the loops. Clarify and justify how vessel mixing will be modeled for SBLOCAs when the loop conditions differ.

Figures IV.2-1 and IV.2-2 represent the nodalization used in the pump trip studies performed for the Maine Yankee and Yankee Plant at Rowe, respectively. Similar noding schemes will be used for small break calculations. The recirculation loops will be modeled as two loops. One will represent the broken loop, the other will represent the intact loops. Several nodes are used to model the recirculation loops accurately. The downcomer and other regions of the reactor vessel are modeled with a number of axially stacked volumes. However, the vessel nodalization does not specifically model azimuthal variations in these areas to account for differences between the recirculation loops. This nodalization is considered adequate for SBLOCAs for the following reasons:

1) Only uniformly applied operator actions are used in licensing analyses. For example, reactor coolant pumps are either all running or all tripped; steam generators are either all bottled up or all available for cooling. Even the ECCS is available in all recirculation loops. Therefore, the various loops are not expected to behave significantly different from each other.

2) The fluid conditions at the inlet to the core is expected to be very nearly uniform even if different loop conditions are introduced in the upper downcomer regions. This is because: a) The fluid experiences a change in direction at the injection nozzles. The exact fluid trajectory in the downcomer depends on the loop flow differences and the resistance to flow in the vertical or annular direction. The annular region is quite free and a uniform flow is expected to exit the downcomer; b) The downcomer exit flow is going to experience a change in direction with a higher probability of mixing. The various structures present in the lower plenum area (such as a flow skirt in Maine Yankee) and the core support plates with substantial reduction in flow area are expected to enhance mixing; c) PWRs use an open core configuration. This geometry promotes fluid mixing in the core. No major liquid level differences are expected to exist at various azimuthal locations in the core.

3) A voided pressurizer does not play a significant role for those phases of a LOCA where core cooling is a concern. During the pressurizer refill period, the pressurizer loop may behave differently than the other loops. But its impact on LOCA calculations will be negligible as the core is expected to be fully covered during this period.

Q.VI.17

Page 9 of Reference 8 states: "The two-fluid nonequilibrium hydrodynamic model includes three options for simpler hydrodynamic models. These are a quasi-steady flow model, a homogeneous flow model, and a thermal equilibrium model. The two-fluid, quasi-steady, or homogeneous flow models can be used with either the nonequilibrium or equilibrium thermal models (that is, six combinations). Most of the development effort was performed using the two-fluid nonequilibrium model". Clarify if anything but the two-fluid nonequilibrium model will be used in any part of the system for SBLOCA calculations.

A.VI.17

The nonequilibrium option is generally used for volumes in our current Yankee, Maine Yankee and Vermont Yankee plant models. The exceptions to this general approach occur for several Time Dependent Volumes (TMDPVOLs) that represent boundary conditions in each model. Of these TMDPVOLs, only the feedwater and ECCS supply volumes act as fluid sources which deliver liquid to the systems. The remaining TMDPVOLs act as fluid sinks for which only the pressure is an important parameter. Therefore, the cases where the equilibrium option, rather than the nonequilibrium option, is used to represent certain boundary conditions makes no difference.

The two-velocity ("two-fluid") option is also generally used in these plant models. The Maine Yankee input deck contains no one-velocity junctions. The Yankee input deck contains three one-velocity junctions. These represent the connection for the flow path from the downcomer to the tube bundle region at the bottom of the steam generator in the single broken loop, the single intact loop, and the

combined two intact loops. This region generally contains single-phase liquid; thus, the one-velocity option is appropriate. The Vermont Yankee input deck contains two one-velocity junctions. The first represents the very small leakage path from the lower plenum to the control rod guide tube region at the 42-inch elevation in the vessel. The second represents the very small leakage path from the isolated portion to the active segment of the recirculation header. This latter junction and the nearly isolated portion of the recirculation header will be removed when the plant completes the pipe replacement program since it will no longer exist.

Q.VI.18

Clarify if there is some type of boiling droplet breakup in addition to the Weber number criteria that models mechanical breakup.

A.VI.18

RELAP5YA assumes that droplets are present in the annular-mist flow regime (voids between 0.85 and 0.95) and the mist flow regime (voids above 0.95). The average droplet size is used in estimating the interphase drag in these regimes. In the annular-mist regime, the average droplet size is postulated to be at its maximum and is characterized by a critical Weber number criterion. In mist flow, the average droplet size is assumed to be below its maximum value and the model for droplet size calculation is described in Section 3.1.3.4 of Reference VI.18-1. The maximum droplet size, defined by a critical Weber criterion, is assumed to occur at a void fraction of 0.95, and corresponds to the transition point between the annual-mist and mist flow regimes. Droplet breakup due to boiling is not explicitly modeled, but the decrease in droplet size at void fraction above 0.95 indirectly accounts for mechanisms other than mechanical breakup.

Reference

(VI.18-1) Fernandez, R. T., et al., "RELAP5YA - A Computer Program for Light-Water Reactor System Thermal-Hydraulic Analysis, Volume I," YAEC-1300P, October 1982.

Q.VI.19

Page 33 of Reference 8 states: "The phase-wetted perimeter has been assumed proportional to void fraction." Clarify if this is done even for the annular flow regime and if so justify what approximations are introduced for SBLOCA calculations.

A.VI.19

The wall drag calculation in RELAP5YA is directed primarily at calculating the overall two-phase pressure drop correctly. The partitioning of the total wall drag into wall-vapor and wall-liquid components is done somewhat simplistically by using the void fraction to determine the phase-wetted perimeter. This approach ensures a smooth transition between single phase and two-phase conditions, but does not explicitly account for the effect of flow regimes on the partitioning of the wall drag. Thus in the annular-flow regime, even though the wall is supposed to be completely wetted by the liquid phase, all the wall drag is not apportioned to the liquid phase. However, the total pressure loss due to wall drag is preserved due to the phasic sum momentum equation.

The wall drag has an impact on the phasic momentum equations in RELAP5YA which are solved for the phasic velocities. Also, the wall drag generally has a larger impact on the phase velocities at conditions of high mass flux. For PWR SBLOCA conditions, the annular flow regime generally occurs as a transition regime during the formation of two-phase levels in the system. In these situations, the annular flow regime persists only for a short time interval and the mass fluxes are relatively low. Hence, the partitioning of the wall drag in annular flow is expected to have negligible impact on the calculation of phasic velocities for SBLOCA calculations.

Q.VI.20

Equation 128 on Page 35 of Reference 8 defines the HTFS two-phase friction multiplier correlation. Clarify what value of C, the correlation parameter, is used.

A.VI.20

The correlation parameter, C, is based on the HTFS correlation (Reference VI.20-1) for two-phase pressure drop and is calculated as:

$$2 \leq C = -2 + (28.0 - 0.5 \times G)\exp\left[\frac{(\log_{10}(f_p) + 2.5)^2}{G \times 10^{-4} - 2.4}\right]$$

where:

$f_p$ = Baroczy property index

$$= \frac{\rho_g}{\rho_f}\left(\frac{\mu_f}{\mu_g}\right)^{0.2}$$

G = mass flux

$$= \alpha_g \rho_g v_g + \alpha_f \rho_f v_f$$

Reference

(VI.20-1) Claxton, K. T., et al., "HTFS Correlation for Two-Phase Pressure Drop and Void Fraction in Tubes," AERE-R7162, 1972.

Q.VI.21

Page 35 of Reference 8 also states: "For countercurrent two-phase flow, the HTFS two-phase friction correlation is invalid. However, for countercurrent two-phase flow, the phases are approximately separated and the friction factors, $\lambda_f$ and $\lambda_g$, are used directly with reasonable accuracy." Clarify if any problems occur in using this approach because of the discontinuities in models that occur in switching from countercurrent to cocurrent flow.

A.VI.21

There will be some discontinuity in the calculation of the phasic wall drag components when the code shows a transition from countercurrent to cocurrent flow. However, this transition generally occurs at low flow

conditions. At these conditions, the calculation of phasic momentum is dominated by gravity and the interphase drag component, which is smoothly behaved, and the wall drag component has minimal impact. Hence, these discontinuities in wall drag are expected to have negligible impact in the estimation of the overall drag on each phase.

Q.VI.25

Page 18 of Reference 13 states: "...the assumption of zero mass transfer is questionable for large area changes. Large area changes give relatively large pressure changes and hence mass transfer due to P that could change the void redistribution as the fluid passes through the area change. Clarify what limitations will be placed on the use of the abrupt area change model for SBLOCAs to justify the zero mass transfer assumption.

A.VI.25

No formal limitations have been placed on the use of the abrupt area change model. The partial quotation, taken out of context from the cited reference, and the question imply several misconceptions concerning the abrupt area change model. The following explanation is intended to clarify the role of the abrupt area change model and situations where we use it.

The pressure change between two adjacent volumes connected by an unchoked junction is determined by the solution to the full set of conservation equations, not simply the area change between volumes. Examination of Equations 231 and 232 in Appendix A of Reference VI.25-1 shows that this pressure change, $(P_K - P_L)^{n+1}$, includes the following phenomena:

a. Temporal and spatial phasic acceleration.

b. Phasic gravitational forces.

c. Phasic wall friction forces.

d. Interphase drag forces.

e. Virtual mass effects.

f. Interphase mass/momentum transfer.

Section 2.1.3.4 of Reference VI.28-1 states that RELAP5YA and RELAP5 MOD1 contain models to account for local irreversible pressure losses from abrupt area changes in the geometry of flow paths. These models provide additional terms to the two momenta equations, as discussed in Section 2.1.3.4, even though they are not shown explicitly in the two equations cited above. These models are <u>not</u> a replacement for the two momenta equations. The abrupt area change model provides one of two options to account for the additional local pressure losses. The RELAP5 MOD1 authors have attempted to formulate this model in a manner that accounts for downstream void-fraction redistribution and that is consistent with the basic conservation equations (Dr. Trapp states this on Page 17 of the cited reference). The authors have assumed that mass transfer is negligible in the localized region of the abrupt area change. However, mass transfer is accounted for in momentum control volume as shown in Equations 231 and 232 cited above. Finally, large area changes tend to increase the loss coefficients, but do not necessarily lead to "relatively large pressure changes." The net pressure change that affects mass transfer is the sum of many effects identified above. The local pressure loss terms depend not only on the loss coefficients, but also on the magnitude of the phasic dynamic pressure. In SBLOCAs, the dynamic pressures tend toward small values as the velocities subside and the system becomes gravity dominated.

We generally do not use the abrupt area change model in plant-specific input decks, except for certain cases. Instead, we generally use the smooth area change option and enter forward and reverse loss coefficients that are based upon standard references or plant data. The exceptions occur when we use the motor valve component available in RELAP5YA. The current SBLOCA model for the Yankee plant at Rowe uses motor valve components to represent the nonreturn valves in the primary side cold legs and the secondary side steam lines. The current SBLOCA

model for the Maine Yankee plant does not use any motor valve components. The current LOCA model for the Vermont Yankee plant uses motor valve components to represent the following:

a. Pump discharge valves in each recirculation loop.

b. Main steam line isolation valves.

c. Pressure regulator valve upstream of the turbine.

d. Safety/relief valves on the main steam lines.

e. Safety valves on the main steam lines.

Q.VI.26

Clarify how the abrupt area change model has been assessed against data for conditions expected in SBLOCA calculations.

A.VI.26

The abrupt area change model has only been used in conjunction with the motor valve component in current plant LOCA models as discussed in the answer to Question Q.VI.25. The main effects to be simulated are the opening and/or closing time of certain valves. This can and has been assessed by verifying that the valves open, close or remain in position according to the time of their trip signals and corresponding valve operating rates.

Q.VI.27

Clarify how L1 and L2 are defined for the abrupt area change model on Page 58 of Reference 8.

A.VI.27

The upstream length, L1, and downstream length, L2, used in the abrupt area change model are defined as follows:

Expansion

$$L1 = 0.0$$

$$L2 = 10.0\ DIAMV(L)\sqrt{ARAT(L)}$$

Contraction

$$L1 = 1.0\ DIAMV(K)\sqrt{ARAT(K)}$$

$$L2 = 10.0\ DIAMV(L)\sqrt{ARAT(L)}$$

where:

| | | |
|---|---|---|
| K | = | upstream volume number. |
| L | = | downstream volume number. |
| DIAMV( ) | = | hydraulic diameter of designated volume |
| ARAT( ) | = | partitioned area ratio in the designated volume associated with the abrupt area change junction. |

Note that we do not generally use the abrupt area change option as discussed in the answer to Question Q.VI.25.

Q.VI.28

Page 103 of Reference 8 describes modeling valves using flow coefficients rather than the abrupt area change model and converting the flow coefficients to energy loss coefficients. Clarify how the flow coefficients are defined in terms of energy loss coefficients.

A.VI.28

Information contained in Appendix A, Page 103 and Appendix B, Pages 111 to 112 of Reference VI.28-1, and Page 63 of Reference VI.28-2 indicates that tabular values of flow coefficients ($C_v$) can be entered as a user option to account for local form losses (K) through motor and

servo valves. The latter two references also define the method presumably used to convert the flow coefficients to local energy losses (K) within the computer code. This information is not correct.

RELAP5 MOD1 and RELAP5YA contain two options for modeling local pressure losses across these two types of valves. The first option is to specify that the abrupt area change model is to be used for the valve. The code will then internally compute the loss coefficients based upon the current time geometry. We generally use this option for these two types of valves. The second option is to specify that the smooth area change model is to be used for the valve. This option requires the user to enter a table of loss coefficients versus normalized valve stem position. Although the User's Manuals indicate flow coefficient ($C_v$) values are to be entered, the algorithm actually assumes that energy loss coefficients (K) were entered. Therefore, loss coefficients must be entered.

References

(VI.28-1) R. T. Fernandez, R. K. Sundaram, J. Ghaus, A. Husain, J. N. Loomis, L. Schor, R. C. Harvey and R. Habert, "RELAP5YA - A Computer Program for Light-Water Reactor System Thermal-Hydraulic Analysis, Volume I: Code Description," Yankee Atomic Electric Company Report YAEC-1300P, Volume I (October 1982). (Proprietary)

(VI.28-2) R. T. Fernandez, R. K. Sundaram, J. Ghaus, A. Husain, J. N. Loomis, L. Schor, R. C. Harvey and R. Habert, "RELAP5YA - A Computer Program for Light-Water Reactor System Thermal-Hydraulic Analysis, Volume II: User's Manual," Yankee Atomic Electric Company Report YAEC-1300P, Volume II (October 1982). (Proprietary)

Q.VI.29

Page 49 of Reference 10 states: "In addition, the Two-Dimensional Branching technique described in Section 3.2.7.2 of Appendix B is not recommended since it is known that this technique can create nonphysical recirculation through the adjacent junctions." Clarify how

$90^{o}$ tees will be modeled and justify why nonphysical behavior will not result.

A.VI.29

Ninety degree ($90^{o}$) tees are modeled using two rather than the three junctions shown on Figure 4 in Section 3.2.7.2 of Appendix B (Reference VI.29-1). Either Junction J2 or J3 would not be used. This technique prevents the occurrence of nonphysical recirculation between Volumes VI, V2 and V3 via Junctions J1, J2 and J3. Appropriate loss coefficients for the branch and run junctions, based upon standard references, are calculated and entered.

References

(VI.29-1) R. T. Fernandez, R. K. Sundaram, J. Ghaus, A. Husain, J. N. Loomis, L. Schor, R. C. Harvey and R. Habert, "RELAP5YA - A Computer Program for Light-Water Reactor System Thermal-Hydraulic Analysis, Volume I: Code Description," Yankee Atomic Electric Company Report YAEC-1300P, Volume I (October 1982). (Proprietary)

Q.VI.30

Clarify how the $90^{o}$ tee model has been assessed against data for single-phase and two-phase flow conditions.

A.VI.30

The $90^{o}$ tee modeling technique described in the answer to Question Q.VI.29 has been used extensively in both our Separate Effects and our System Effects code assessment cases. Table VI.30-1 summarizes the nodalization diagrams which show where this technique has been used. These tests include steady and transient single- and two-phase flow through tees. This modeling technique contributed toward the generally good assessment results that were obtained.

TABLE VI.30-1

Test Facility and Nodalization Diagrams With Tees

Q.VI.31

Page 101 of Reference 8 discusses how gravity effects are modeled with a branch volume. Clarify how the gravity head is included.

A.VI.31

The gravity head is included in the phasic sum momentum equation for all junctions. This appears in the second term on the right side of Equation (13) on Page 12, Equation (224) on Page 81 and Equation (231) on Page 83 of Appendix A in Reference VI.31-1. The gravity head term is computed as variable DELPZ in Subroutine VEXPLT:

$$DELPZ = \left[(\alpha_g \rho_g)_K^n + (\alpha_f \rho_f)_K^n]\Delta Z_K + [(\alpha_g \rho_g)_L^n + (\alpha_f \rho_f)_L^n)\Delta Z_L\right]\frac{g_Z}{g_c}$$

where $\Delta Z_K$ and $\Delta Z_L$ are half the elevation change in the upstream and downstream volumes, respectively. This term is then added to the SUMOLD variable. When horizontal stratified flow exists, then an additional term given by Equation (25) on Page 14 of Reference IV.31-1 is added to the right side of the phasic difference momentum equation. This term is then added to the DIFOLD variable in Subroutine VEXPLT.

Reference

(VI.31-1) Fernandez, R. T., R. K. Sundaram, J. Ghaus, A. Husain, J. N. Loomis, L. Schor, R. C. Harvey and R. Habert, "RELAP5YA - A Computer Program for Light-Water Reactor System Thermal-Hydraulic Analysis, Volume I: Code Description," Yankee Atomic Electric Company Report YAEC-1300P, Volume I, October 1982. (Proprietary)

Q.VI.32

Clarify if the statement is correct that "A gravity head is included in the branch volume $V_3$ and $V_4$ and results in a corresponding separation effect due to buoyancy" (Page 101 of Reference 8).

A.VI.32

The cited statement is perhaps too cryptic. Gravity head terms are generally accounted for in the momentum equations associated with junctions as stated in Answer A.VI.31. Each junction has a momentum cell that connects the adjoining halves of adjacent volumes. When an adjacent volume is vertical (for example V2 and V4 in Figure 33 of the cited reference), then its nonzero elevation change contributes a gravity term to the phasic sum momentum equation. When an adjacent volume is horizontal (for example V1 and V3 in Figure 33), then its zero elevation change will not contribute a gravity term to the phasic sum momentum equation. However, when stratified flow exists in a horizontal volume, then a buoyancy term is added to the difference momentum equation. Therefore, volume V4 will always have a gravity head term. Volume V3 will have a buoyancy term when stratified flow exists within it.

Q.VI.33

Page 19 of Reference 13 states: "The area change seen at a branch junction gives a crude representation of the expansion or contraction losses seen by each junction flow. But it should be noted that the partitioning used to determine the area changes is algebraic in character and not based upon any physical principals. In fact, the partitioning fails to preserve the mass flow of each junction stream because volumetric flow is preserved by the partitioning instead of mass flow." Clarify how much error this could introduce in SBLOCA calculations.

A.VI.33

The hydrodynamics within a volume that contains two or more inlet and/or outlet junctions is a complicated process that generally involves local three-dimensional flow patterns. In reality, these local 3-D flow patterns determine the expansion and contraction losses (and momentum mixing losses discussed in the answer to the next question). These fluid mechanical energy losses are converted to

relatively small thermal energy sources by dissipation. In one-dimensional codes such as RELAP5YA, these losses are approximated by the product of form loss coefficients (from standard references) and the phasic kinetic energy terms. Although this approximation may not be exact, it appears to be reasonable based upon the generally good code assessment results contained in Reference VI.33-1. These assessment cases cover a very broad range of thermal-hydraulic conditions. In particular, they include a PWR small break test (LOFT L3-6/8-1) and a BWR small break test (TLTA 6432/1). Therefore, we conclude that the error introduced by this approximation is small and acceptable.

We disagree with the last sentence in the cited statement. The mass flow rate for all junctions is preserved by inclusion and solution of the conservation of mass equations within the limits of the code.

Reference

(VI.33-1) Fernandez, R. T., R. K. Sundaram, J. Ghaus, A. Husain, J. N. Loomis, L. Schor, R. C. Harvey and R. Habert, "RELAP5YA - A Computer Program for Light-Water Reactor System Thermal-Hydraulic analysis, Volume III: Code Assessment," Yankee Atomic Electric Company Report YAEC-1300P, Volume III (October 1982). (Proprietary)

Q.VI.34

Page 19 of Reference 13 also states: "Because each junction momentum equation is calculated independently of the other junction flows connected to the branch volume (except for the reduced area) the momentum mixing terms are neglected." Clarify how neglecting these momentum mixing terms affects SBLOCA results, and if they have been included in RELAP5YA or just in the jet pump modeling.

A.VI.34

The momentum mixing terms have only been included in the jet pump model. Our studies indicate they are significant primarily at or near

normal jet pump operating conditions. In this region, the very high velocity drive nozzle stream mixes with the much lower velocity suction nozzle stream. The momentum mixing terms have not been included for other RELAP5YA hydrodynamic components. The generally good code assessment results obtained over a broad range of thermal-hydraulic conditions indicate these terms are generally not significant except for jet pumps.

## VII. CORE STEAM COOLING

### Q.VII.13

For the three steady-state film boiling tests, Page 167 of Reference 12 states: "RELAP5YA provides a reasonable prediction of the CHF location but overpredicts the wall temperature in the post-CHF regime." Justify this statement about the CHF location because Pages 180-181 of Reference 12 only show the wall temperature data above the CHF location so the CHF location is not given.

### A.VII.13

The precise location of the CHF is not presented in the Experimental Data Report (Reference VII.13-1) for the THTF steady-state tests. The exact location of the dryout point cannot be determined and is, in fact, rarely clearly defined in a rod bundle. However, the data report presents the calculated quality at the CHF location and the quality at every axial location for which post-CHF temperature are presented.

We inferred that the dryout point was located between the thermocouple at which film boiling was detected and the thermocouple below it. Table VII.13-1 provides the reported quality at CHF, the inferred CHF location, and RELAP5YA calculated CHF location.

TABLE VII.13-1

| Test No. | Reported Quality at CHF | Inferred Expt. CHR Loc. (ft) | RELAP5YA CHF Loc. (ft) |
|---|---|---|---|
| 3.07.9B | 0.368 | 4.8 - 5.2 | 4.7 - 6.0 |
| 3.07.9K | 0.887 | 9.3 - 9.5 | 7.5 - 8.3 |
| 3.07.9X | 0.84 | 8.2 - 8.8 | 6.0 - 7.5 |

### Reference

(VII.13-1) Yoder, G. L., et al., "Dispersed Flow Film Boiling in the Rod Bundle Geometry Steady-State Heat Transfer Data and Correlation Comparisons," ORNL/8822 (Preliminary Draft).

Q.VII.14

For the transient film boiling test, clarify why the RELAP5YA sheath temperature data at the elevations shown on pp. 183-184 of Reference 12 underpredicts the temperature during the period immediately after CHF occurs. There is some confusion in the curves on these two pages where the same curve changes from a dashed line on the left part of the graph to a solid on the right and the data and RELAP5YA curves apparently cross.

A.VII.14

The underprediction by RELAP5YA of the temperature in the THTF Test 3.08.6C during the period immediately after CHF is due to the fact that CHF is predicted to occur by about 0.5 to 1 second later than the experimental data. The data curves and RELAP5YA curves are shown more clearly in the attached figures.

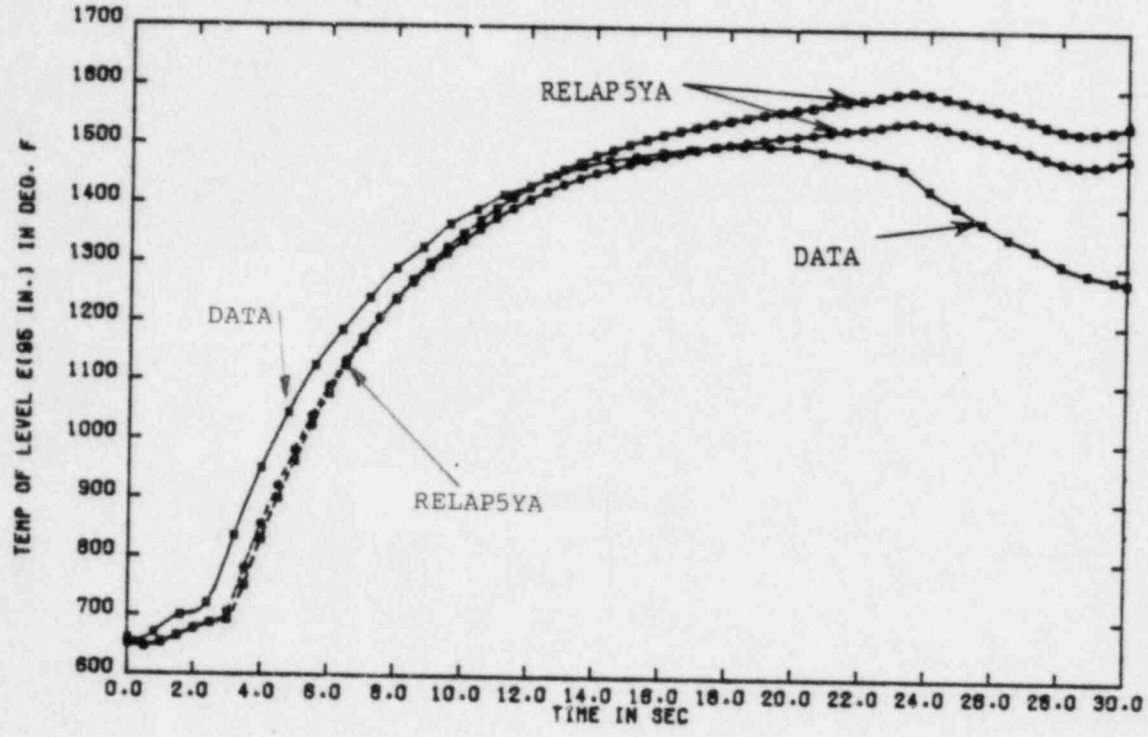


Figure 5.1-9: FRS Inner Sheath Temperature at Level E(95in.)

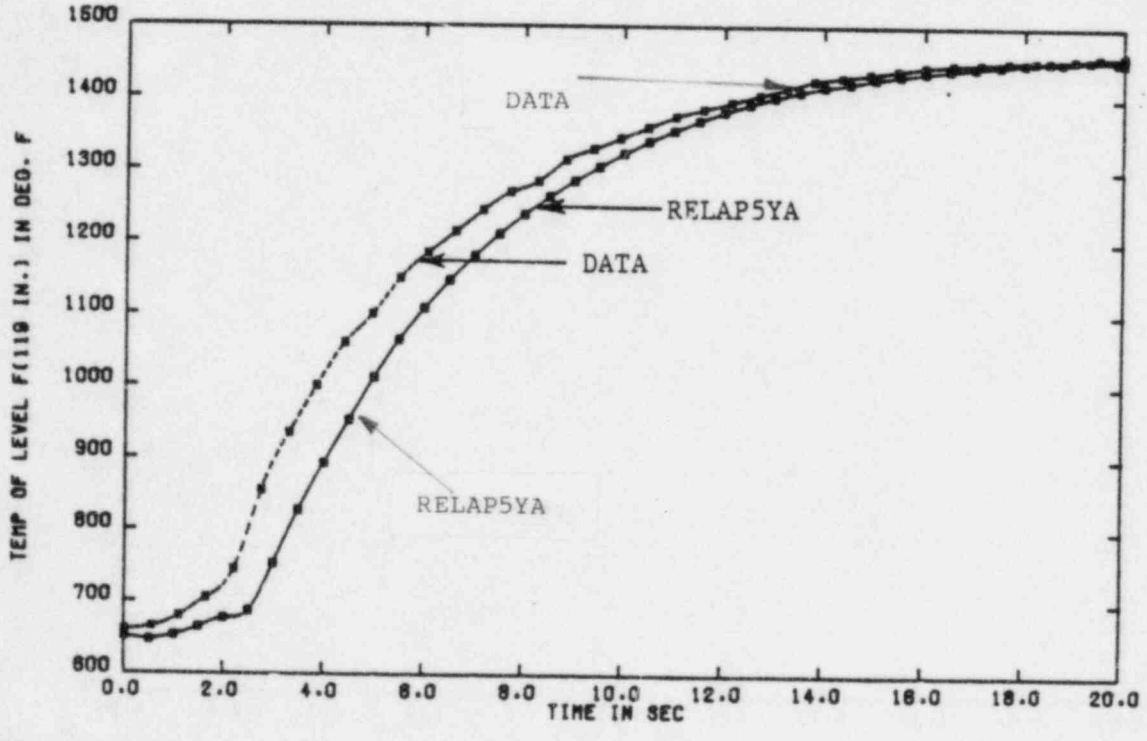


Figure 5.1-10: FRS Inner Sheath Temperature at Level F(119in.)

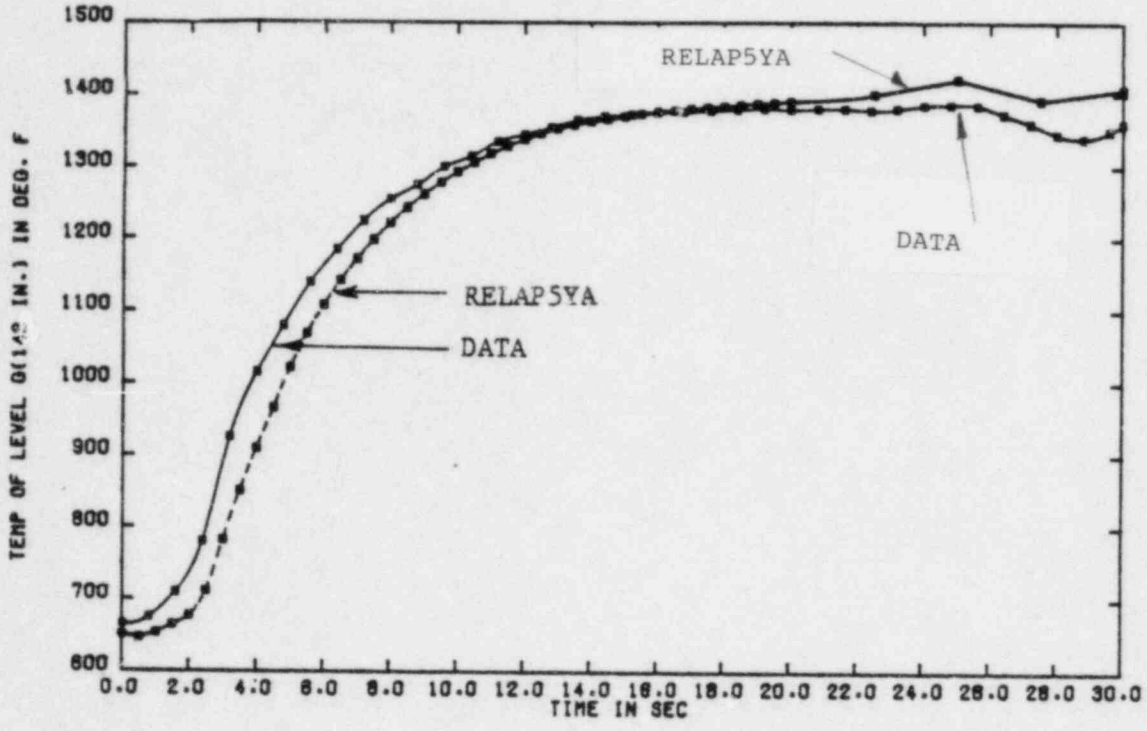


Figure 5.1-11: FRS Inner Sheath Temperature at Level G(142 3/4 in.)

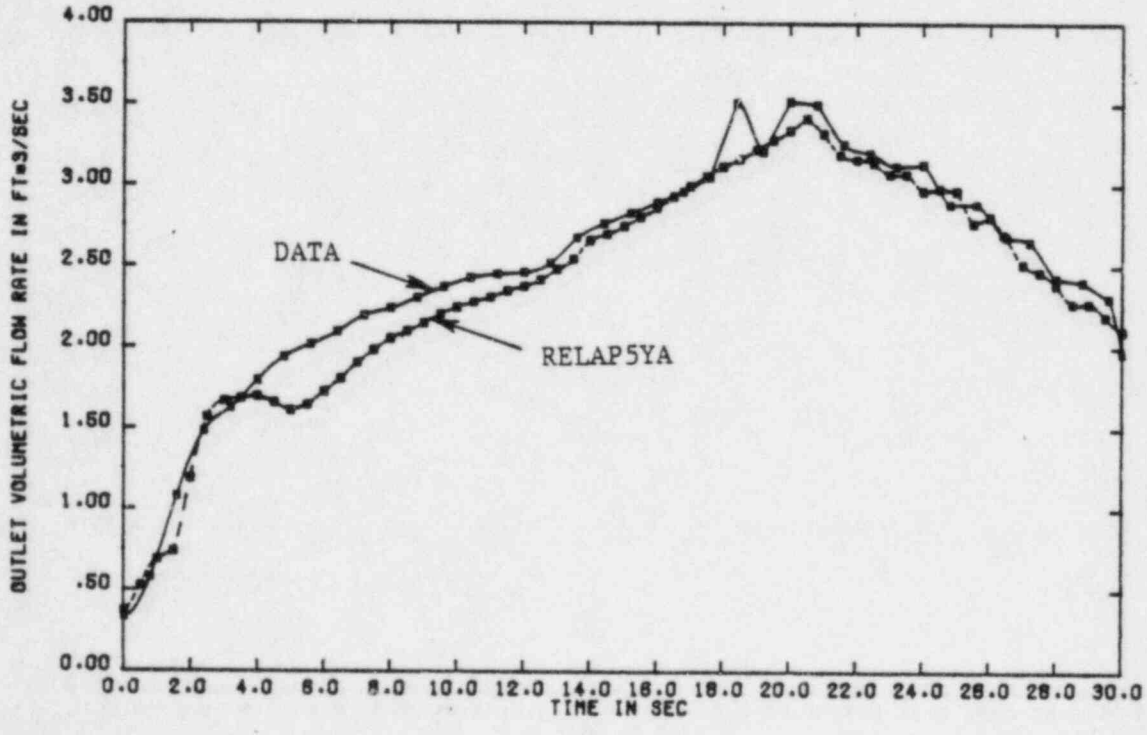


Figure 5.1-12: Comparison of Measured And Calculated Outlet Volumetric Flow

Q.VII.15 Clarify what causes the shape of the outlet fluid temperature curve after 22 s as shown in Figure 5.1-13 of Reference 12.

A.VII.15

The increase in the outlet fluid temperature, which occurs in both the test and the RELAP5YA predictions, is due to the fact that the pump was tripped at 20 seconds in the transient. The inlet flow rate fell quickly after the pump was shut off. At 21 seconds, the bundle power was reduced from 7.8 MW to approximately 3.4 MW over a 4-second time interval. The inlet flow rate dropped faster than the power. This resulted in the power flow mismatch that produced a fluid temperature excursion.

Q.VII.16

For the quasi-steady-state boil-off test, Figure 5.1-15 of Reference 12 shows the RELAP5YA void fraction is greater than the data above the 4-foot elevation. Page 169 of Reference 12 states: "This figure indicates that the interphase drag values calculated by RELAP5YA may have been somewhat high beyond the 4-foot elevation for this assessment case." Clarify why this is true because it would seem that high drag values would cause more liquid to be carried upward and therefore give lower rather than higher void fractions.

A.VII.16

The RELAP5YA calculation for this test started with a full bundle with constant inlet flow and bundle power. A very slow boil-off transient of 380 seconds was run until the outlet steam flow matched the bundle inlet flow. The high drag values at the upper elevations entrained more liquid out of the bundle during the boil-off transient. The void profile presented in Figure 5.1-15 of Reference (VII.16-1) established at about 50 seconds in the transient. We can infer that RELAP5YA calculated higher drag values than existed in the test which caused a substantial part of the initial liquid inventory to leave the bundle. Hence, more of the bundle is dry and the calculated void fractions are higher.

Reference

(VII.16-1) Fernandez, R. T., R. K. Sundaram, J. Ghaus, A. Husain, J. N. Loomis, L. Schor, R. C. Harvey and R. Habert, "RELAP5YA - A Computer Program for Light-Water Reactor System Thermal-Hydraulic Analysis, Volume III: Code Assessment," Yankee Atomic Electric Company Report YAEC-1300P, Volume III, October 1982. (Proprietary)

Q.VII.17

Page 169 of Reference 12 also states: "A dryout CHF is calculated to occur at a much lower elevation that corresponds to the predicted two-phase mixture level in the bundle." Clarify how this statement is justified by the wall temperature and void fraction figures given on Page 186 of Reference 12.

A.VII.17

Figure VII.17-1 from Reference VII.17-1 indicates that the inferred mixture level for this test is at about 8.6-foot elevation. The RELAP5YA calculated mixture level at a void fraction of 0.96 is 4.6 feet as shown in Figure 5.1-15 of Reference VII.17-2. Figure 5.1-16 shows that RELAP5YA predicted a dryout CHF that corresponds to the predicted mixture level at 4.6 feet. The test report does not specifically give the CHF location. However, we assume the experimental CHF location occurred at the reported mixture level.

Reference

(VII.17-1) Anklam, T. M., et al., "Experimental Investigation of Uncovered Bundle Heat Transfer and Two-Phase Mixture Level Swell Under High Pressure, Low Heat Flux Conditions" (Final Report for THTF Tests 3.09.10I-N and 3.09.10AA-FF-DRAFT), Oak Ridge National Laboratory, September 1981.

(VII.17-2) Fernandez, R. T., R. K. Sundaram, J. Ghaus, A. Husain, J. N. Loomis, L. Schor, R. C. Harvey and R. Habert, "RELAP5YA - A Computer Program for Light-Water Reactor System Thermal-Hydraulic Analysis, Volume III: Code Assessment," Yankee Atomic Electric Company Report YAEC-1300P, Volume III, October 1982. (Proprietary)

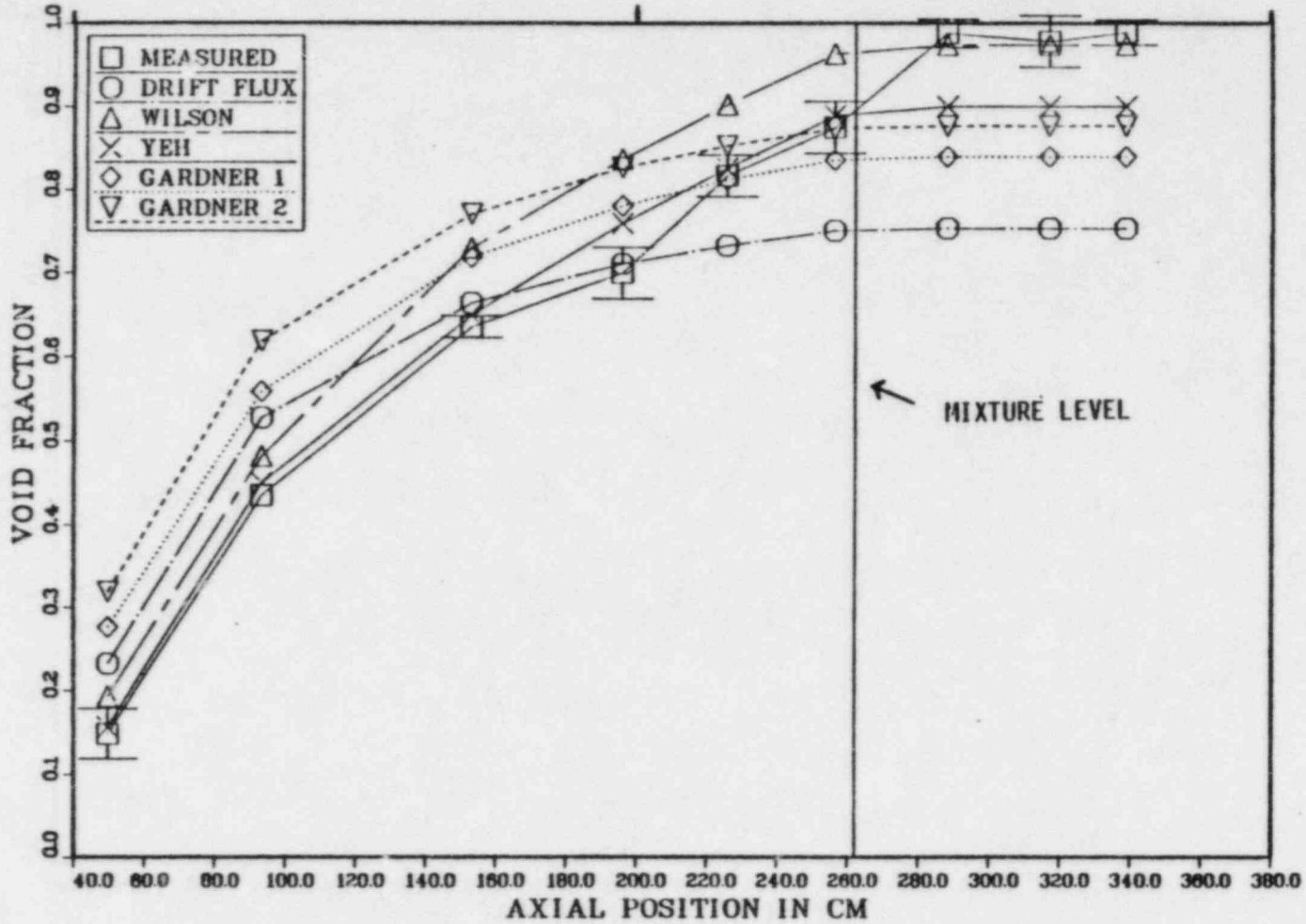


Figure VII.17-1 Experimental and Predicted Void Fraction Profiles; Test 3.09.101.

Q.VII.18

Pages 169-170 of Reference 12 state: "The above disparity between the calculated and measured results might be attributed to the method used in modeling this test. The RELAP5YA calculation resulted in a very slow boil-off transient with constant inlet flow and bundle power. The thermal power transferred to the fluid did not match the bundle power until 380 seconds into the transient. When they matched, the results were accepted as the values to compare to the test data. By this point in time, a substantial part of the initial liquid inventory was calculated to have left the system. In these experiments, power was applied to the bundle and then was reduced to produce peak FRS temperatures of about 1400°F (maximum temperature imposed by safety limits). The differences between the power histories applied to the bundle in the test (which are not reported), compared with the fixed power in the RELAP5YA simulation may account for the differences between the calculated and measured results." Clarify why this test was picked for assessment purposes if the power history was unknown.

A.VII.18

This test was selected because it was thought to represent a condition that might be encountered during SBLOCAs. The test procedure indicates that the bundle power and inventory were adjusted over a period of time until the loop stabilized. Then a 20-second data scan was taken. We simulated this test using the reported data that were obtained "after the loop was stabilized." We do not know what effect the previous unrecorded history might have had on the RELAP5YA results. However, RELAP5YA has a tendency to underpredict the two-phase mixture level for low flow conditions. This results in a conservative PCT response for slow boil-off situations expected during SBLOCA.

Q.VII.19

For the reflood tests discussed on Pages 170-172 of Reference 12: Clarify how quench level is measured.

A.VII.19

The quench level is determined based on the response of the FRS sheath thermocouple (Reference VII.19-1). For the THTF tests, the quench level is defined as the point during a reflood when precursory cooling stops and a precipitous drop in surface temperature begins (Figure VII.19-1).

Reference

(VII.19-1) Hyman, C. R., et al., "ORNL Small Break LOCA Heat Transfer Test Series II: High Pressure Bundle Boil-Off and Reflood Test Analysis" (Final Report for THTF Boil-Off and Reflood Tests 3.09.100-X-DRAFT), Oak Ridge National Laboratory, September 1981.

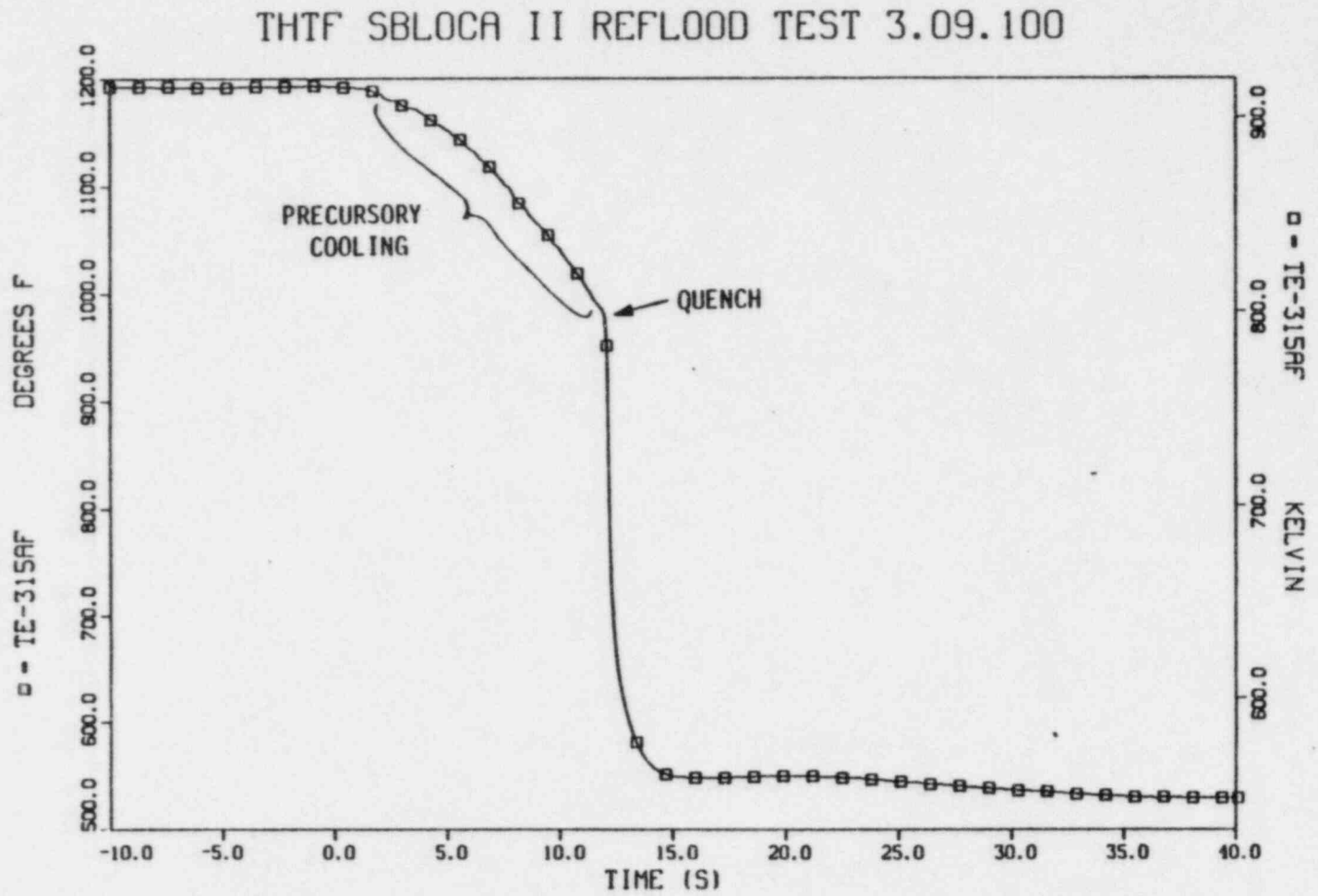


Figure VII.19-1 Example of Precursory Cooling and Quenching Indicated by FRS Sheath Thermocouple Response

Q.VII.20

Clarify how "the measured void profile at time zero was used to calculate the initial liquid and vapor velocities" (Page 170 of Reference 12).

A.VII.20

The dynamic quality at each nodal volume is calculated from an energy balance assuming thermal equilibrium. The phasic velocities and the static quality are determined from these dynamic qualities and the measured void fraction at these locations. To initialize the test, the following calculations were performed:

A. Dynamic quality in each node:

$$x(i) = \frac{Q \cdot z(i)}{\dot{m}\, h_{fg}} - \frac{h_{sub}}{h_{fg}} \qquad (1)$$

where:

$x(i)$ = "dynamic equilibrium" quality in each node

$z(i)$ = elevation of the node center from the bottom of the heated length (ft)

$h_{fg}$ = latent heat of vaporization ($\frac{Btu}{lb}$)

$h_{sub}$ = inlet subcooling ($\frac{Btu}{lb}$)

$Q$ = liner heat generation rate (Btu/ft-sec))

$\dot{m}$ = mass flow rate (lb/sec)

B. The slip ratio in each node:

$$S(i) = \frac{x(i)}{1 - x(i)} \cdot \frac{1 - \alpha(i)}{\alpha(i)} \frac{\rho_f}{\rho_g} \qquad (2)$$

where:

$\alpha(i)$ = nodal void fraction (from void fraction distribution at time "zero" from Reference VII)

$\rho_f$ = saturated fluid density ($lb/ft^3$)

$\rho_g$ = saturated vapor density ($lb/ft^3$)

C. Vapor velocity in each node:

$$V_g(i) = G\, x(i)/\rho_g \alpha(i) \tag{3}$$

we replace x(i) in (3) by

$$x(i) = \frac{\rho_g \alpha(i)\, S}{\rho_g \alpha(i) S + \rho_f (1 - \alpha(i))} \tag{4}$$

where:

$$S = V_g/V_f \tag{5}$$

to get:

$$V_g(i) = G/[\rho_g \alpha(i) + \rho_f (1 - \alpha(i))/S]$$

D. Liquid velocity:

$$V_f(i) = V_g(i)/S \tag{6}$$

F. Static quality:

$$x_s(i) = \frac{1.0}{1.0 + \frac{\rho_f}{\rho_g} \frac{(1 - \alpha(i))}{\alpha(i)}} \tag{7}$$

The values of $V_g(i)$, $V_f(i)$ $x_s(i)$, calculated above are used for the initial conditions.

Q.VII.21

Clarify why the liquid mass inventory peak agrees almost exactly with the data at 17.5 s in Figure 5.1-18 of Reference 12 when the calculated collapsed liquid level at 17.5 s in Figure 5.1-19 of Reference 12 is significantly below the data.

A.VII.21

The test data and calculation have been re-examined to address this question. According to Reference VII.21-1, the local void profile in the heated bundle was determined from the nine differential pressure transducers. This experimental void profile is compared to that calculated by RELAP5YA in Figure 5.1-17 of Reference VII.21-2. These two void profiles agree reasonably well at 20 seconds. The experimental void profile was then used to calculate the collapsed liquid level at 20 seconds. This calculation yields a value of 124.9 inches which compares well with the RELAP5YA value of 125.0 inches. However, it is substantially lower than the 134.3-inch collapsed liquid level at 20 seconds in the test report. We have not been able to account for this discrepancy in the reported test data. Finally, the test report states that the liquid mass in the heated bundle was calculated by the following formula:

$$M_{liquid} = \rho_f A_{flow} Z_{CLL}$$

where:

$\rho_f$ = saturated liquid density

$A_{flow}$ = bundle flow area

$Z_{CLL}$ = collapsed liquid level

Their use of the saturated liquid density (47.5 lbm/ft$^3$ at 20 seconds) does not account for the more dense subcooled liquid (50 to 55 lbm/ft$^3$ at 20 seconds) in the bundle below the two-phase region. However, their collapsed liquid levels appear to be too large. Nevertheless, the product yields a liquid mass of 35.4 lbm versus 34.9 lbm calculated by RELAP5YA at 20 seconds.

References

(VII.21-1) Hyman, C. R., et al., "ORNL Small Break LOCA Heat Transfer Test Series II: High Pressure Bundle Boil-Off and Reflood Test Analysis" (Final Report for THTF Boil-Off and Reflood Tests 3.09.10O-X-DRAFT), Oak Ridge National Laboratory, September 1981.

(VII.21-2) Fernandez, R. T., R. K. Sundaram, J. Ghaus, A. Husain, J. N. Loomis, L. Schor, R. C. Harvey and R. Habert, "RELAP5YA - A Computer Program for Light-Water Reactor System Thermal-Hydraulic Analysis, Volume I: Code Description," Yankee Atomic Electric Company Report YAEC-1300P, Volume I, October 1982. (Proprietary)

Q.VII.22

Clarify why the peak in the liquid mass inventory is predicted almost exactly by RELAP5YA for Test 3.09.100 and yet is significantly underpredicted for Test 3.09.10Q.

A.VII.22

The saturated versus subcooled liquid densities are about 9.5% different for reflood test 3.09.100. The collapsed liquid levels versus those determined from the void profile test data are about 5% to 7.5% different.

Both the liquid density and collapsed liquid level enters the determination of liquid inventory in the bundle. Therefore, the combined uncertainty in the reported inventory is about $\pm$11%. The calculated liquid inventory for both reflood tests are within $\pm$11% of the test data, and show the same distinct trends as the experimental data.

Q.VII.28

Page 142 of Reference 11 states that for medium flow ranges the maximum of the high and low flow heat-transfer correlations is used. This

applies for subcooled or saturated transition boiling, subcooled or saturated film boiling, saturated film boiling or forced convection of superheated vapor. Clarify why this procedure is conservative if the maximum of the two correlations is used.

A.VII.28

The RELAP5YA heat transfer correlations are meant to be best-estimate correlations rather than provide conservatism. In licensing analyses, YAEC will use these correlations along with EM assumptions to ensure that heat transfer from the rods will be calculated conservatively. The logic used in the RELAP5YA selection of heat transfer correlations essentially uses a set of "high-flow" correlations with a lower bound provided by a set of "low-flow" correlations. This is because the high-flow correlations are not applicable at very low mass fluxes. The selection of the maximum of the two sets of correlations ensures that the correlations are used in their applicable ranges of flow rates.

Q.VII.29

Clarify how the reflood model has been assessed for falling film from the top and for bottom quench.

A.VII.29

The reflood model has been assessed by modeling two separate effect tests for the bottom quench, and three integral tests which included both falling film and bottom quench.

The separate effects tests are the THTF tests 3.09.10O and 3.09.10Q. The integral tests are test TLTA 6425/2, TLTA 6441/6, and LOFT L8-1.

Q.VII.30

Clarify how closely the assessment conditions match the expected possible SBLOCA reactor conditions.

The reflood tests used for the assessment of the bottom quench were part of the second series of PWR Small Break Loss Of Coolant Accidents (SBLOCA) conducted at Oak Ridge National Laboratory in the Thermal-Hydraulic Test Facility (THTF). The objective of the reflood tests was to study bundle quenching behavior under conditions of system pressure, linear power and flooding rate expected in a SBLOCA. Five reflood tests were performed from which two were selected for assessment.

Table VII.30-1 summarizes the parameters for the reflood SBLOCA II THTF tests. Average inlet flooding velocities in SBLOCA II ranged from a low of 2.33 in/sec to a high of 4.82 in/sec. Initial system pressure ranged from 563 psia to 1092 psia. Linear power ranged from 0.304 kW/ft to 0.659 kW/ft).

The tests chosen (underlined in Table VII.30-1) were at low pressure and at various flooding velocity and liner power, conditions which are expected to occur during a SBLOCA in the plants modeled.

All the integral tests used in the assessment of RELAP5YA used the quench model option at ECCS initiation. Since these were transient tests, the conditions in the test facilities varied with time. A detailed account of the integral test conditions are presented in Reference VII.30-1.

TABLE VII.30-1

Summary of Initial Conditions for Reflood Tests

| Test No. | Pressure [MPa (psia)] | Linear Heat Rate (LHR) [kW/m (kW/ft)] | Bundle Mass Flow [kg/s (lbm/s)] | Inlet Subcooling [K ($^{o}$F)] | Outlet Superheat [K ($^{o}$F] | Maximum FRS Temperature [K ($^{o}$F)] |
|---|---|---|---|---|---|---|
| 3.09.10O | 3.88 (563) | 2.03 (0.618) | 0.156 (0.343) | 74 (134) | 198 (356) | 1055 (1440) |
| 3.09.10P | 4.28 (621) | 1.10 (0.304) | 0.075 (0.164) | 65 (117) | 209 (377) | 1089 (1500) |
| 3.09.10Q | 3.95 (573) | 1.02 (0.311) | 0.078 (0.172) | 66 (118) | 168 (303) | 1027 (1390) |
| 3.09.10R | 7.34 (1065) | 2.16 (0.659) | 0.170 (0.373) | 113 (203) | 133 (239) | 1033 (1400) |
| 3.09.10S | 7.53 (1092) | 1.38 (0.421) | 0.085 (0.188) | 105 (189) | 164 (295) | 1077 (1480) |

Reference

(VII.30-1) Fernandez, R. T., R. K. Sundaram, J. Ghaus, A. Husain, J. N. Loomis, L. Schor, R. C. Harvey and R. Habert, "RELAP5YA - A Computer Program for Light-Water Reactor System Thermal-Hydraulic Analysis, Volume III: Code Assessment," Yankee Atomic Electric Company Report YAEC-1300P, Volume III, October 1982. (Proprietary)

Q.VII.31

Clarify how the ability of the quench-front velocity model to track the quench front has been assessed and under what conditions it has been assessed.

A.VII.31

The quench-front velocity model, which is based upon Reference VII.31-1, is part of the Rewet-Quench Model (Reflood Model). The assessment of this model was clarified in A.VII.29.

Reference

(VII.31-1) Andersen, J. G. M., et al., "NORCOOL - A Model of Analysis of a BWR Under LOCA Conditions," NORHAV-D-32, Research Establishment, R150, Denmark, December 1976.

Q.VII.32

Appendix K Requirement I.D.3 includes the requirement that: "The effects on reflooding rate of the compressed gas in the accumulator which is discharged following accumulator water discharge shall also be taken into account" (Page 269 of Reference 10). Clarify how the effects of the noncondensible gas are included in the reflood models.

Compressed gas in the accumulators will only be discharged for those LOCAs which are large in size and do not depend upon the steam generators for the removal of decay heat. Therefore, the degradation of steam generator heat transfer as a result of U-tube blanketing is of no concern.

For these larger SBLOCAs, the following scenarios may be postulated:

a. Cold Leg Break

Nitrogen, due to its lighter density, would either stay in the cold leg or upper portions of the downcomer while finding its way to the break via the downcomer annulus. If the break size is large enough, the nitrogen venting will not impact the core at all. However, for smaller breaks, the upper downcomer annulus may temporarily be pressurized which may depress the water level in the downcomer and transfer some liquid to the core. This liquid transfer to the core will cause quenching of that portion of the core which may not have already been quenched.

b. Hot Leg Break

The nitrogen injected will collect into the upper downcomer region. If leakage paths are available to the upper head or the upper plenum, the nitrogen will migrate to these regions on its way to the break. The core will be unaffected during this period.

If no such leakage path is available, the nitrogen may leak via the suction leg with no impact on the core. Some of the nitrogen in this case may also bubble through the core via the downcomer. This scenario will experience a swelling of the core level and consequently quenching of those portions of the core which are still unquenched.

c. Suction Leg Break

This break will be covered under scenarios (a) and (b).

Thus, we conclude that the compressed gas in the accumulator which is discharged following accumulator depletion is expected to have no negative impact on the outcome of a SBLOCA and is not considered in our calculations.

Q.VII.40

Clarify what effect the following two assumptions given on Page 244 of Reference 10 have on the temperatures calculated: "Fuel rod deformation does not affect radii used in heat conduction and convection except in the gap region." "Zircaloy-water reaction does not change material properties of cladding."

A.VII.40

This question requests clarification of the effect of two assumptions made in fuel behavior modeling.

The first assumption is that "fuel rod deformation does not affect radii used in heat conduction and convection except in the gap region." For the majority of SBLOCA cases, clad rupture does not occur. Fuel rod deformation is small and the effect on temperatures is truly negligible. For cases in which clad temperatures approach or exceed rupture temperature, clad swelling can be significant. However, in this case, the increased fuel rod surface area available for heat removal is conservatively neglected.

The second assumption is that "zircaloy-water reaction does not change material properties of cladding." This assumption is not expected to have much effect for the results of cases in which zircaloy-water reaction is small. However, the RELAP5YA fuel behavior model is being modified to include oxide conductivity and heat capacity when cladding is oxidized.

Q.VII.41

Page 268 of Reference 10 states: "During small breaks, the fluid velocity in the core region is expected to be small. Various regions in the core are expected to communicate with each other and the fluid conditions at various radial locations are not expected to be significantly different at a given elevation. The entire core, therefore, may be represented by an average core for small break calculations." Clarify for very low flows that could occur during loss of natural circulation in the loops during a SBLOCA why the fluid conditions in the high power regions could not be significantly different than in the low power regions.

A.VII.41

The difference in fluid conditions between the high and low reactor power regions during low flow conditions will depend upon the core loading schemes. For textbook type cases utilizing homogeneous fuel loading schemes, the power generation will be the lowest at the core periphery and will monotonically increase toward the center of the core. For such radial power profiles, the fluid conditions in the high and low power regions are going to be different. Also, for canned fuel assemblies, the fluid conditions will depend upon the assembly power due to the lack of free communication with the adjacent bundles.

Fuel assemblies used in PWRs do not use assembly cans and experience free fluid communication with the adjacent bundles. Also, the fuel management schemes try to achieve uniform radial power generation rates throughout the core. Figures VII.41-1 and VII.41-2 provide typical assembly radial peaking factors for the Yankee plant at Rowe and Maine Yankee, respectively. For the Yankee plant, Assembly 47 is the peak power assembly with a radial peaking factor of 1.3033. However, if one takes a region of 9 assemblies around Assembly 47 (Assemblies 36, 37, 38, 46, 47, 48, 56, 57 and 58) the average radial peaking is only 1.002. For the Maine Yankee plant, quarter assembly 65 is the peak power quarter assembly with a radial peaking factor of 1.32240. It

resides in assembly comprised of quarter assemblies 51, 52, 64 and 65. However, if one takes a region of 8 assemblies around the hot assembly (quarter assemblies 27, 28, 29, 30, 38, 39, 40, 41, 49, 50, 51, 52, 53, 54, 62, 63, 64, 65, 66, 67, 77, 78, 79, 80, 81, 82, 92, 93, 94, 95, 96 and 97) the average radial peaking is only 0.95.

We conclude that the entire core, therefore, may be represented by an average core for small break calculations.

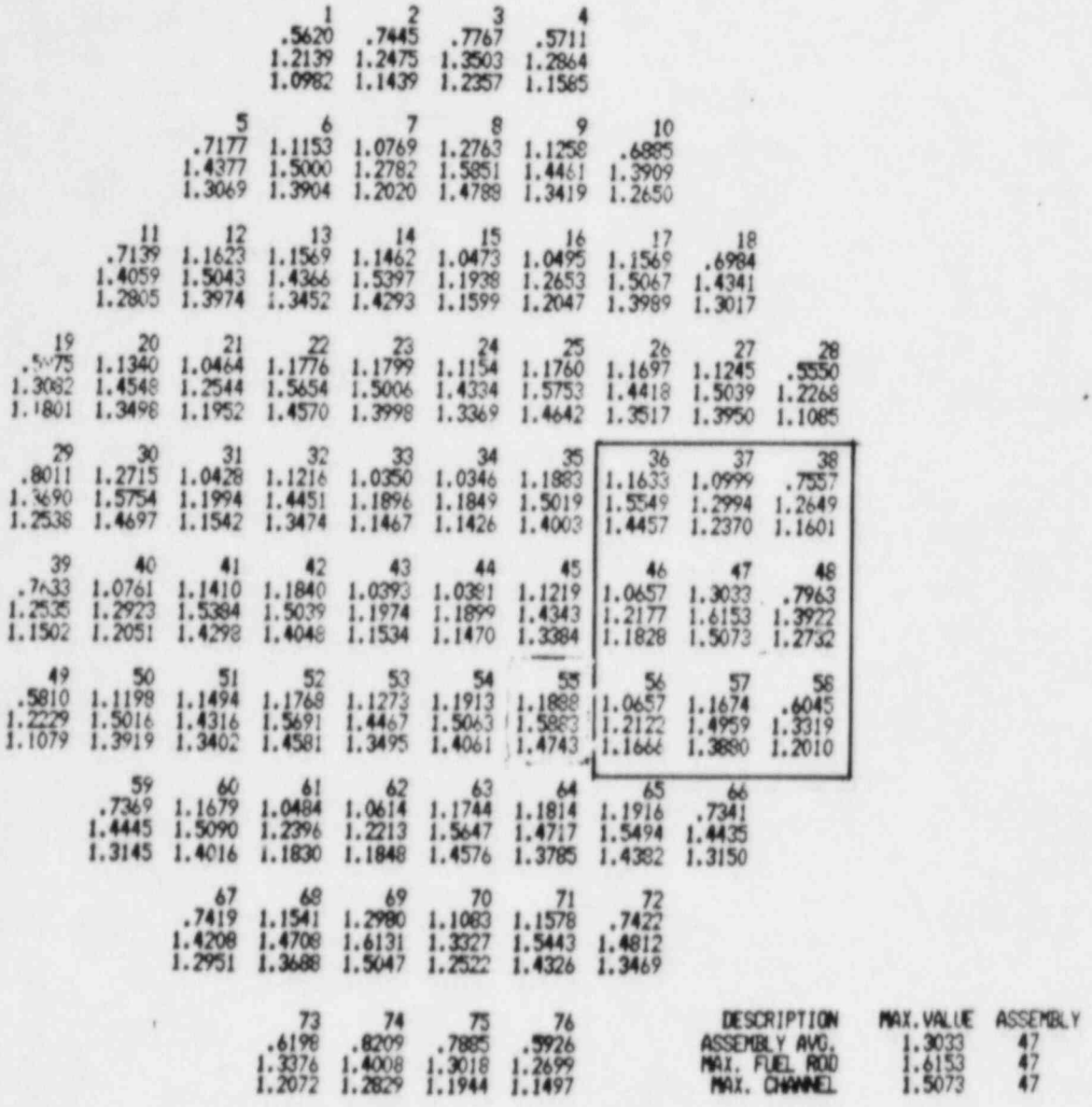


Figure VII.41-1 Typical Assembly Radial Power Peaking Factor for The Yankee Plant

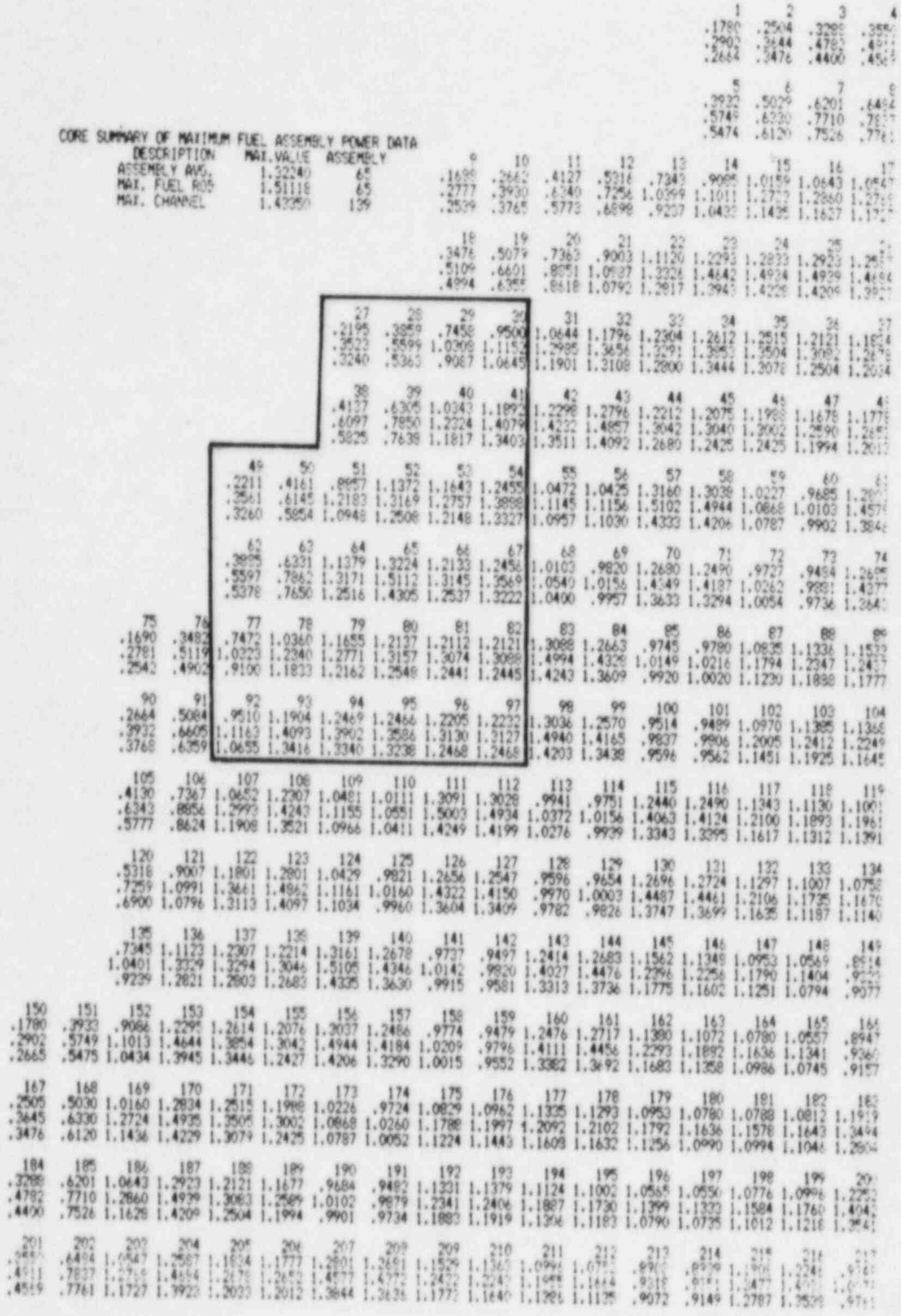


Figure VII.41-2 Typical Quarter Assembly
Radial Power Peaking Factor
For The Maine Yankee Plant

## VIII. METAL HEAT

Q.VIII.1

Clarification and justification should be given for the metal slabs associated with all of the nodes used in all SBLOCA-related analyses.

A.VIII.1

Figures IV.2-1 and IV.2-2 represent the nodalization used in the pump trip studies performed for the Maine Yankee plant and the Yankee plant at Rowe, respectively. Similar noding schemes will be employed for the small break calculations. As is seen, Yankee uses a detailed nodalization of the plant. Also, the noding does include the representation of the reactor vessel wall, the piping wall and other major internal structures present in the plant.

A list of metal slabs used at various nodes will be provided with each plant application. Clarification and justification of metal structures not represented in the analysis will also be provided at that time.

Q.VIII.2

Clarify especially the modeling to be used for the pressurizer walls, upper head and upper part of the steam generator U-bends because these areas will affect the pressure during the SBLOCA refill processes.

A.VIII.2

The pressurizer wall and the reactor vessel wall in the upper head region will be modeled in our analyses. In addition, the major heat structures present in the upper head region will also be represented.

The steam generator U-tube model is shown in Figures IV.2-1 and IV.2-2 for the Maine Yankee plant and the Yankee plant at Rowe, respectively. The U-tube region has been nodalized in detail and the U-tube bend region is explicitly represented by two heat structures.

## IX. BREAK FLOW

Q.IX.5

Break flow depends on conditions of the fluid reaching the break. If HPI or accumulator flow is not injected into the cold leg with the break, then the resulting break flow will be very different in the model from the actual transient because of the difference in void fraction and temperature of the fluid at the break. Also, HPI and accumulator water injected into the intact cold legs that bypasses the core and goes out the break needs to be modeled to accurately model break flow. Clarify how the treatment of HPI and accumulator flows affects the break flows calculated.

A.IX.5

Figures IV.2-1 and IV.2-2 represent the nodalization used in the pump trip studies performed for the Maine Yankee plant and the Yankee plant at Rowe, respectively. Similar noding schemes will be used for small break calculations. As seen in these figures, the cold legs are modeled in detail for the two plants. The ECC has been modeled to inject into the cold legs very close to their actual injection points. The break is modeled in the injection node. This nodalization maximizes the amount of ECC flow going out of the break and minimizes the depressurization rate due to the presence of two-phase fluid at the break location. Therefore, we model the ECC locations accurately and select the break at a conservative location.

Q.IX.7

Clarify for stratified flow which critical flow model is applied above the interface and which is applied below it and how any switching process between the models is modeled.

A.IX.7

When critical flow is determined to exist at a junction, then the code selects the appropriate critical flow model based upon the junction void fraction, $\alpha_j$. The determination of the junction void fraction for stratified flow is discussed in the answer to question Q.VI.7. For $\alpha_j < 0.05$, the Subcooled Critical Flow Model is selected. For $\alpha_j \geq 0.05$, either the Moody or the RELAP5YA Standard Two-Phase Critical Flow Model is used depending upon the option selected by the user. If the junction void fraction lies within the transition region defined by $0.01 < \alpha_j < 0.1$, then the underrelaxation scheme defined on Page 90, Appendix A of Reference IX.7-1 is used.

Reference

(IX.7-1) Fernandez, R. T., R. K. Sundaram, J. Ghaus, A. Husain, J. N. Loomis, L. Schor, R. C. Harvey and R. Habert, "RELAP5YA - A Computer Program for Light-Water Reactor System Thermal-Hydraulic Analysis, Volume I: Code Description," Yankee Atomic Electric Company Report YAEC-1300P, Volume I, October 1982. (Proprietary)

Q.IX.8

Deleted.

Reference

(IX.8-1) Memo, Ed D. Throm, Reactor System Branch DSI to Brain W. Sheron, Chief, Reactor System Branch, DSI, "Summary of 6/22/84 YAEC-NRC Meeting on RELAP5YA PWR SBLOCA EM Analysis," July 17, 1984.

Q.IX.9

Clarify why the calculation showed more depressurization than the data between 10 and 60 for Marviken Test 10 and yet the calculated break flow was lower than the data for this same period (pp. 39-40 of Reference 12).

The original RELAP5YA case underpredicted the pressure and escaped mass at 60 seconds because the initial liquid level in the vessel was incorrectly set too low at 17.06 meters rather than 17.66 meters. This input error has been corrected, and the two cases (RELAP5YA Standard Critical Flow Model and RELAP5YA Moody Critical Flow Model) have been rerun. Revision 1 for Figures 2.2-12 through 2.2-19 are attached. These revised figures also contain data uncertainty bars, where possible, from information now available in Reference IX.9-1.

The maximum error in the vessel pressure measurement has been estimated by the Marviken staff to be ±90 kPa (Page 50, Reference IX.9-1). Figure 2.2-12, Revision 1 shows that the new dome pressure overlays the test data from 5 to 65 seconds. The calculation did not predict the pressure undershoot between 0 and 5 seconds that has been attributed to delayed nucleation in the vessel, nor the brief return to subcritical flow during this period. Therefore, the blowdown period was calculated to be about 2.5 seconds longer as shown on Figure 2.2-12 near 70 seconds.

Figure 2.2-13, Revision 1 compares the calculated break flow rate to that derived from the Pitot Static Method by the Marviken staff. They have estimated the error for this method falls within ±8 to ±15 percent in the two-phase region (Page 48, Reference IX.9-1). Based upon this, we have placed ±10 percent uncertainty bars on this test data. Figure 2.2-12, Revision 1 shows the calculated break flow rate lies within the data uncertainty from 10 to 65 seconds.

Figure 2.2-13A compares the calculated break flow rate to that derived from the Vessel Inventory Method by the Marviken staff. They have estimated the error limit to be ±6 percent for periods of slowly decreasing mass flux and ±12% for periods with more rapid changes in mass flux which occurs prior to 10 seconds in certain tests with 500 mm nozzles (e.g., Test 10). Also, they state this method is not valid when the vessel level drops below 2.3 meters above the bottom. Test data shows this occurred at 57 seconds in Test 10. The comparison

shows the calculated break flow rates agree very well with this test data between 10 to 57 seconds.

Therefore, we conclude that RELAP5YA calculates the two-phase critical flow rate and pressure history from 10 to 65 seconds very well for this test based upon these comparisons to test data with uncertainty bars.

Reference

(IX.9-1) The Marviken Full Scale Critical Flow Tests: Summary Report, Joint Reactor Safety Experiments in the Marviken Power Station Sweden, NUREG/CR-2671, MXC-301, U.S. Nuclear Regulatory Commission, May 1982.

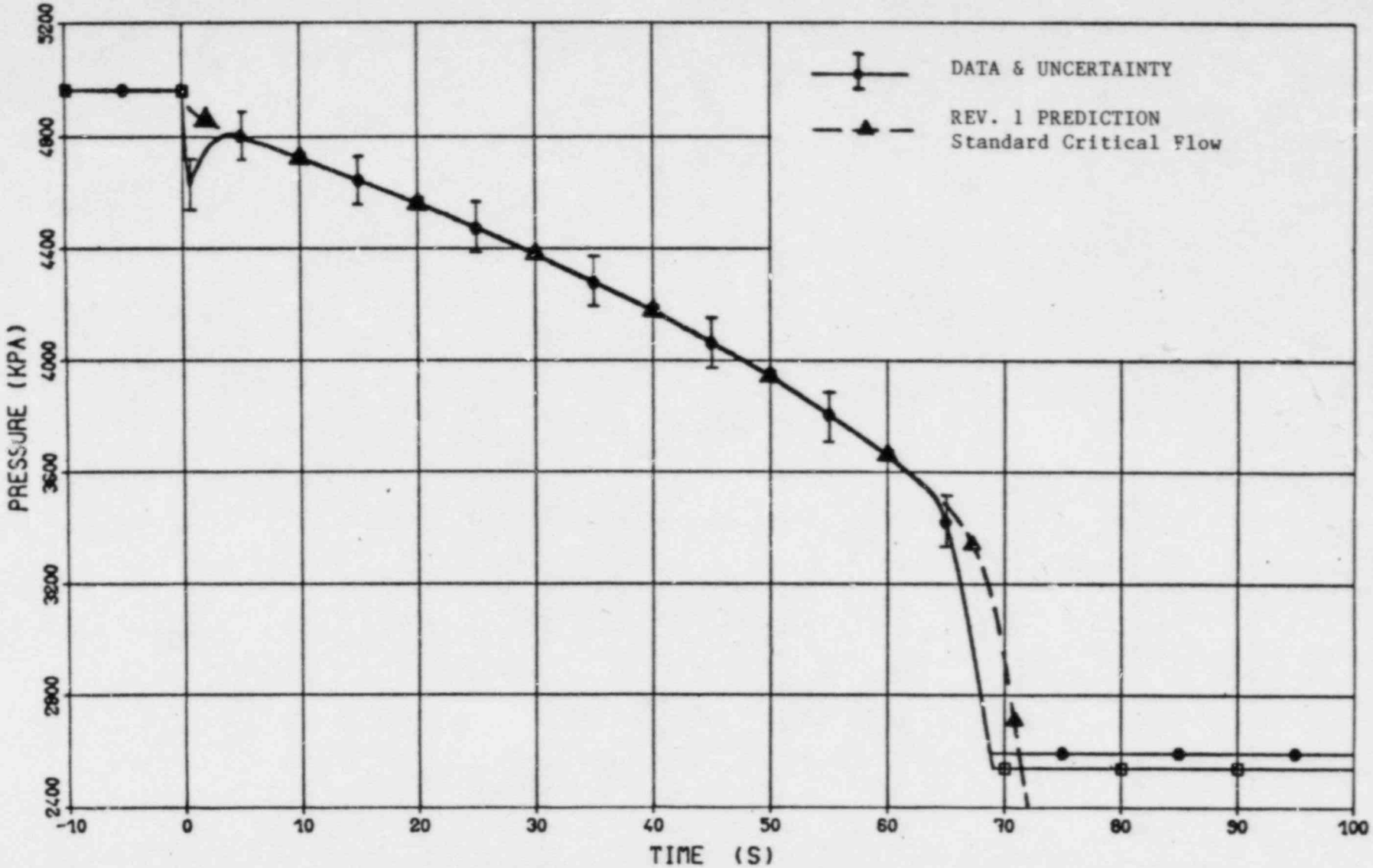


Figure 2.2-12 Marviken Test 10 Dome Pressure
RELAP5YA Standard Critical Flow Model Predictions-Rev. 1

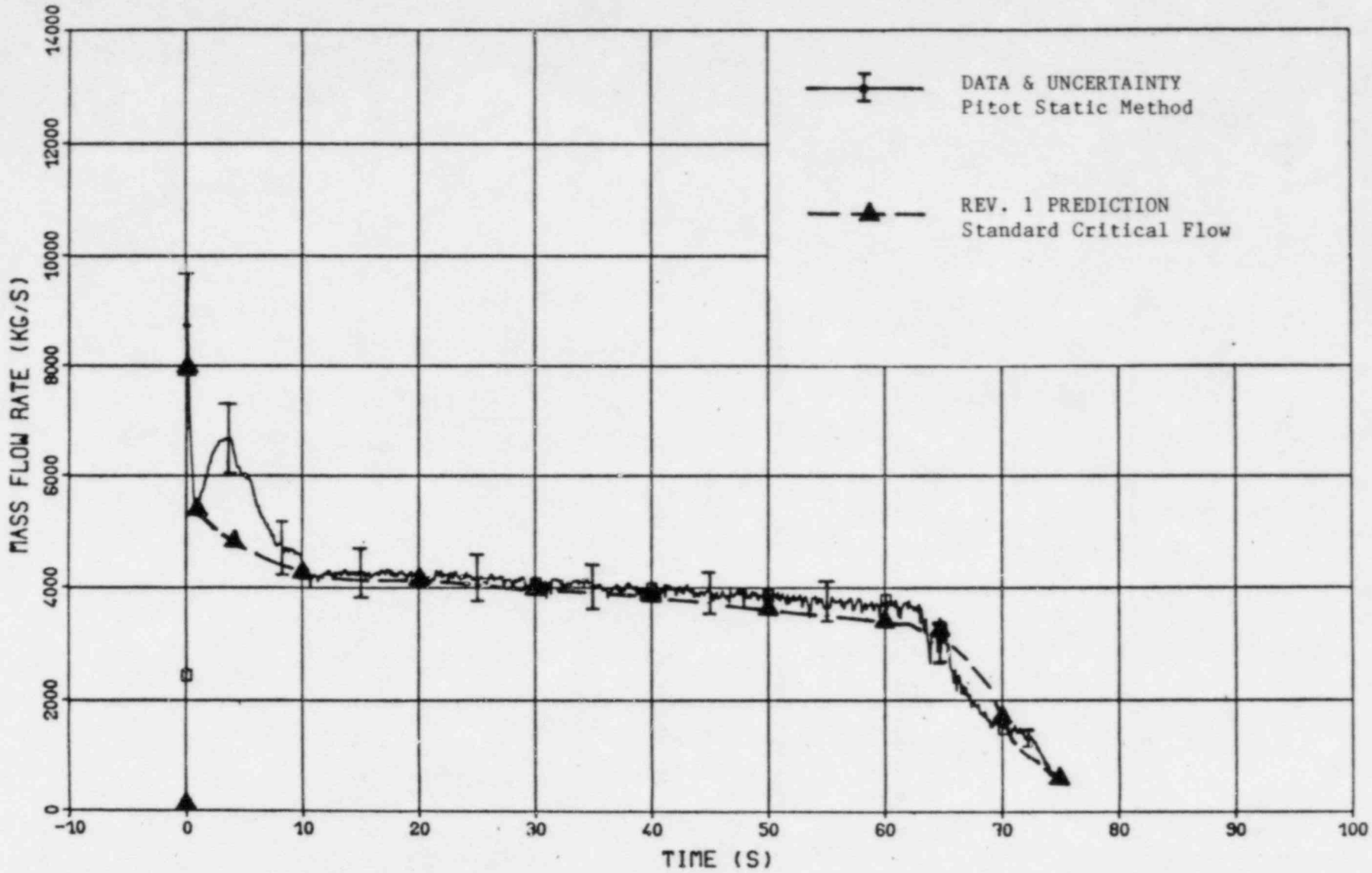


Figure 2.2-13 Marviken Test 10 Break Flow Rate
RELAP5YA Standard Critical Flow Model Predictions-Rev.1

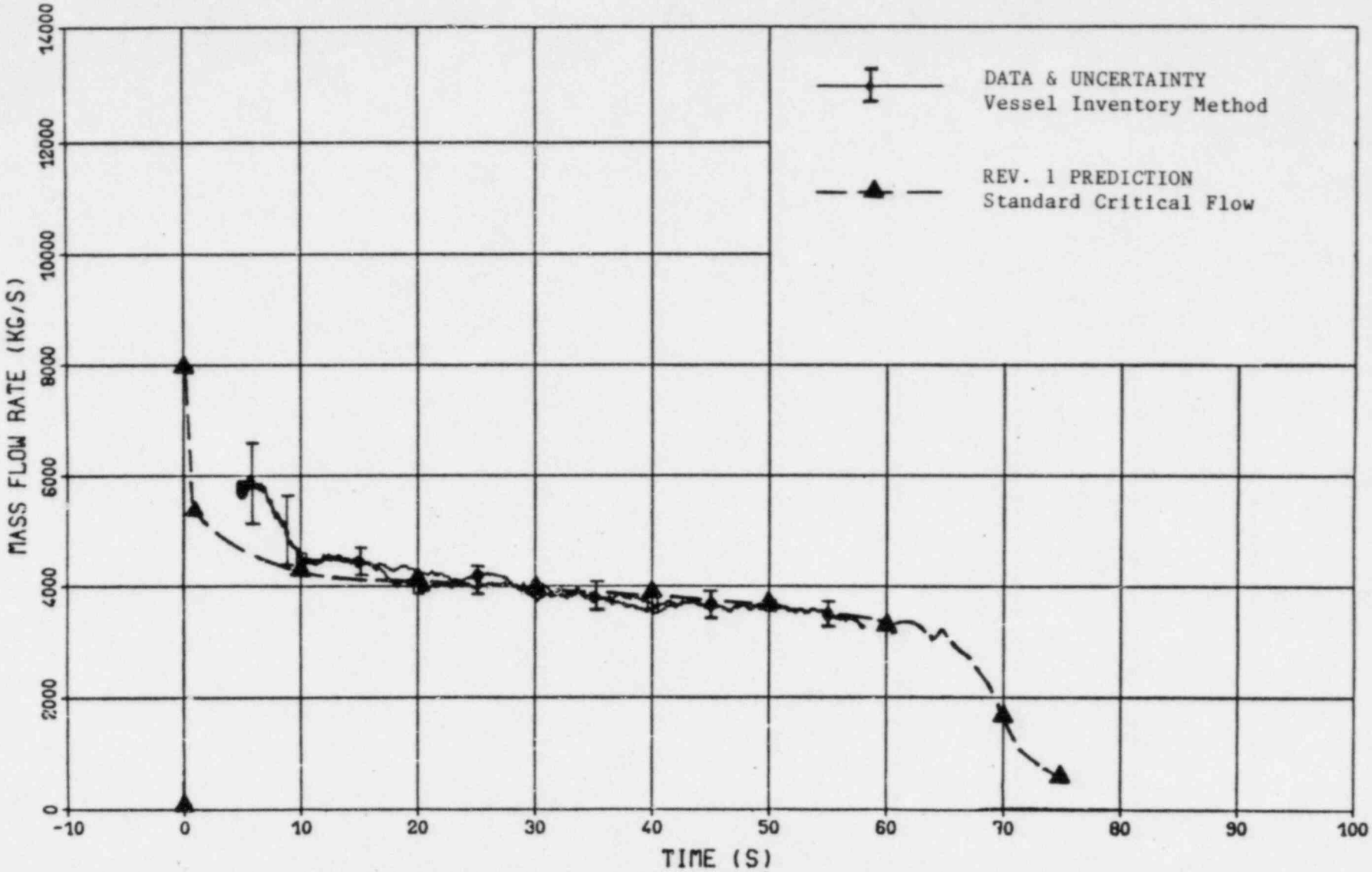


Figure 2.2-13A Marviken Test 10 Break Flow Rate
RELAP5YA Standard Critical Flow Model Predictions-Rev. 1

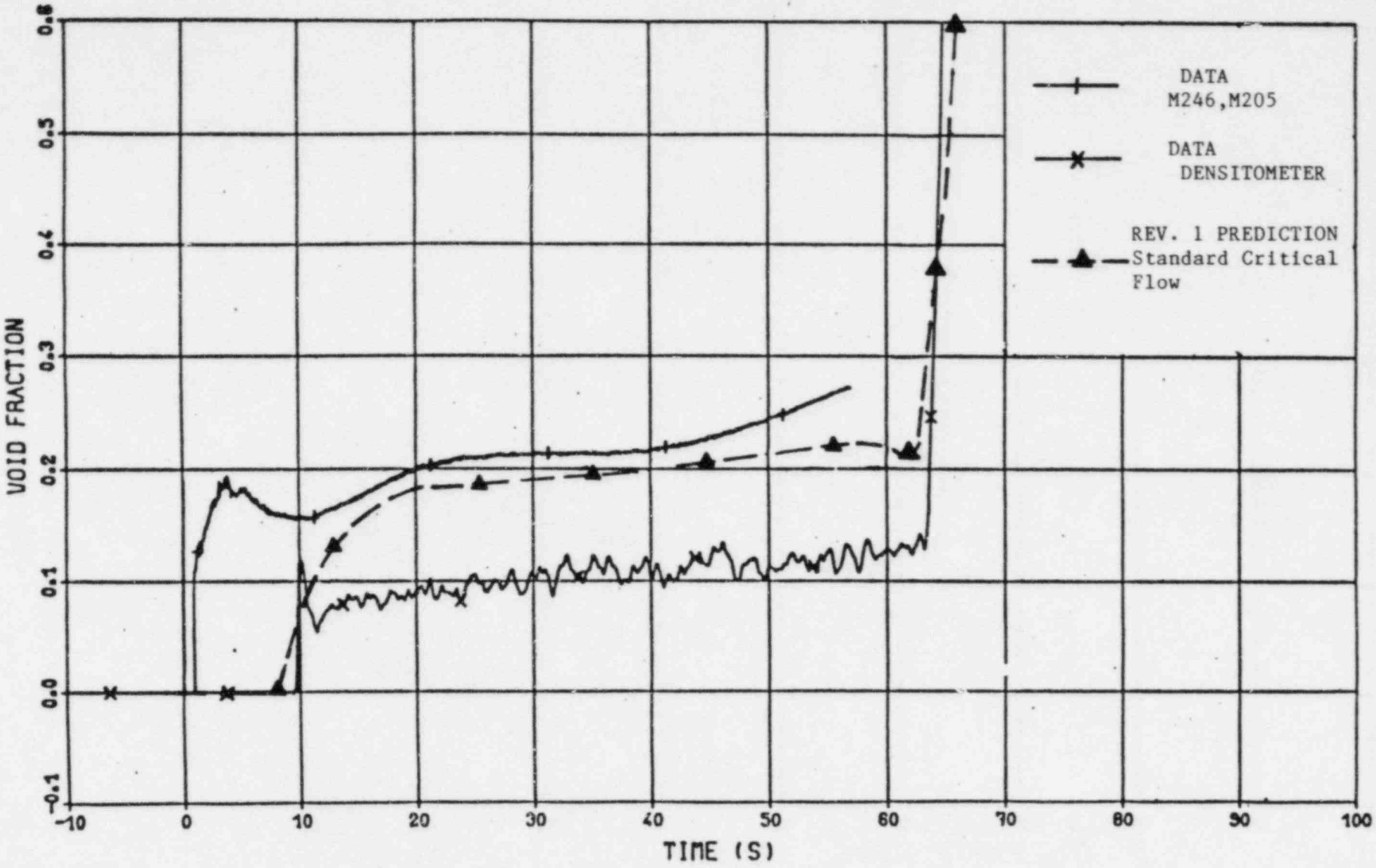


Figure 2.2-14 Marviken Test 10 Void Fraction
RELAP5YA Standard Critical Flow Model Predictions-Rev. 1

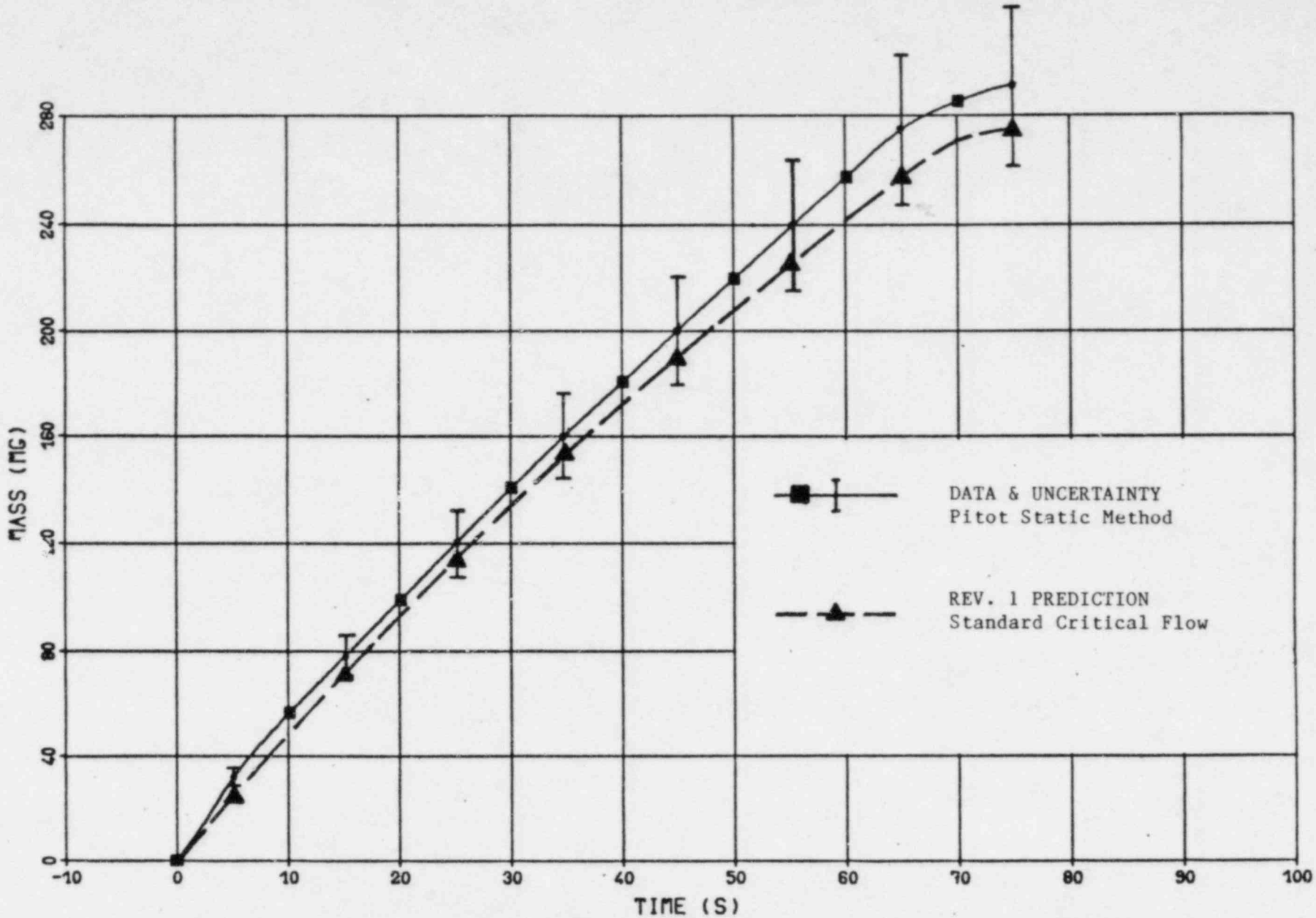


Figure 2.2-15 Marviken Test 10 Excaped Mass
RELAP5YA Standard Critical Flow Model Predictions-Rev. 1

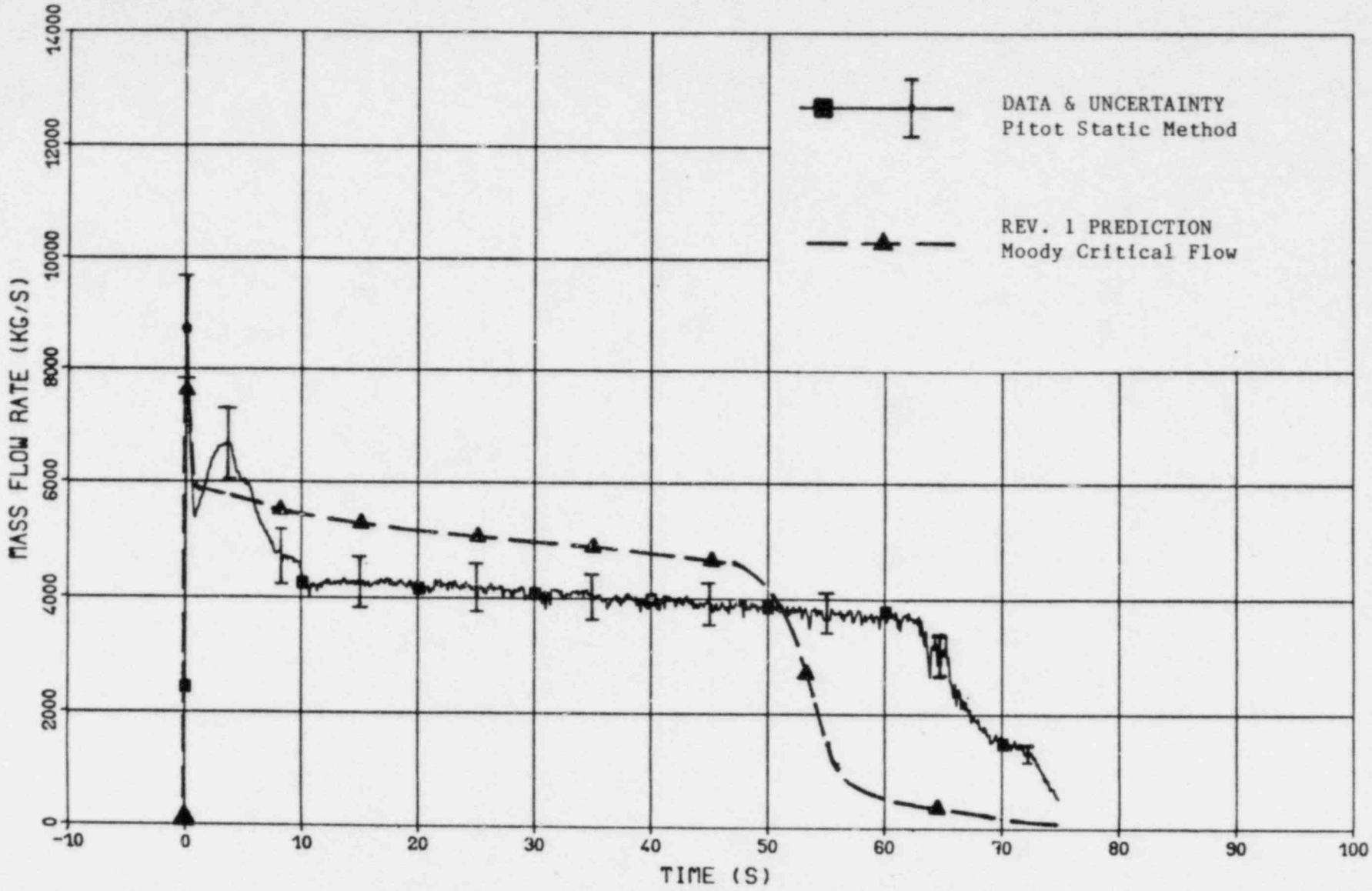


Figure 2.2-16 Marviken Test 10 Break Mass Flow Rate
RELAP5YA Moody Model Predictions-Rev. 1

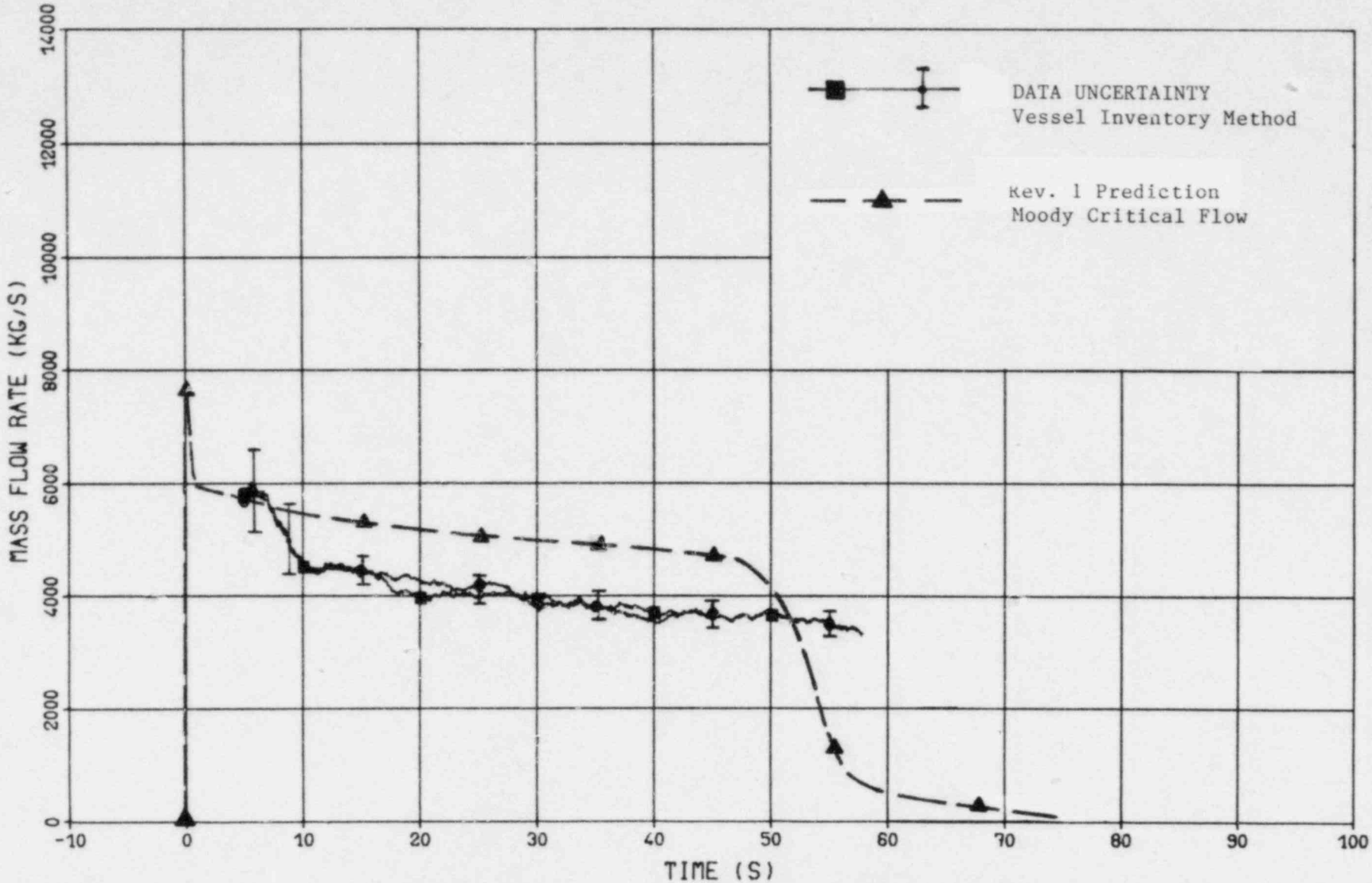


Figure 2.2-16A Marviken Test 10 Break Mass Flow Rate
RELAP5YA Moody Model Predictions-Rev. 1

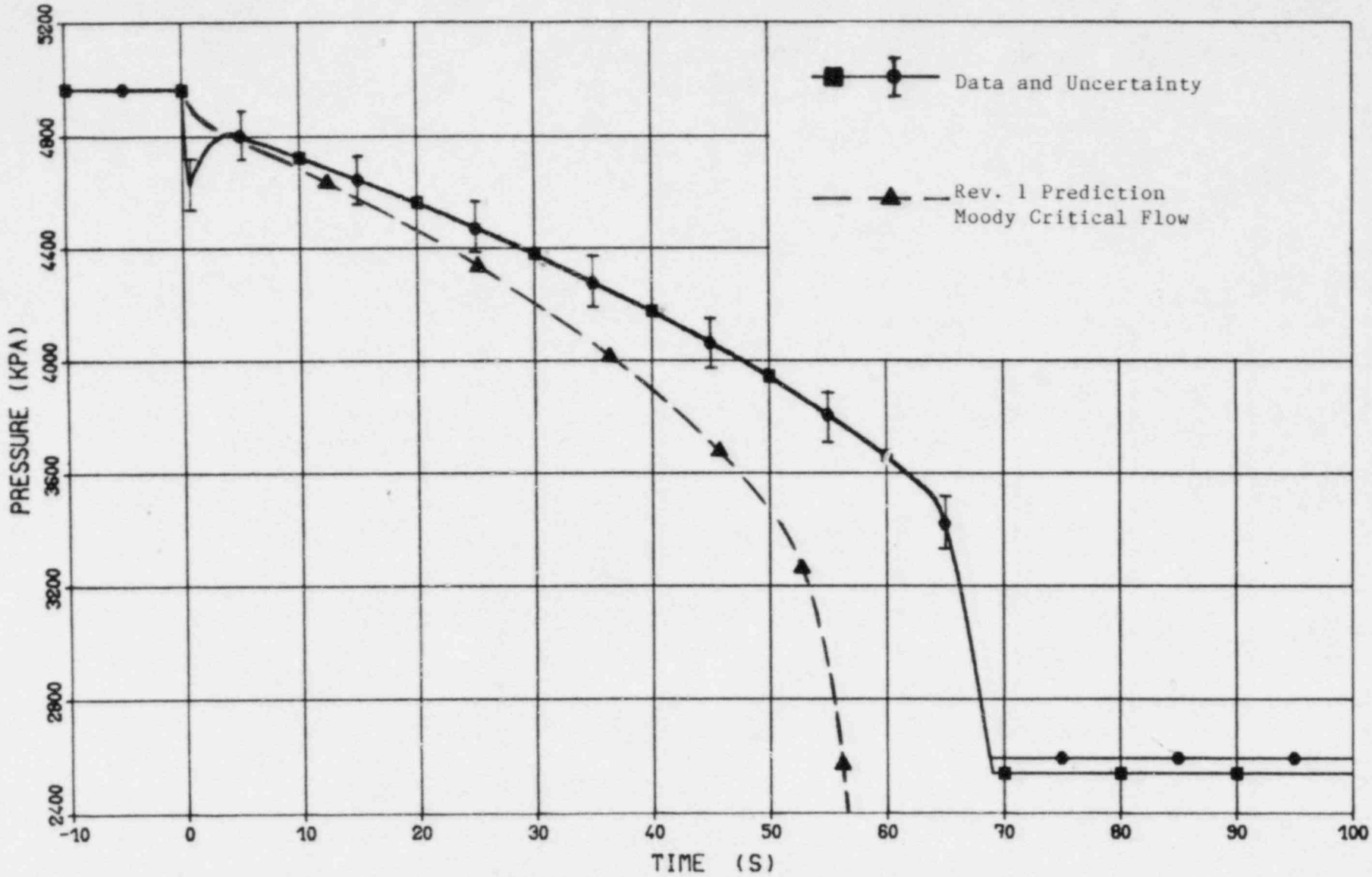


Figure 2.2-17: Marviken Test 10 System Pressure
RELAP5YA Moody Model Predictions - Rev. 1

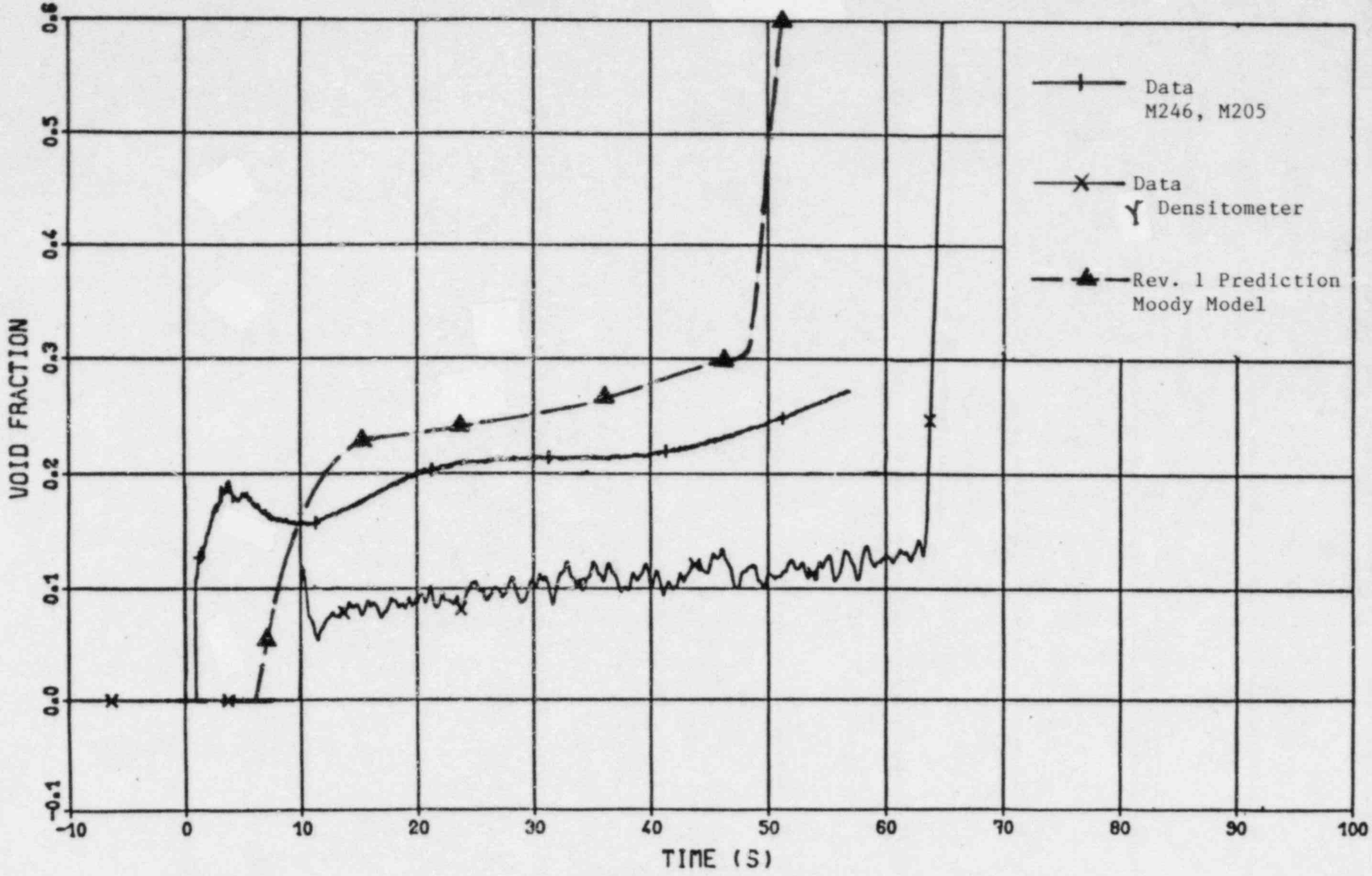


Figure 2.2-18: Marviken Test 10 Void Fraction
RELAP5YA Moody Model Predictions - Rev. 1

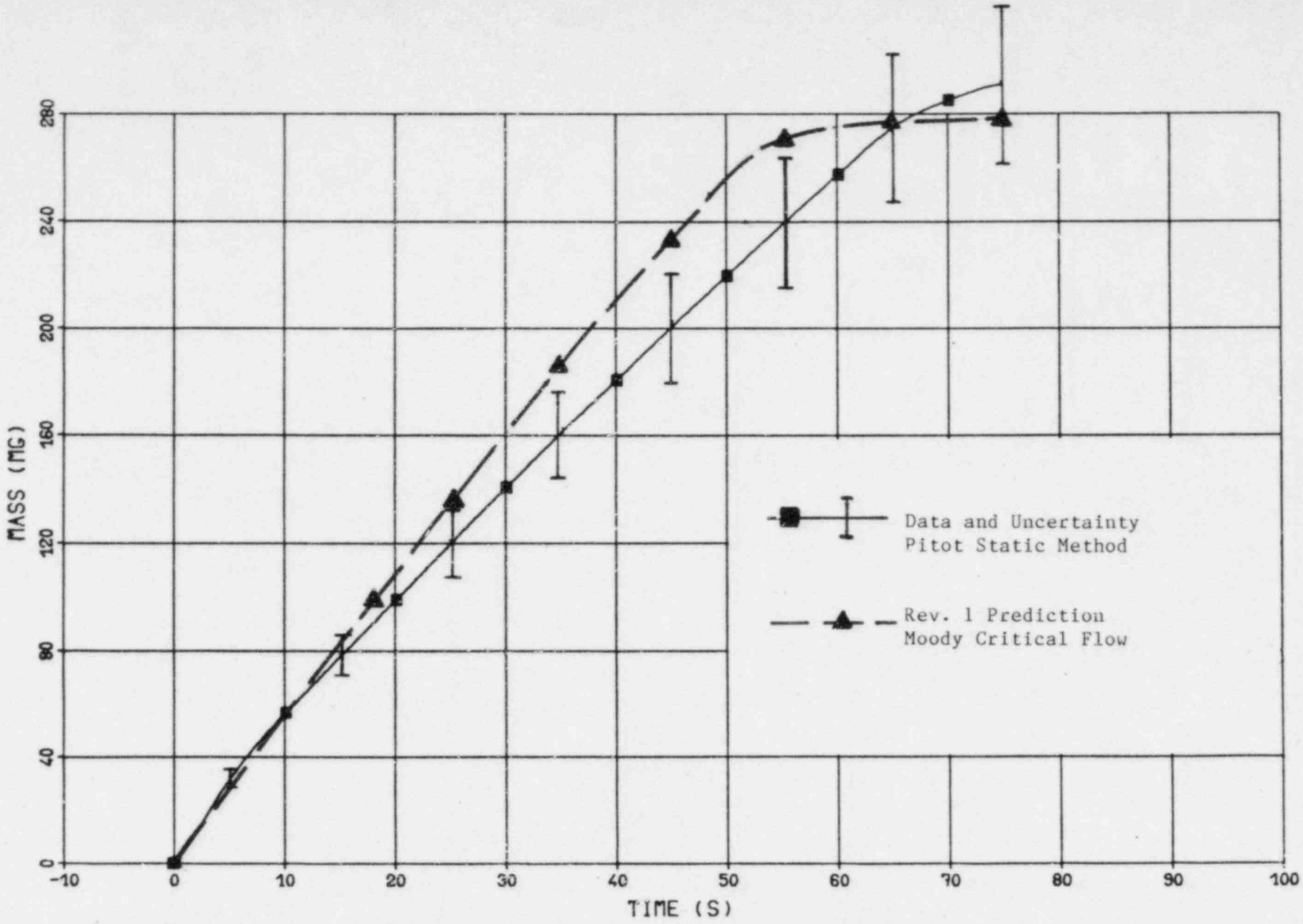


Figure 2.2-19: Marviken Test 10 Escaped Mass
RELAP5YA Moody Model Predicitons - Rev. 1

Q.IX.10

Clarify also why Page 42 of Reference 12 shows the code underpredicted the escaped mass at 60 s and yet it also underpredicted the pressure at 60 s.

A.IX.10

As explained in Answer A.IX.9, the revised case with the correct initial liquid level in the vessel shows that the calculated pressure history agrees with the test data very well from 5 to 65 seconds. However, the calculated escaped mass still lies below the reported data at 75 seconds. Since this computer run had a small mass error (less than 0.2%) at 75 seconds, this discrepancy was investigated further.

The test data shown on Figure 2.2-15 was derived by the Marviken staff from the Integral Pitot Static Method (integral of discharge mass flow rate). Since the estimated error of the Pitot Static Method is $\pm$8% to $\pm$15% for determining the two-phase flow rate, then this error is also reflected in the integral of this parameter. Therefore, $\pm$10% uncertainty bars have been placed on the reported escaped mass test data. This shows that the predicted values lie within the data uncertainty from 10 to 75 seconds.

Next, we note the initial mass in the vessel and discharge pipe is 279,644 kg. A variety of test data indicate the system was essentially filled with vapor by the time the ball valve was closed at 78 seconds. The final system pressure after 78 seconds is 2350 $\pm$ 243 kPa (341 $\pm$ 35 psia) from the six pressure transducers. The saturated vapor density at 2350 kPa is 11.78 kg/$m^3$. The final mass retained in the 427.33 $m^3$ system must have been about 5.034 kg. Therefore, the maximum value for escaped mass at 75 seconds is 274, 610 kg. This value is within 0.065% of the 274,789 kg value predicted by the revised RELAP5YA calculation. This value is also 5.6% below the 290,000 kg value reported as test data at 75 seconds on the figure. Therefore, we conclude that RELAP5YA accurately predicted the total escaped mass from the system at 75 seconds, and that the reported test value is in error.

Q.IX.11

Clarify if the discontinuity in slip between the Moody model and the RELAP5 MOD1 subcooled choking model could cause flow oscillations and potentially mass conservation problems for break flows near the 0.05 void fraction switching point between the models.

A.IX.11

The original implementation of the Moody Critical Flow Model in RELAP5YA included a) tabular values of the Moody critical mass flux as a function of the upstream (donor cell) pressure and enthalpy, and b) Moody's theoretically derived slip ratio given by:

$$K_m = (V_g/V_f) = (\rho_f/\rho_g)^{1/3}$$

This method led to computational problems and large mass errors in the donor cell.

Subsequently, the method of implementing the Moody Critical Flow Model in RELAP5YA was modified. The tabular values of Moody critical mass flux as a function of upstream pressure and enthalpy were retained. However, Moody's theoretically derived slip ratio was replaced by a solution of the difference momentum equation using a relatively large value for the interphase drag coefficient. This approach has yielded well behaved solutions to date. It allows some slip between the phases (1.0 to about 1.3). These slip values are compatible with those calculated by the subcooled choking model which are near unity. The mass flow rates calculated by the Moody Two-Phase Critical Flow Model are still conservatively high compared to those predicted by the RELAP5YA Standard Two-Phase Critical Flow Model.

Several SBLOCA-EM calculations have been reviewed to examine the calculated break flow behavior near the 0.05 void fraction switching point. Two cases each, from the Yankee Plant Pump Trip Study (Reference IX.11-1) and the Maine Yankee Pump Trip Study (Reference IX.11-2) are shown in the attached Figures IX.11-1 and

IX.11-2, respectively. These results show that the transition between the Subcooled Choking Model and the Moody Two-Phase Critical Flow Model is relatively smooth. Note that the subcooled critical flow rates ($\alpha$ less than 0.05) are slightly higher than the Moody two-phase critical flow rates ($\alpha$greater than 0.05). The mass error in each run was small. Therefore, we conclude that the transition between the Subcooled Critical Flow and the Moody Two-Phase Critical Flow models yields well behaved solutions.

References

(IX.11-1) J. N. Loomis, J. H. Phillips, A. Husain, "Reactor Coolant Pump Operation During Small Break LOCA Transients at the Yankee Nuclear Power Stations," YAEC-1437, Yankee Atomic Electric Company, July 1984.

(IX.11-2) L. Schor, S. Haq, A. Husain, J. Ghaus, "Justification of Reactor Coolant Pump Operation During Small Break LOCA Transients for Maine Yankee," YAEC-1423, Yankee Atomic Electric Company, April 1984.

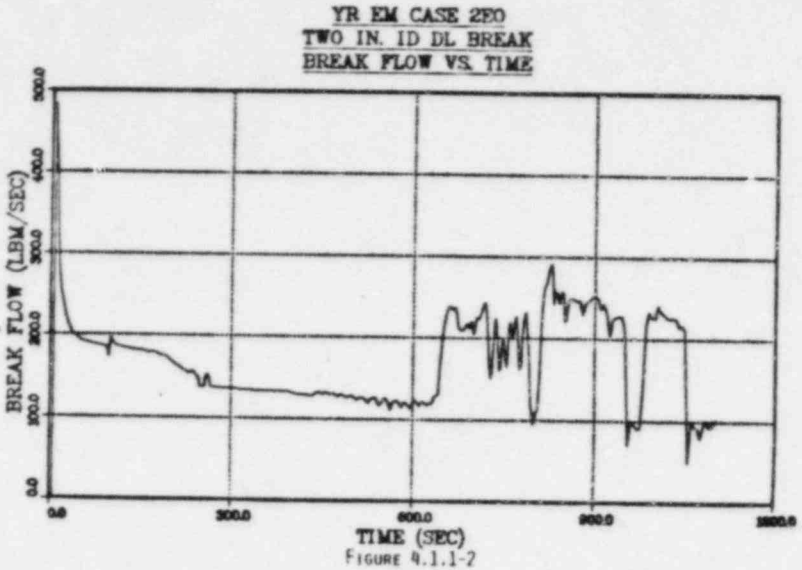

FIGURE 4.1.1-2

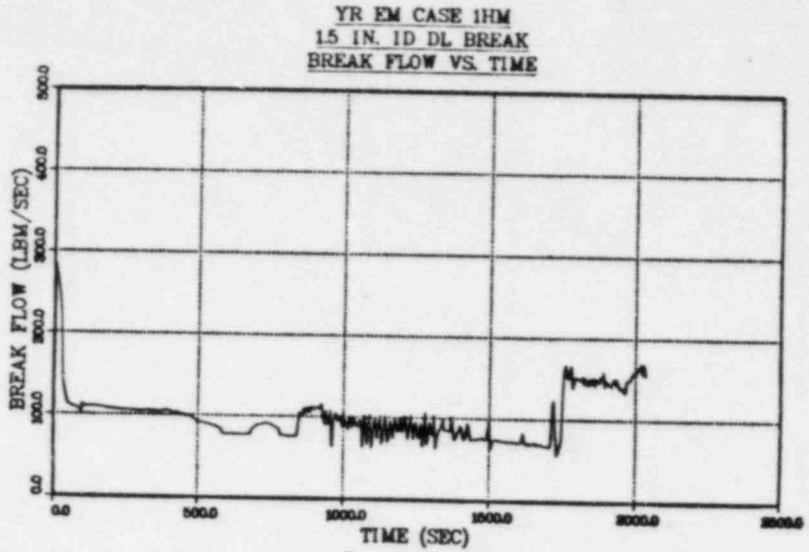

FIGURE 4.1.2-2

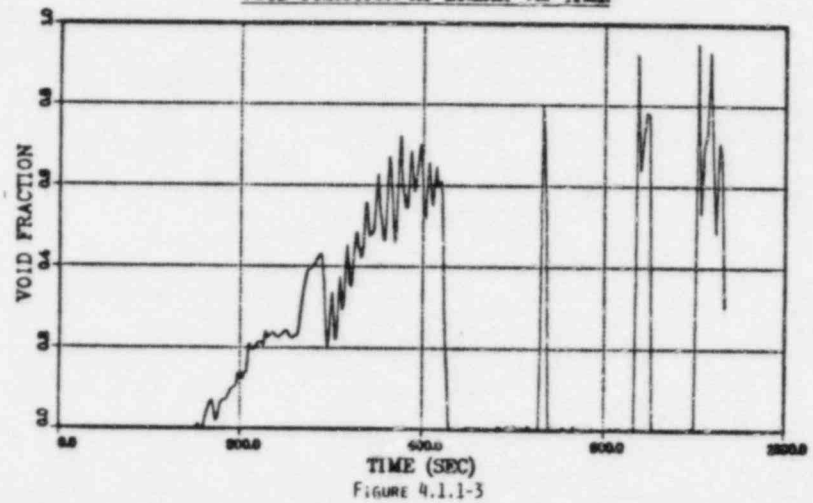

FIGURE 4.1.1-3

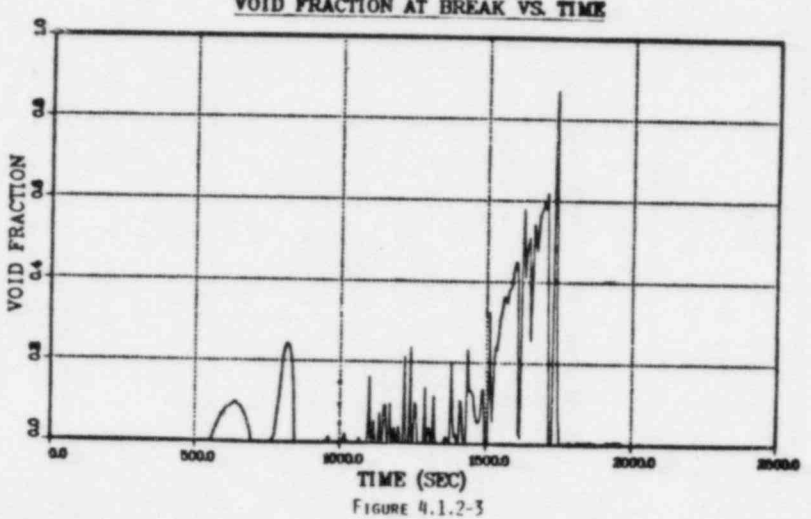

FIGURE 4.1.2-3

Figure IX. 11-1: Yankee Plant SBLOCA-EM Cases

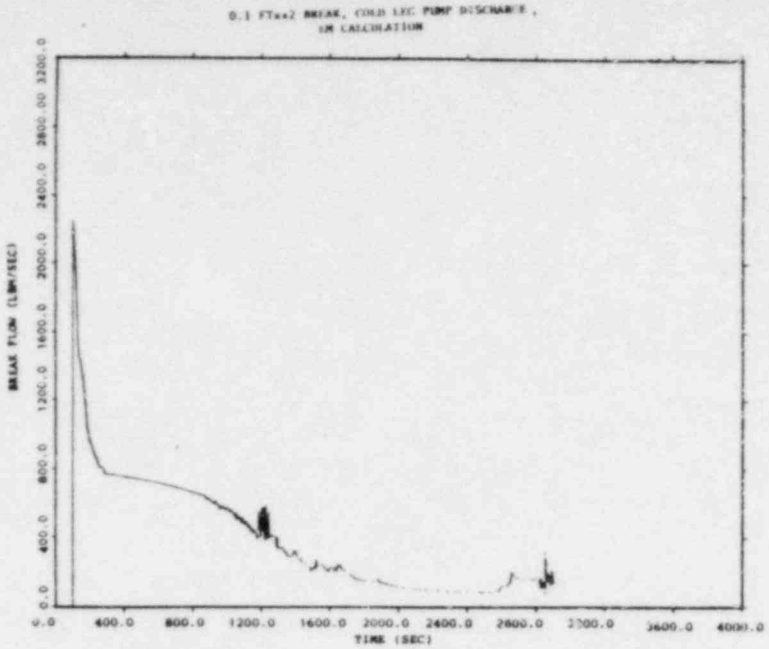


Figure 4.1.1-3 Break Flow

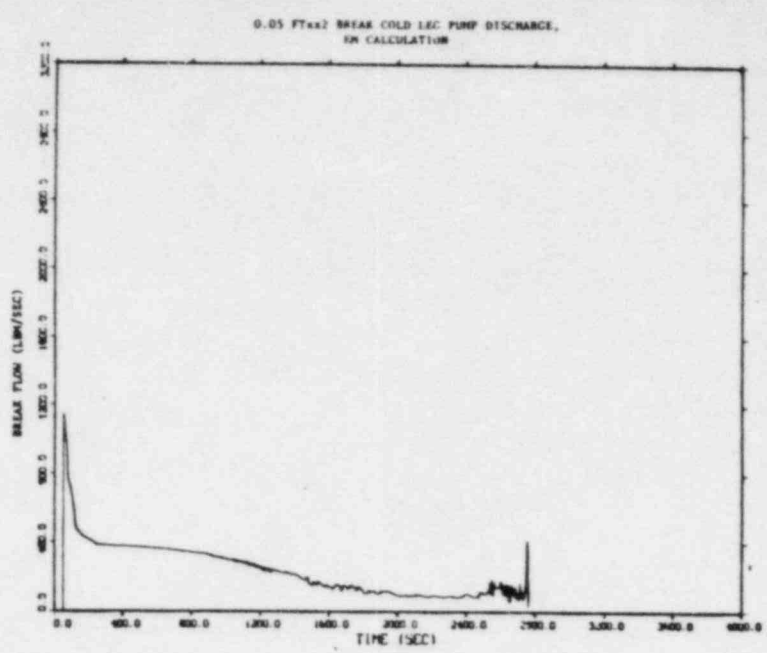


Figure 4.1.2-3 Break Flow

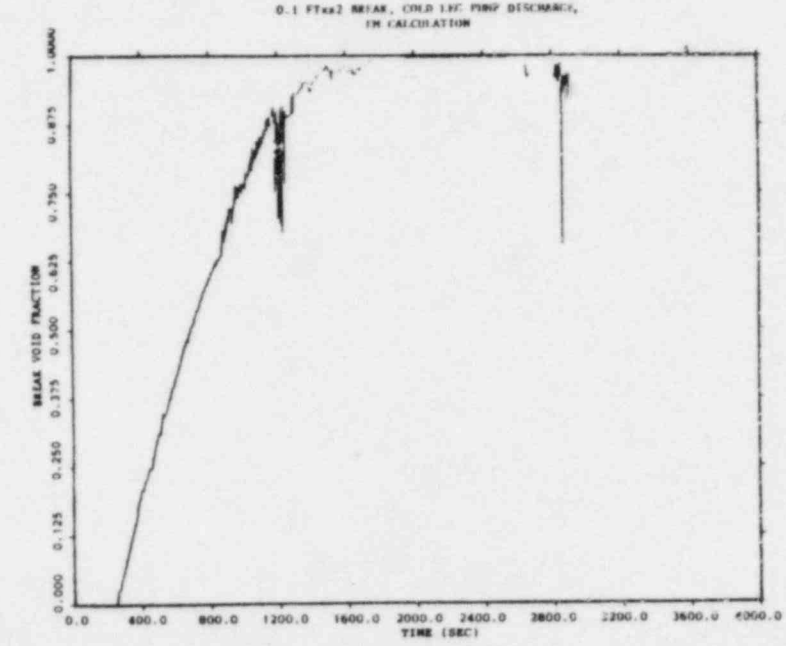


Figure 4.1.1-4 Break Void Fraction

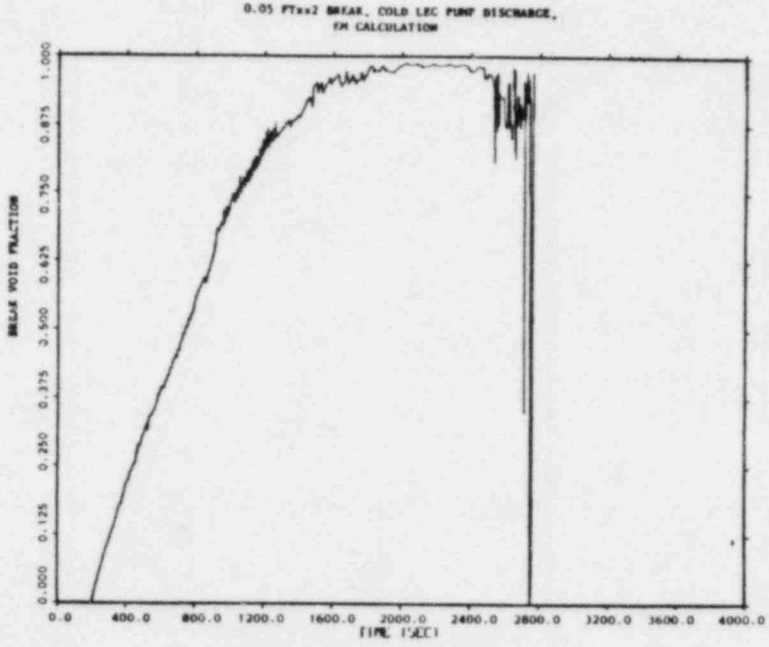


Figure 4.1.2-4 Break Void Fraction

Figure IX. 11-2: Maine Yankee SBLOCA-EM Cases

Q.IX.12

Clarify why using the Moody model only after the void fraction exceeds 0.05 meets the Appendix K Requirement I.C.1.B that for all times after the discharging fluid has been calculated to be two-phase in composition, the discharge rate shall be calculated by use of the Moody model.

A.IX.12

Paragraph I.C.1.6 in Appendix K requires that the Moody Critical Flow model be used after the discharging fluid has been calculated to be two-phase in composition. Restated, one first needs to calculate that two-phase discharge conditions exist at the break location, and then use the Moody Critical Flow Model thereafter. However, this requirement does not specify the void fraction nor quality of the discharging fluid that is to be calculated prior to using the Moody Critical Flow model. Therefore we have selected the small void fraction value of 0.05 as our criterion to begin using the Moody model. This small void fraction was chosen mainly to ensure continuity in the critical flow calculation between single-phase and two-phase conditions. Figures IX.11-1 and IX.11-2 from the answer to the previous question show that the subcooled critical flow rates are slightly higher than those calculated by the Moody Critical Flow Model near the void fraction value of 0.05. Thus, we comply with Appendix K requirement I.C.1.6.

Q.IX.14

Clarify if break-size sensitivity studies will be done for SBLOCA analyses.

A.IX.14

Yes, break-size sensitivity studies will be performed and submitted on a plant-specific basis.

Q.IX.18

Page 89 of Reference 8 states: "Equation (245) can be derived from Equation (153) by neglecting the third C term in D and setting C=0 (stratified) on the right side of Equation (153) and C=∞0(homogeneous) on the left side." Clarify how the opposite extremes of the virtual mass coefficient can be justified for use in the same equation.

A.IX.18

The cited text contains errors, and should state the following:

Equation (245) can be derived from Equation (153) by substituting Equations (148), (149) and (150) into Equation (153) with the following assumptions:

a. Set C=∞ (homogeneous) on the right side of Equation (149).

b. Set C=0 (stratified) and neglect the third term on the right side of Equation (150)

Justification of the model given by Equation (245) is based upon INEL's extensive experience and YAEC's assessment results to date. Although the two assumed values of C are significantly different, nevertheless, the resulting equation produces results that are in good agreement with test data (e.g., Marviken, LOFT, TLTA). The following discussion may explain why.

Figure 15 in Appendix A of Reference IX.18-1 shows that the virtual mass coefficient in Equation (149) has a significant effect upon the two-phase equilibrium sonic speed. Thus, this coefficient will have a significant effect upon the mass mean Mach number defined by Equations (148), (149) and (154). Figure 16 (Reference IX.18-1) shows the coefficient, D, defined in Equation (150) that multiplies the relative Mach number is bounded by $\pm$0.6. The relative Mach number for critical flow conditions is generally an order of magnitude less than

the mass mean Mach number due to the relatively small phasic velocity differences that develop. Thus, the second term on the left side of Equation (155) is generally much smaller than the first term, i.e.:

$$M_v + D\,M_r = \pm 1 \qquad (155)$$

$$M_v \equiv \frac{V_m}{a} > D\,M_r \equiv \frac{D(V_g - V_f)}{a}$$

Therefore, the influence of the virtual mass coefficient, C, is weaker in parameter D given by Equation (150) than it is in the sonic velocity, a, given by Equation (149) when determining critical flow conditions.

This observation was checked by rerunning the Marviken Test 10 Best-Estimate Calculation and assuming C=∞ in Equation (150) consistent with the assumed value in Equation (149). The results are shown in Figures IX.18-1 through IX.18-5 as the sensitivity case indicated by the small dash lines. These results show the break flow rate and discharge pipe void fraction are slightly higher. This causes the vessel dome pressure to decrease faster and moves to outside the uncertainty bars on the measured dome pressure. Both the Revision 1 prediction and the sensitivity case predict the escaped mass history within the uncertainty of the reported test data. Therefore, we believe the original model given by Equation (245) remains the best model to use for critical flow calculations at this time.

Reference

(IX.18-1) R. T. Fernandez, R. K. Sundaram, J. Ghaus, A. Husain, J. N. Loomis, L. Schor, R. C. Harvey and R. Habert, "RELAP5YA - A Computer Program for Light-Water Reactor System Thermal-Hydraulic Analysis, Volume I: Code Description, "Yankee Atomic Electric Company Report YAEC-1300P, Volume I, October 1982. (Proprietary)

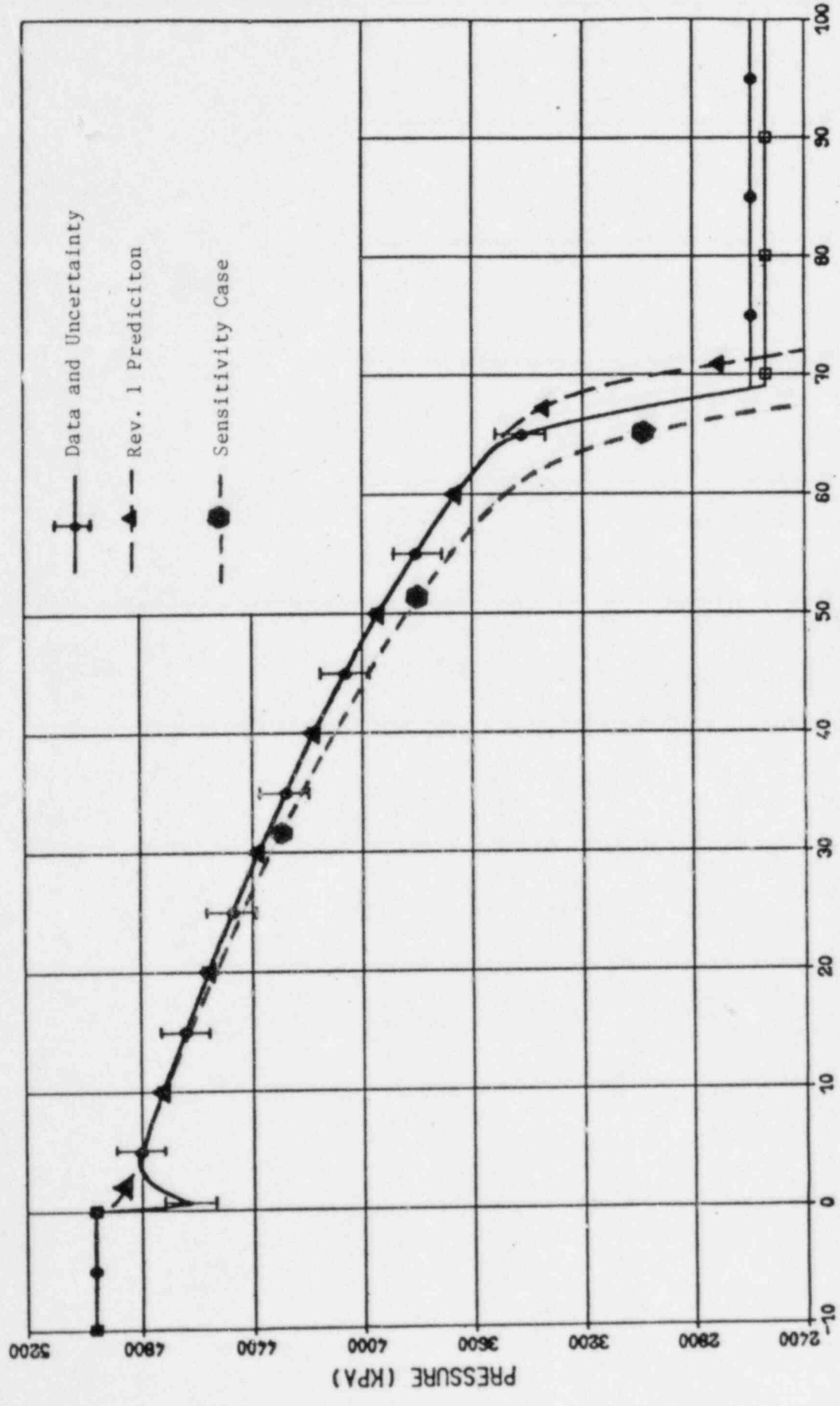


Figure IX.18-1: Marviken Test 10 Dome Pressure
RELAP5YA Standard Critical Flow Model Predictions

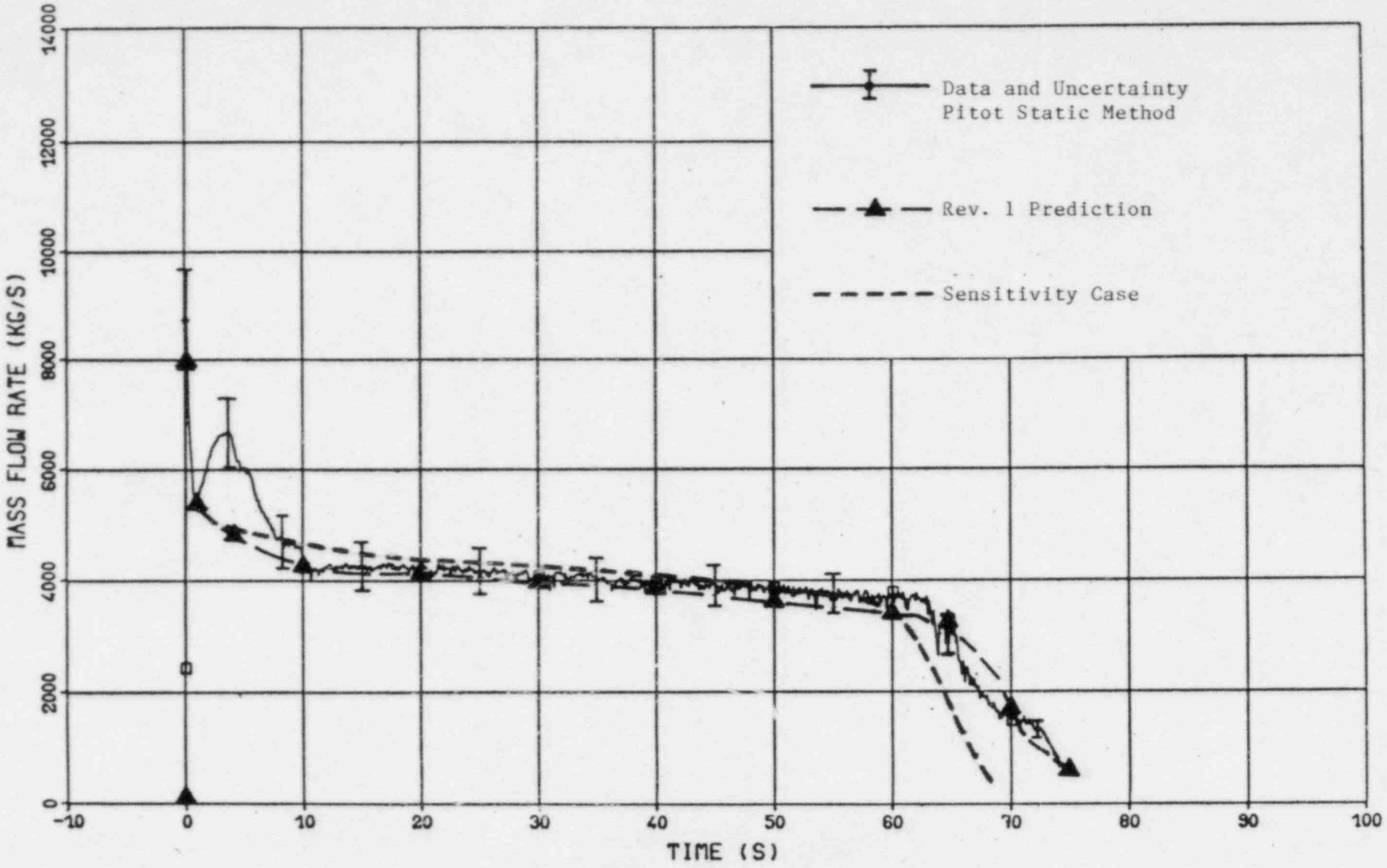


Figure IX.18-2: Marviken Test 10 Break Flow Rate
RELAP5YA Standard Critical Flow Model Predicitons

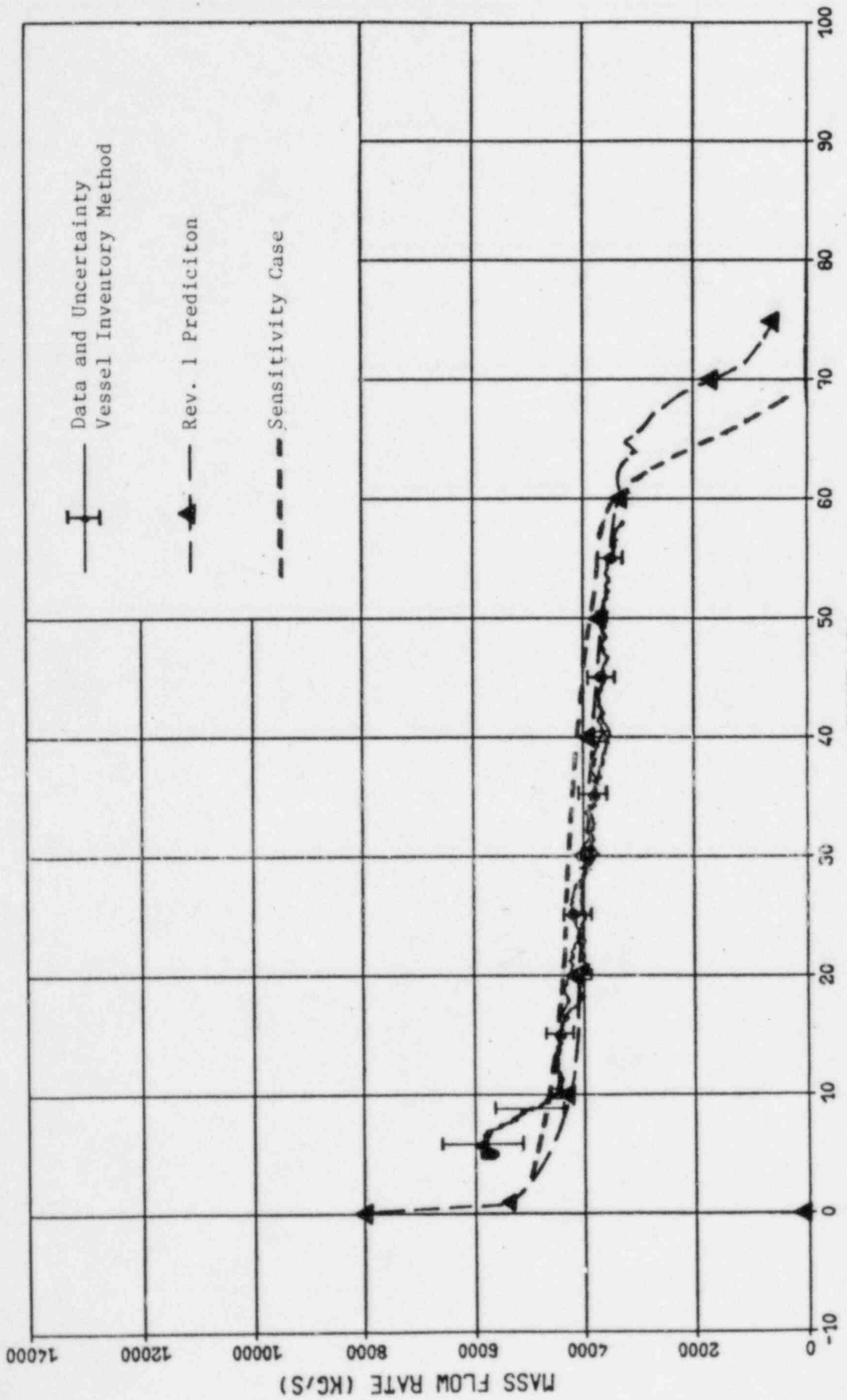


Figure IX.18-3: Marviken Test 10 Break Flow Rate
RELAP5YA Standard Critical Flow Model Predictions

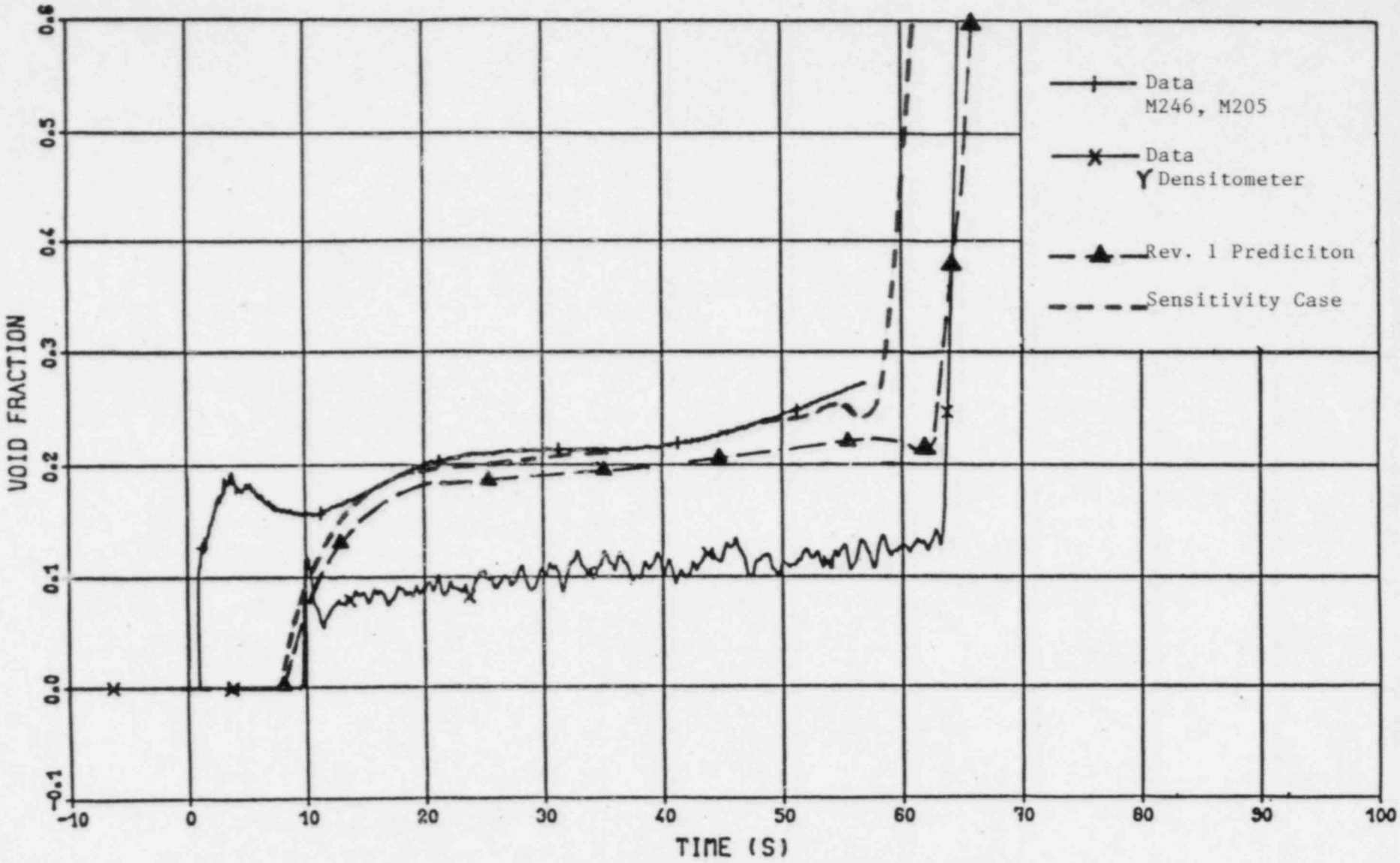


Figure IX.18.4: Marviken Test 10 Void Fraction
RELAP5YA Standard Critical Flow Model Predictions

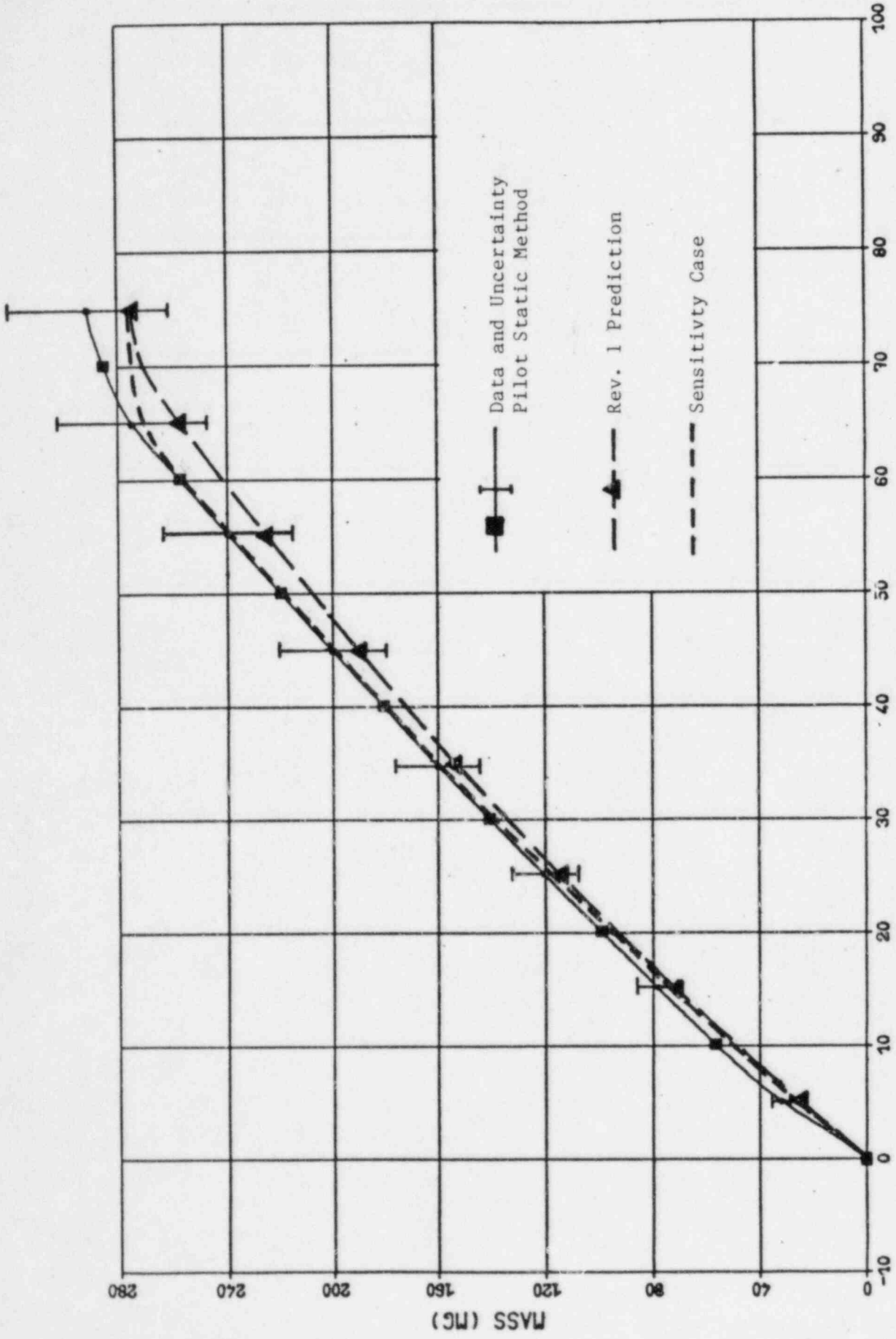


Figure IX.18-5: Marviken Test 10 Escaped Mass
RELAP5YA Standard Critical Flow Model Predictions

Q.IX.19

Justify that break-flow models bound all SBLOCA cases expected.

A.IX.19

RELAP5YA contains two sets of critical flow models. The standard critical flow models are used for best-estimate calculations of the break flow rate for liquid, two-phase fluid and steam conditions. The Moody critical flow model is used for licensing calculations of the break flow rate for two-phase fluid and steam conditions as required by Paragraph I.C.1.6 of Appendix K to 10CFR50.46. All critical flow models account for the break size and location through input data. Separate discharge coefficients can be entered as input data for liquid and for two-phase/steam discharge conditions. All critical flow models account for the upstream fluid conditions that feed the break. The special case of break flow out of a horizontal pipe containing stratified flow is discussed in the answer to Questions Q.IX.7 and Q.VI.7. All models have been favorably assessed against a wide-range of conditions (e.g., break size, pressure, quality) reflected in the six tests identified in Table IX.19-1 that is attached. Therefore, we believe these break flow models bound all LWR LOCA cases that could reasonably be postulated, including small break LOCAs.

TABLE IX.19-1

Assessment of Break Flow Models

| Test Facility and Number | Critical Flow Regime | | |
|---|---|---|---|
| | Liquid | Two-Phase | Steam |
| Marviken Test 10 | R | R, M | R, M |
| GE Level Swell Test 1004-3 | | R | R |
| TLTA Test 6425/R2 | R | R, M | R, M |
| TLTA Test 6426/R1 | R | R | R |
| TLTA Test 6432 | R | R | R |
| LOFT Test L3-6 | R | R | |

Note: R = RELAP5YA Standard Critical Flow Model
M = Moody Two-Phase Critical Flow Model

## X. ADDITIONAL QUESTIONS THAT ARE CONCERNED WITH SEVERAL AREAS

### Q.X.2

During depressurization, the noding detail affects the pressure history after the pressurizer empties. The highest temperature node containing liquid in the upper head, upper plenum, or top of the hot-leg bend (or top of a steam generator U-bend) will determine the saturation pressure at which the fluid begins flashing. If fluid from large regions is combined in one node, the flashing will be determined by the average temperature of the large node rather than the hottest temperature that would be modeled using smaller nodes. Additional nodal sensitivity studies are required to confirm the adequacy of the hot region nodal detail to properly account for flashing during depressurization in a small break LOCA" (Page VIII-43 of Reference 2). Clarify what sensitivity studies have been done to define the noding required to ensure adequate detail will be modeled in SBLOCA calculations.

### A.X.2

This question refers to the noding schemes used by Combustion Engineering, Inc. for their LOCA analyses (Reference X.2-1). As is seen in Figures IV.2-1 and IV.2-2, Yankee plans to use a detailed nodalization of the plant. This detail has been utilized to represent the plant configuration accurately and to capture the important aspects of the transients. A very detailed noding of the upper head and upper plenum region is employed. With this kind of noding, we feel that the flashing of different regions following a LOCA will be accurately modeled. As such, we cannot justify the need to perform noding sensitivity studies to assure the adequacy of noding detail in the upper portions of the reactor vessel.

### Reference

(X.2-1) CEN-114-P, Amendment 1-P, "Review of Small Break Transients in CE NSSS," Pages 3.3-29 and 3.3-30," July 1979.

Q.X.3

Appendix K, Requirement II.2 states: "For each computer program, solution convergence shall be demonstrated by studies of system modeling or noding and calculational time steps (Page 274 of Reference 10). Clarify what noding sensitivity studies have been performed.

A.X.3

It has been pointed out in A.X.2 that we intend to use a detailed nodalization of the plant in our LOCA analyses. This detail has been utilized to represent the plant configuration accurately and to capture the important aspects of the transient. With this kind of noding detail, Yankee does not see the need to perform noding sensitivity studies to demonstrate computer program solution convergence.

Q.X.4

Clarify what time step sensitivity studies have been performed.

A.X.4

Time step sensitivity studies will be performed on a plant-specific model and documented in submittals.